Benzothiophene-based Fragments Act as Reversible and Irreversible Covalent Probes for Dynamic Coactivator Med25

by

Phoenix NiaImani Williams

A dissertation submitted in partial fulfillment
of the requirements for the degree of
Doctor of Philosophy
(Chemistry)
in The University of Michigan
2023

Doctoral Committee:

Professor Anna K. Mapp, Chair
Associate Professor Alison Narayan
Professor Melanie Sanford
Assistant Professor Wenjing Wang

Phoenix N. Williams

niaimani@umich.edu

ORCID iD: 0000-0002-5305-8586

DEDICATION

I'd like to dedicate this work to my grandparents. Especially, my great-grandfather Ranford L. Williams (Papa) and my grandmother Sheila Moppin (Ma Sheila) who both supported me and believed that I could achieve anything I put my mind to but have unfortunately passed away before the completion of this document. Thank you for your love and encouragement and may your souls rest in peace. Also, to my great grandmother who's been a continual support to me through all my ups and downs. Last, I want to dedicate this to my friends and family who continue to inspire me every day. I'm not sure how I'd be the person I am today and who I'm destined to become without your influence.

ACKNOWLEDGMENTS

First, I would like to acknowledge my advisor Dr. Anna Mapp. I've enjoyed the time I've had to see her in action. She is so inspiring, kind-hearted, and passionate. She's taught me so much in terms of mentoring and connecting organic chemistry to biochemistry and how to apply it to a research setting. I appreciate the wisdom and support you've given me throughout this process. You also remind me that every scientist is still a person, and that it's ok to enjoy science AND have other hobbies. Even though we all make mistakes, we can learn from them and incorporate our unique perspectives and talents towards outcomes we never thought possible.

Additionally, the Mapp lab is full of inspiring scientists each with their own unique outlook on research and personal development. Thank you, Dr. Stephen Joy and Dr. Brittany Morgan, for guiding me through the COVID19 pandemic as great mentors while simultaneously making it fun to come to lab. Thank you, Dr. Steve Sturlis, Dr. Olivia Patteli, and Dr. Sam DeSalle, for teaching me different biochemical techniques and how to use different instruments. I owe a huge thanks to Dr. Kevon Stanford for mentoring me when I joined the lab and teaching me some of the basics of peptide synthesis and peptidomimetics.

I also need to highlight my current lab member Ayza Croskey. Not only has she always had such an enthusiasm for research, but she also brings peace and serenity to the lab. I've also watched her develop as a mentor to newer research colleagues while always adding insightful responses to research questions. Thank you for assisting me with DSF and talking me through different experimental plans.

I owe a thanks to the Rackham Merit Fellowship Program through the University of Michigan, to the PPG Summer Research Fellowship for assistance in research funds. As well I must thank the Chemistry department, Life Science Institute, Rackham Graduate School, and the ACS for travel funds for conferences and recruitment efforts.

I must thank my family members who have continued to support me in all that I do. I think of you all often and I look forward to the times when we get to come together again. You all may not understand what I'm saying most of the time, but you always continue to motivate me to never give up.

Thank you to the friends that come and go and to the friends that stay, I want to highlight how you all come from different walks of life and have different specialties and I simply hope that you all continue to believe in yourselves with the same intensity you believed in me. I keep you in my prayers and must remember that I learn a lot from all our interactions and can use them to always remember to keep an open mind to different perspectives and unconscious biases. Huge acknowledgments go to the Chemistry graduate student services team. From recruiting me to pursue a degree at the University of Michigan to advising me on my next career moves to

listening to my woes, they have always made me feel supported and have made this process so much easier than it could have been.

I'd also like to acknowledge one of my best friends, Takana H. Tubo. Even though we don't always see eye to eye your intelligence and continues to inspire me. Thank you for taking the time to help me understand different biological aspects to my work that were harder for me to grasp and even reviewing drafts of statements and presentations I've submitted or presented throughout my scientific career. You've seen the most of my development through this process and continued to encourage me to be my best even when times were difficult. Also, thank you for being there through some of the harder moments of this journey, such as when both of my grandparents passed away. These times made earning a PhD in chemistry seem impossible and I vividly remember telling you I wanted to give up. Thank you for letting me rant and then when I was calm reminding me how I even got here in the first place.

Even though I already brought up my family, I wanted to shout my mom out once more. Mom, you know you inspire me as I watch you do anything you put your mind to. I get my determination to succeed and stubbornness not to quit from you. The only reason I believe I can succeed is because I watch you do it. Not that it's a straightforward, easy process, and maybe you don't feel like "you've won" yet, but don't forget to celebrate the small victories that add to your overall goal.

Finally, I must quote my Papa. He'd always tell me that the process was equal to the fulfilment. After this journey it makes sense. Through trial and error, amidst many failures, I've learned you can get through any challenge if you simply don't give up and remember that the failure isn't a reflection of yourself rather a lesson on what doesn't work. It may not be easy, but there are creative solutions to any problem if you look at it from the right angle.

With that thank you all for your love, encouragement, and support.

PREFACE

The following dissertation outlines the development of two novel thermostabilizers of Med25 AcID in search of small molecule modulators of Med25-related Protein-Protein Interactions. We develop small molecules identified from a Cysteine Tethering Screen into Irreversible modulators and investigate their interaction with Med25 AcID.

Table of Contents

LIST OF FIGURES

Chapter 4 Figures

LIST OF SCHEMES

LIST OFAPPENDICIES

ABSTRACT

Transcriptional coactivators mediate transcriptional activity within cells by forming transient protein-protein interactions (PPIs) to facilitate the assembly of the RNA polymerase machinery. Dysregulation of these PPIs results in disease. Transcriptional coactivators consist either of multiple protein subunits or multiple subdomains that assist the transcriptional activation process through a PPI network with transcriptional activators. For example, Med25, a subunit of the Mediator complex, has been shown to play a role in bridging the Mediator complex and RNA Polymerase II at Med25-dependent gene targets, ultimately resulting in transcriptional upregulation. Mis-regulation of Med25-transcriptional activator PPIs contributes to viral infection, oncogenesis, and stress response disorders. For this reason, there is great interest in identifying druglike modulators of Med25. The motif that Med25 uses to form activator PPIs is the Activator Interaction Domain (AcID). It contains two binding surfaces, the H1 and H2 faces, that are large (900 A^2) and have little topology for small-molecule interactions. However, Med25 AcID contains two solvent-exposed cysteine residues adjacent to the H1 binding surface, suggesting that a site-directed screening approach might be an effective method for ligand discovery. Towards that end, the Mapp lab identified reversible covalent modulators of Med25 AcID using a disulfide Tethering approach in collaboration with the Wells lab. When the hits from the screen were examined, we noted the unusual structure of a benzothiophene-containing ligand that Tethered Med25 AcID at C506 selectively and potently and thus appeared to be an excellent candidate for further development.

The lead fragment contains both a benzothiophene moiety and an isonipecotic acid moiety, along with a disulfide used for Tethering. In **Chapter 2** a study dissecting the roles of each of these functional groups and their contribution to the affinity of the lead fragment for Med25 was carried out. Each of the molecules was assessed using single-point Tethering experiments in a time-dependent fashion. The results indicate that both the benzothiophene and the nipecotic acid groups have some affinity for Med25 AcID but that neither recapitulates the affinity of the lead fragment. Taken together, the data suggest that both moieties make important contacts with Med25 AcID.

In **Chapter 3** we transformed the reversible ligands from **Chapter 2** into irreversible covalent ligands through the incorporation of α-bromoacetamide into each of the ligands. Each of the ligands was synthesized using standard methods and then tested in single-point alkylation experiments. We also used these experiments to evaluate the effects of stereochemistry on small molecule binding to Med25. Through this we demonstrate that benzothiophene-based ligands discovered through disulfide Tethering can be transformed into irreversible probes that target Med25 AcID. **We show that both (*R*)- and (*S*)-benzothiophene nipecotic acetyl bromides not only irreversibly bind to Med25 AcID but also shift the melting temperature of Med25 AcID, suggesting that these two compounds stabilize particular Med25 AcID conformations.** Thus, these two molecules are useful probes for us and others for the study of Med25 function. Future efforts will examine the effect of the conformational stabilization on Med25 PPI networks in vitro and in cells.

CHAPTER I Dynamic Coactivator Med25 Protein-Protein Interactions and Disease

Chapter 1.1 Background and Introduction

Transcriptional coactivators mediate transcriptional activity of cells by forming transient protein-protein interactions (PPIs) to facilitate the assembly of the RNA polymerase machinery (**Figure 1.A**). Dysregulation of these PPIs results in disease.[1–18]Transcriptional coactivators are proteins consisting either of multiple protein subunits or multiple subdomains that assist the transcriptional activation process through a PPI network with transcriptional activators. For example, Med25, a subunit of the Mediator complex has been shown to play a role in recruiting both the remaining Mediator subunits and RNA Polymerase II to Med25-dependent gene targets, ultimately resulting in transcriptional upregulation (**Figure 1.1B**). Med25 was first discovered in 2004 by Tomomori-Sato et al. as an ortholog of Saccharomyces cerevisiae Mediator subunit Cse2.[19] Tomomori-Sato et al. used several different Mediator preparations combined with various biochemical analyses to validate that Med25 is a bona fide subunit of Mediator. Med25 is

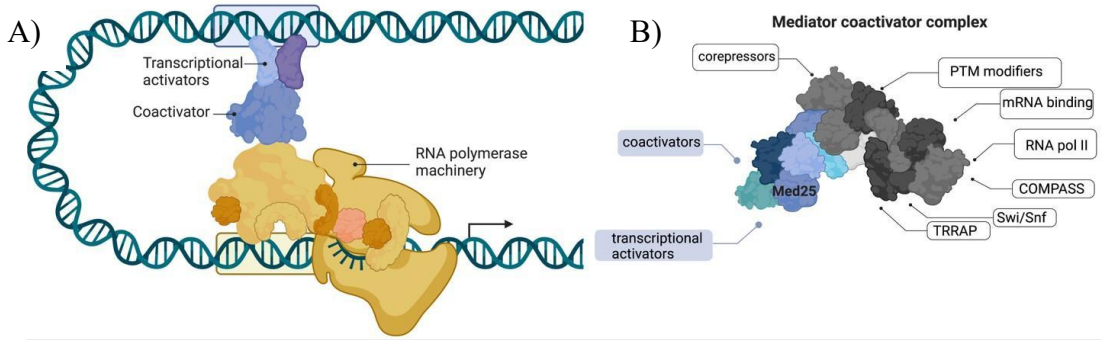

Figure 1. Med25 PPIs and Transcription .(1A) *Transcriptional coactivators bind to promoter-bound activators for the recruitment of RNA Pol II and other related general transcription factors to initiate transcription.[1–9]* ***(1B)*** *Med25 is a subunit of the Mediator coactivator complex that forms PPIs with transcriptional activators. While the coactivator complex Mediator is ubiquitous in species from yeast to mammals, the subunit composition and functions can be species specific.* [3,5,6,10,11]

expressed within higher order eukaryotes (rats, mice, human, and plants) suggesting this subunit plays more of a role in species-specific regulatory processes.[2,3,9,11,12,20–31]

Over time researchers have shown that Med25 is a 747-residue protein subunit of Mediator (**Figure 1.2**) consisting of three main domains.[32–34] The von Willebrand factor A (VWA) domain, (AAs 17-226) which recruits and secures the other relevant Mediator subunits for transcriptional activation, the **Ac**tivator **I**nteracting **D**omain (AcID) (AAs 394-543), which is responsible for Med25's activator interactions, and the Nuclear Receptor Domain (NR) (AAs 646-650) which participates in PPIs with nuclear receptors such as the retinoic acid receptor [35]

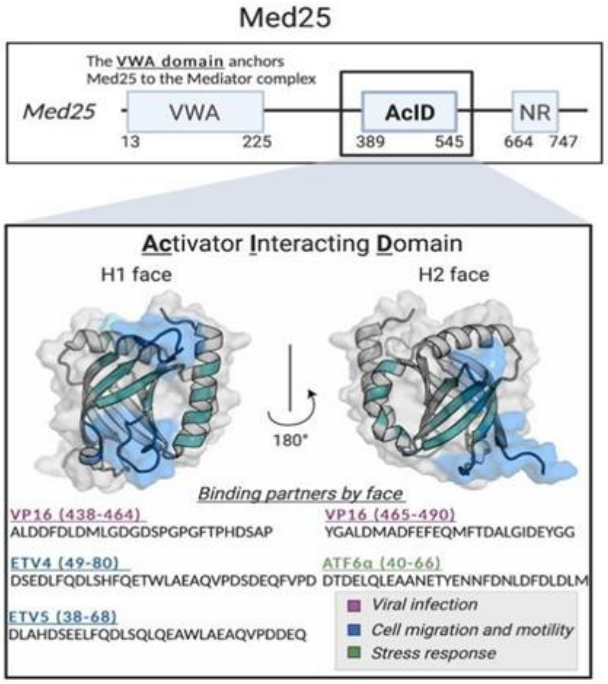

Figure 1.2 Med25 and its Activator Binding Interactions using AcID. *The Activation Interacting Domain (AcID) of Med25 binds disparate transcriptional activators using the H1 or H2 binding face. Viral activator VP16 can interact with both sites simultaneously, while Ets-related activators ETV4 and ETV5 distinctly bind the H1 face and ATF6α binds the H2 face.* [4,21,32,34–36,38–41]

Chapter 1.1 Med25 AcID PPIs and Disease

Since its discovery, Med25 AcID has been shown to be necessary for interacting with disparate activators such as the viral protein VP16[27,36–39], Ets-related factors such as ERM[36,37] and the stress response protein ATF6α.[14,30,34,38,39] Med25 AcID contains two binding surfaces termed H1 and H2. While VP16 binds to both sites simultaneously, ERM interacts with the H1 face while ATF6α binds the H2 face. (**Figure 1.2**) These interactions have been characterized by protein MR studies as well as genetic and biochemical experiments in an attempt to better understand the overall mechanisms involved.[1,2,5,10,29,31,26,27,20,21,30,23,22,24,35,40–51]

Developing a chemical probe that disrupts or enhances Med25-related PPIs allows us to better understand their mechanisms and leads to the discovery of transcription-targeting therapeutics. Since its been demonstrated[52] In the case of the Ets-related factors ETV1/4/5 are often overexpressed in prostate cancer and have been shown to be functionally important for the transcription of genes regulated by these types of enhancers [36]Additionally AP1-motifs which bind to JUN and FOS transcription factor families can be observed in Med25-occupied regions with both TFs making specific contacts with Med25. It's interesting to note that the differences between these two TFs shows that FOS is able to strongly bind to the same Med25 site as ETV4, while JUN interacts with two other distinct sites.[36]

Additionally, it has been recently demonstrated that Med25's H1 and H2 sites are allosterically connected as the Koff rates of both VP16 and ATF6α are reduced when Med15's H1 face is pre-engaged with ERM either covalently or noncovalently, but neither of their Kon rates are affected by ERM's presence. It is hypothesized that tethered ERM forces Med25 through a conformational change that adds to the binding affinity of ATF6α for Med25 AcID.[39] These results encourage the development of small molecule modulators that could tether to Med25 and recapitulate these allosteric effects and thus act as regulators for the conformational changes that Med25 undergoes upon binding. This could lead to chemical probes that for example can dissect the role of ETV-Med25 PPIs in initiating and progressing metastatic breast cancers or other related diseases.[52] Chapter 1.3 Med25 AcID Utilizes Large and Flexible Binding Surfaces for Activator PPIs The previous examples of Med25-related activators all vary greatly in amino acid sequence, characteristics, as well as functional output. The mapped Med25-activator PPI sites that participate in various transient interactions cover a large surface area (**Figure 1.3A**) of each protein suggesting the absence of characteristic binding pockets which typically aid in traditional ligand

discovery techniques[53–57] While traditionally success has been made using protein-ligand NMR experiments [32–34,36] and computational docking experiments [58] in identifying the interaction surface of Med25 PPIs, currently there are no available crystal structures of Med25 AcID that would aid in identifying small molecule lead fragments to guide the rational design of therapeutic candidates and computational docking can only provide limited information if the fragment's binding site is unknown. These challenges have previously rendered dynamic transient protein interactions and their interaction surfaces as untargetable.[53,59]

Additionally, dynamic proteins tend to exist in varying degrees of disorder. (**Figure 1.3B**) As an example, in solution, both Med25 and ERM exist as floppy unstructured states[32,34] adding

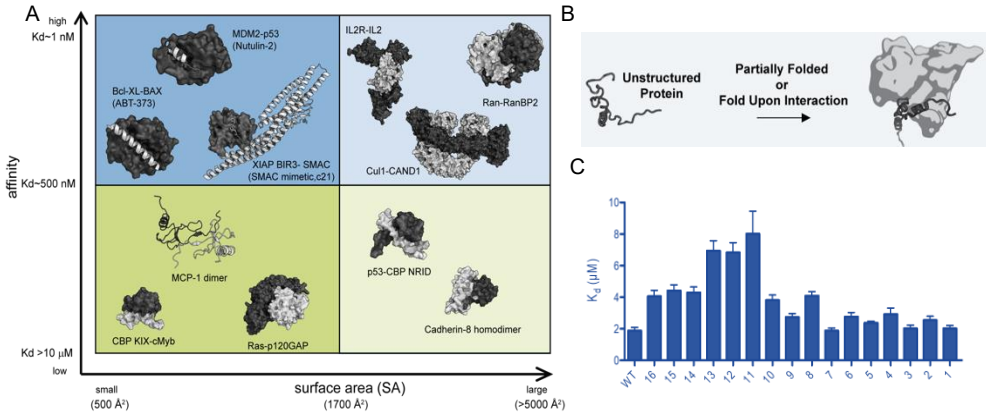

Figure 1.3 Challenges Targeting Dynamic Protein-Protein Interactions. ***(A)*** *Med25 is a dynamic coactivator with large and flexible surface areas and characteristic strong affinity binding interactions with related activators like the PPIs shown in the upper right corner.* ***(B)*** *A schematic of how mutations at different amino acid sites change the binding affinity (K_d) of an interaction.* ***(C)*** *Unstructured proteins or regions within proteins have been shown to gain a secondary structure upon binding to related partners.*[61–70]

to their difficulty to target. Protein NMR experiments combined with mutational analysis experiments have shown specific amino acid contacts that facilitate the binding interaction (**Figure 1.3C**) and that upon binding these two proteins transiently form secondary structures using specific key amino acid residues[36] indicating a conformational change that ultimately results in transcriptional activity.

Even though disparate activators use the same AcID binding surface for these interactions, it is hypothesized that each activator would promote the formation of unique conformations that would properly communicate the transcriptional signal to the cellular machinery. Since dynamic coactivators like Med25 utilize large and flexible binding surfaces instead of traditional pockets, the search for small molecule therapeutics has been rather challenging. This leaves the question of how can you possibly design a small organic molecule that selectively inhibits/enhances one of these Coactivator/Activator PPIs?[60–66,59,67–71]. For the regulation of related Med 25 related PPIs, I propose identifying small molecule modulators that recapitulate this transient structural change and therefore trap Med25 in specific conformations that would alter this protein's ability to bind to its endogenous activators and thus allow us to better understand the mechanistic underpinnings of transcriptional regulation.

Chapter 1.4 Identifying Small Molecule Scaffolds for Med25 AcID-PPI Modulation

Despite the challenges of targeting Med25 AcID, co-workers in the Mapp lab have had some success in the development of inhibitors of Med25-activator PPIs. For example, natural product screening led to the identification of depsides and depsidones as relevant inhibitors of Med25 PPIs likely by binding to one of Med25's flexible loops. Recently Dr. Garlick was able to show that the depsidone natural product Norstictic acid (**Scheme 1.1**) inhibits Med25 AcID-related PPIs **by covalently targeting a dynamic loop binding site and flanking one canonical binding surface allowing for both orthosteric and allosteric inhibition** [62,72] This added natural products to the repertoire of Med25 inhibitors, however natural products when isolated from naturally sources are typically obtained in low yields and are synthetically challenging to make limiting their therapeutic use.

Norstictic acid

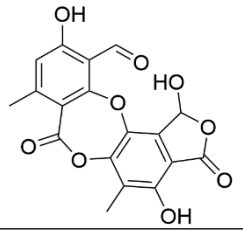

Scheme 1.1 ***Norstictic Acid***
The depsidone natural product ***norstictic acid*** *has been shown to interact with Med25 AcID's H2 face.*[80]

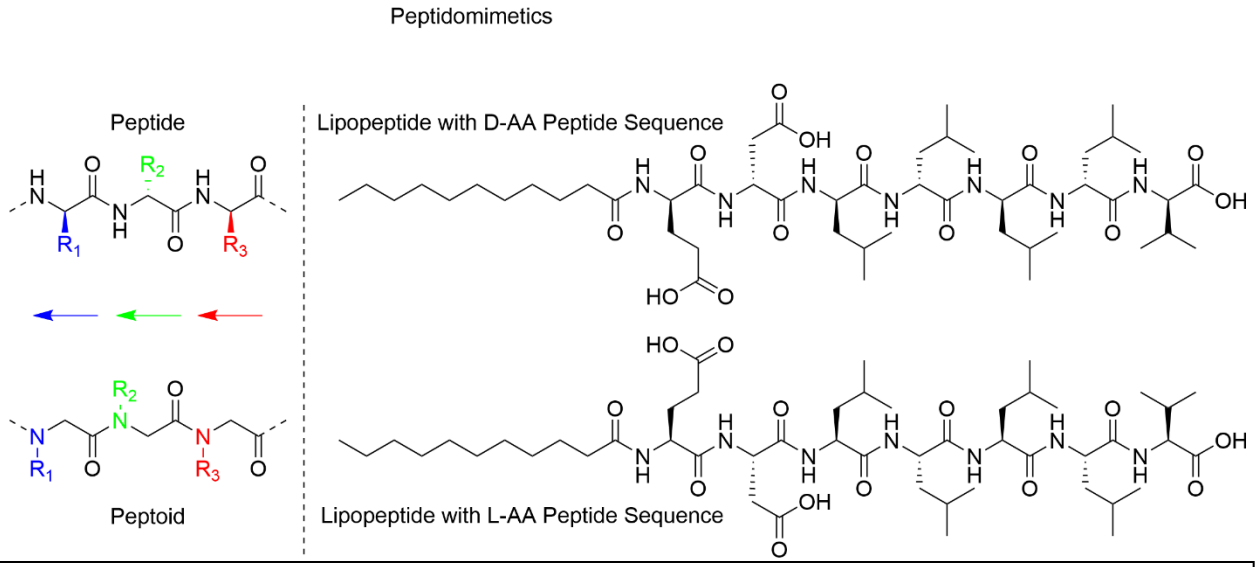

Scheme 1.2 Peptidomimetics towards the development of Med25 PPIs. *Peptidomimetics can be used to target dynamic coactivator proteins. A general schematic of peptoid based inhibitors.* [73] ***(left)*** *A sample lipopeptide sequence that targets Med25 AcID's H2 face.* [74] ***(right)*** *Both methods allow for the generation of large diverse libraries by utilizing SPPS.*

Peptidomimetics (**Scheme 1.2**) have also been developed to untwine the governing mechanism of Med25-related transcriptional activation such as Dr. Stanford's use of peptoids[73] and Dr. Patelli's use of Lipopeptide binders.[73,74] These methods can result in therapeutic leads and can be easily modified using standard solid phase peptide synthesis (SPPS), but these molecules be so large that they have trouble crossing cellular membranes and thus are not typically considered as drug candidates.

Taken together these studies have demonstrated the **targeting of the K519-521 loop** adjacent to the **H2 binding surface** within Med25 AcID is effective for both orthosteric and allosteric inhibition of Med25-activator PPIs. However, there are at least 2 additional dynamic substructures within Med25 AcID that we have not previously been able to engage with small molecules or peptidomimetics and thus need to use alternative discovery strategies to develop such probes.

Chapter1.5 Disulfide Tethering Screening the Wells Lab Disulfide Library

A promising technique to discover small organic molecules to act as inhibitors/enhancers is a site-directed ligand discovery method known as disulfide Tethering (**Figure 1.4**)[75,76] This technique can be used on any proteins either by using native cysteine residues or engineered cysteine residues. When the cysteines must be engineered, it is crucial that the cysteine(s) be solvent exposed and placed between 5-10 Å from the expected binding pocket or surface, as to ensure the small organic molecule reaches the binding surface.[75] Small molecule fragments with any affinity for the protein of interest (POI) can be identified through mass spectrometry (MS) analysis as small molecule-protein complexes Additionally, this technique can be used in a high throughput manner to rapidly identify small molecule binders or several molecules can be tested at once, so long as the fragments tested vary in molecular weight by about 5 Da, otherwise it can be difficult to interpret the MS readout as observed equilibrium complexes could have multiple identities. Fragments with higher affinity will display higher complex formation than weaker binders allowing for an additional method to rule out fragments. Disulfide Tethering **can be used**

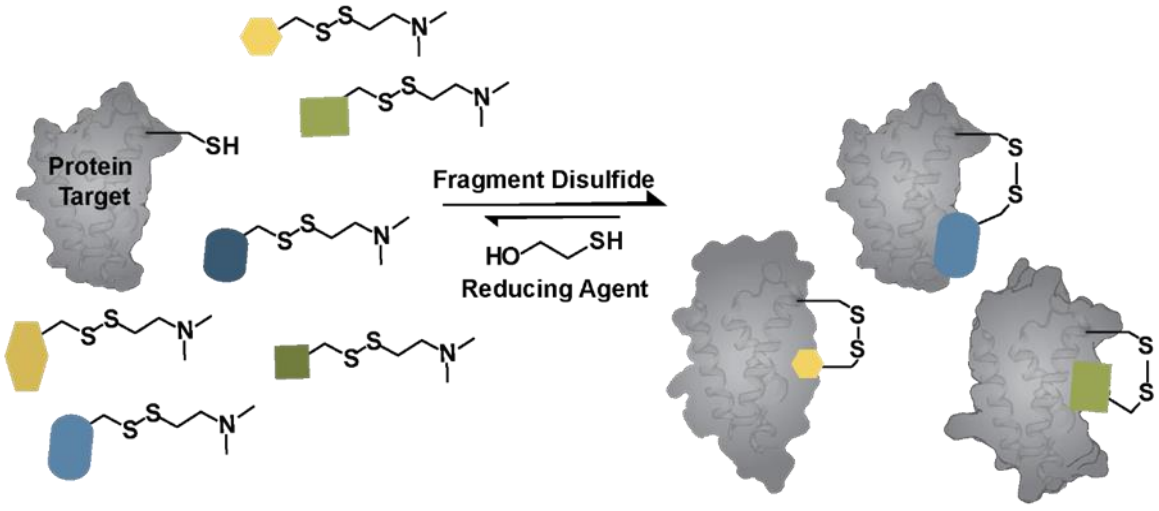

Figure 1.4 General Disulfide Tethering Schematic. *A general schematic of Site Directed Cysteine Disulfide Tethering. A protein target is incubated with a library of disulfide fragments. At equilibrium, small molecules with innate affinity for the protein of interest will form small molecule protein complexes that can be detected using q-Tof MS*[39,75,76]

to identify potential small molecules that can act as probes for dynamic PPIs; this was previously

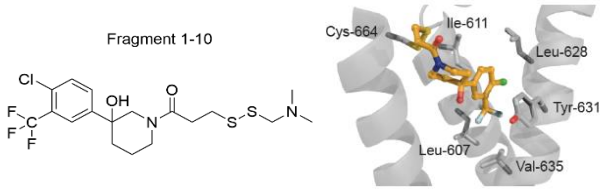

Scheme 1.3 Binding of Fragment 1-10 to KIX and First KIX Crystal Structure. *The structure of fragment* ***1-10*** *identified from a site-directed disulfide Tethering screen.*[75,77] ***(left)*** *The first crystal structure of CBPKIX-* ***1-10*** *bound.* ***PDB: 4I90 (right)***

demonstrated by the Mapp lab's successfully use of this technique to obtain the first crystal structure of ligand bound CBP KIX using fragment **1-10** (**Scheme 1.3**) from a Tethering screen.[75,77]

Chapter 1.5a Advantages of this technique:

Since Med25 AcID's allosterically connected binding sites are large and dynamic, it can be challenging to know where small molecules target AcID. This technique allows us to directly target Med25 AcID's H1 face resulting in site-specific small molecule probes that can bind with either or both of Med25's native cysteines (**C497**, **C506**). Because the fragments interact with AcID through a reversible, covalent disulfide bond, this method also allows for the identification of molecules with moderate-to-weak binding affinity, thus allowing for the identification of fragments that would normally be ruled out to be considered as starting points for designing therapeutic probes. Within the H1 face of AcID, **C506** rests on one its dynamic loops. It's been shown that Med25 uses its dynamic loops for allosteric regulation of its binding sites, so targeting **C506** with small molecules could lead to both orthosteric and allosteric regulation of Med25 PPIs.

Chapter 1.5b Previous uses of Disulfide Tethering:

Dynamic regions within proteins are typically viewed as untargetable. Nonetheless, the Mapp Lab has used disulfide Tethering to target dynamic transcriptional coactivators. After initial success with the CBP KIX domain, where a ligand-bound crystal structure was derived, they attempted a similar screen with Med25 AcID.[77] As noted earlier, Med25 has two solvent-exposed cysteines (**C497** and **C506**) readily available for Tethering experiments. Given that both cysteines

reside within the H1 binding surface of Med25 AcID, **C497** on the stable β-barrel core and **C506** on one of Med25 AcID's dynamic loops, it was hypothesized that these cysteines would be reactive enough for Tethering.[78] From the resulting screen 24 lead compounds that bound to Med25 AcID with equilibrium concentration values of at least 16% were identified, some of which were able to react at both cysteines shown in **Chapter 2** (**Scheme 2.4 and 2.5**). These results suggest that both cysteines on Med25 AcID are targetable to different extents. Additionally, both the CBP KIX and Med25 AcID Tethering studies highlight **how dynamic regions within proteins are indeed targetable and that targeting these dynamic regions may lead to the development of small molecule probes for Med25 AcID-related PPIs.** Recently our lab has performed follow up studies on the hits in this library.[78] For example, Compound **22 (Scheme 1.4)**, a fragment derived from a combination of naproxen and isonipecotic acid moieties, was bound to Med25 AcID and used transient kinetics to test the allosteric effect of the tethered compound. Here the K_{off} values were reduced by 25% suggesting Med25 AcID dissociates from VP16 or ATF6α faster than **22**-bound Med25 AcID.[39] This exemplifies that small molecules can recapitulate the allosteric communication between Med25's sites just as prebound activator ERM[36], and suggests the need to develop specific probes that capture significant protein conformations necessary for molecular recognition and gene transcription.

Fragment 22

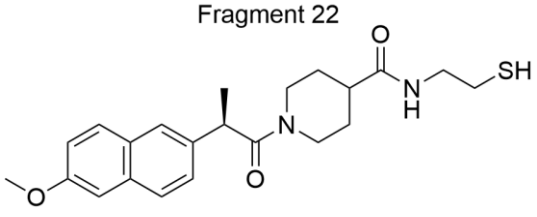

Scheme 1.4 Structure of Compound 22*. Compound **22** was identified from a 2017 Tethering screen against Med25 AcID.[39,78,79] It has been drawn without the disulfide tether to highlight the interacting fragment.*

Chapter 1.5c Disulfide Tethering as a screening tool for SAR

Disulfide Tethering permitted the investigation of small organic fragments with intrinsic binding affinity for Med25 AcID. Hits were defined as fragments that display a detectable equilibrium concentration greater than 15% termed the active set. Through a cheminformatics analysis of Med25 AcID's 2017 Tethering screening results carried out by Dr. Clint Regan, it was hypothesized that the certain sub-fragments within the active set of fragments may have enhanced binding activity towards Med25. Many fragments within the tethering library have similar structural features. For example, within the Hits described in **Chapter 2 Scheme 2.5**, Three out of the twenty-four hits contain a benzothiophene moiety, six contain a nipecotic or isonipecotic moiety, and all 24 contain aromatic regions. It is also significant to note that the benzothiophene moiety seems to be localized to the active set as there were only four total benzothiophene based fragments in the entire 1600 compound library, and three of them were hits, while the (R)-nipecotic or isonipecotic substructures, and aromatic fragments are ubiquitously seen within the entire library. Considering these observations, the benzothiophene fragment may have unique affinity for Med25 Acid. Thus, active compound **5** that was composed of both a benzothiophene and an isonipecotic acid moiety (**Scheme1.5**) was selected for further investigation and thus is the basis of this study investigating how each feature adds to the overall binding interaction. We decided to explore different structure activity relationships regarding the disulfide tail, the N-substitution, and stereochemistry and their role in fragment **5**'s ability to engage with Med25 AcID.

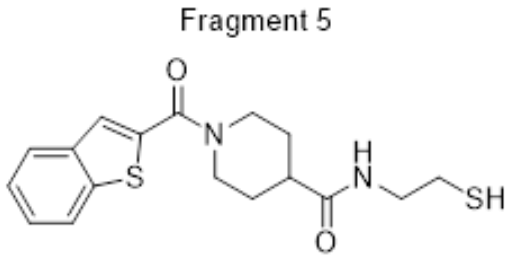

Scheme 1.5 Structure of Compound 5. *Compound **5** was identified from a 2017 Tethering screen against Med25 AcID.[1,2] This fragment and its components are the basis of this study. **5** is drawn without its disulfide tether to emphasize the fragment responsible for binding to AcID.*

Chapter 2 describes how I synthesized various disulfide sub-fragment analogues of **5** and performed single point Tethering (SPT) experiments against wtMed25 AcID at two different BME concentrations (1mM high stringency and 0.1mM low stringency). By comparing percentages of the equilibrium species detected using qTOFMS, we determined that both sub fragments play a role in compound **5** binding to Med25 AcID, and that the isonipecotic acid fragment is more than just a chemical spacer. We also demonstrate that the benzothiophene fragment alone is reactive enough to bind both of Med25 AcID solvent exposed cysteines and thus binds less specifically than either the iso-nipecotic acid fragment or the combined analogue **5**.

Chapter 1.5d Disadvantage of Using Reversible Fragments as Modulators

A major disadvantage of disulfide Tethering as a ligand discovery method is that reversible probes are limited to in vitro experiments as disulfide tethered fragments would be less stable in the cellular environment. Since these disulfide probes can be so easily reduced off the POIs, any activity observed cannot be directly correlated to small molecule binding.[79–83] To evaluate these different constructs as potential ligands of Med25 capable of inhibiting related PPIs and to increase the lifetime of these fragments for cellular experiments, reversible probes must be further functionalized into irreversible probes for used in cell-based studies.

Chapter 1.6 Alkylation Background:

Chapter 1.6a Irreversible Covalent Ligands:

Covalent ligands can be used to create small molecule probes to target proteins and their PPIs to better understand their mechanistic roles. Utilization of the Wells lab disulfide Tethering library resulted in the identification of reversible covalent ligands that target Med25 AcID. The newly formed covalent bond allows small organic fragments with moderate or weak affinity for

the protein to bind to the protein's binding surfaces. However, this bond can be easily reduced and thus renders this probe unusable within a cellular context due to its reducing nature of the chance for off target effects and toxicity.[80,82–86] **Chapter 3** begins with the synthesis of irreversible analogues of the compounds studied in **Chapter 2** that bind to Med25 AcID's solvent exposed cysteines through reversible tethering. Irreversible modulators were made by converting the disulfide tail necessary for reversible tethering into a thiol reactive electrophile capable of reacting to form irreversible bonds.

Irreversible ligands have gained popularity within the therapeutic world due to their ability to fully bind a POI, however, there still remains skepticism over the efficacy of using irreversible probes due to their off-target activity, lifetime within the cell, and toxicity.[87–91] Irreversible ligands can be developed through several different methods such as using amino acid R group activity to our advantage. There are several thiol reactive moieties which allow Cysteines to irreversibly bind with small organic molecules.[30,92–99] For example, Iodoacetamide, a known thiol reactive compound can singly label Med25 roughly 30%, and double labeling can be seen roughly 12% over two hours at various concentrations. (**Figure 3.4**) However, this small molecule is very reactive and generally used to probe cysteine reactivity for any POI. For **Chapter 3** we've chosen to use bromo acetyl bromide to transform the fragments explored in **Chapter 2** from reversible probes to irreversible probes.

Chapter 1.6b Assessing Thermostability:

Finally, we use the results from **Chapter 3** to compare whether irreversible fragment binding could lead to stabilization of the protein.[100,101] Differential scanning fluorimetry (DSF) (**Figure 1.5**) was used to assess whether the small molecules when complexed to Med25 AcID would alter wtMed25 AcID's melting temperature (T_m). This technique has been a powerful

screening tool for dynamic proteins as changes in thermostability can be detected even without knowledge of the binding sites. The melting temperature (T_m) of the protein is interpreted as the inflection point of the resulting melt curve.[102] While allosteric effects of small molecules cannot be determined using this method, their effect on protein stability can be determined. In a high throughput screen, molecules can be sorted by their ability to increase or decrease protein temperature. Combined with further binding studies allosteric inhibition can be inferred using modified tethering hits.

Chapter 1.7 Summary of Dissertation Findings:

In this Dissertation, we first selected compound **5** as a point of reference and synthesized disulfide analogs of the composite sub-fragments. Using SPT experiments, we evaluate the role that each substructure plays in binding to dynamic transcriptional coactivator Med25 AcID's H1 face. We hypothesized that the benzothiophene fragment would exhibit significant equilibrium tethering percentages, while the isonipecotic acid fragment may just act as a spacer that better positions relevant aromatic groups towards Med25 AcID for an enhanced reaction as other benzothiophene based probes also appeared within the active set of molecules but had lower equilibrium binding concentrations.

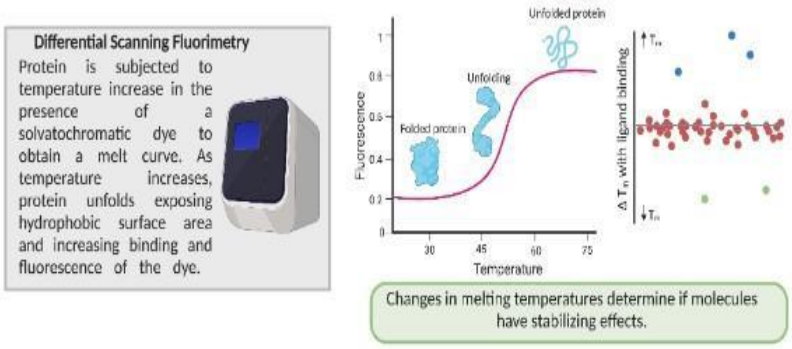

Figure 1.5 DSF to Assess Protein Stabilization. *Differential Scanning Fluorimetry (DSF) uses fluorophores to detect a protein's melting temperature (T_m) by binding hydrophobic regions on proteins that become exposed as the protein melts and unfolds. This method can be performed on ligand-bound proteins to assess stabilization through observed changes in T_m.*[100–103]

We then transform the reversible probes tested in **Chapter 2** into irreversible ligands using bromo acetyl bromide. We then utilize

Single Point Alkylation studies in comparison to iodoacetamide and BME alkylation, to evaluate the effects stereochemistry plays in ligand binding to AcID. After determining experimental conditions where at minimum 25% alkylation occurs these probes were incubated with Med25 AcID over 24 hours and DSF was performed on each complex to assess the thermostabilization resulting in the identification of 2 novel benzothiophene-based fragments that alter Med25 AcID's Tm greater than 3 standard deviations of the mean. It has been shown that binding ability of a fragment doesn't always correlate with inhibition or enhancement activity of other endogenous interactions.[39,78] For example, compound **22** was the 3rd worst binding fragment within the hits, yet it's capable of teasing out mechanistic details between Med25 and the Ets-related family of activators. Therefore, future work will be focused on exploring these benzothiophene-based probes with competitive binding studies such as Fluorescence Polarization (FP) to compare wtMed25 and small molecule-bound Med25's abilities to bind canonical binding partner. Since these molecules target the H1 face of Med25, any interference with Med25-ERM PPIs is a direct result of an orthosteric interaction, while interference with Med25-ATF6α would suggest an allosteric one. Assessment of the functional results of these experiments would facilitate the development of novel Med25 AcID-related transcriptional therapeutics.

Chapter 1.8 References

(1) Bajracharya, A.; Xi, J.; Grace, K. F.; Bayer, E. E.; Grant, C. A.; Clutton, C. H.; Baerson, S. R.; Agarwal, A. K.; Qiu, Y. PHYTOCHROME-INTERACTING FACTOR 4/HEMERA-Mediated Thermosensory Growth Requires the Mediator Subunit MED14. *Plant Physiol.* **2022**, *190* (4), 2706–2721. https://doi.org/10.1093/plphys/kiac412.

(2) Richter, W. F.; Nayak, S.; Iwasa, J.; Taatjes, D. J. The Mediator Complex as a Master Regulator of Transcription by RNA Polymerase II. *Nat. Rev. Mol. Cell Biol.* **2022**, *23* (11), 732–749. https://doi.org/10.1038/s41580-022-00498-3.

(3) Mao, X.; Weake, V. M.; Chapple, C. Mediator Function in Plant Metabolism Revealed by Large-Scale Biology. *J. Exp. Bot.* **2019**, *70* (21), 5995–6003. https://doi.org/10.1093/jxb/erz372.

(4) Napoli, C.; Schiano, C.; Soricelli, A. Increasing Evidence of Pathogenic Role of the Mediator (MED) Complex in the Development of Cardiovascular Diseases. *Biochimie* **2019**, *165*, 1–8. https://doi.org/10.1016/j.biochi.2019.06.014.

(5) Kazan, K. The Multitalented MEDIATOR25. *Front. Plant Sci.* **2017**, *8*.

(6) Xu, J.-Y.; Wu, L.; Shi, Z.; Zhang, X.-J.; Englert, N. A.; Zhang, S.-Y. Upregulation of Human *CYP2C9* Expression by Bisphenol A via Estrogen Receptor Alpha (ERα) and Med25: BPA Upregulates Human *CYP2C9* Expression Through ERα and Med25. *Environ. Toxicol.* **2017**, *32* (3), 970–978. https://doi.org/10.1002/tox.22297.

(7) Cánovas, V.; Lleonart, M.; Morote, J.; Paciucci, R. The Role of Prostate Tumor Overexpressed 1 in Cancer Progression. *Oncotarget* **2016**, *8* (7), 12451–12471. https://doi.org/10.18632/oncotarget.14104.

(8) Figueiredo, T.; Melo, U. S.; Pessoa, A. L. S.; Nobrega, P. R.; Kitajima, J. P.; Correa, I.; Zatz, M.; Kok, F.; Santos, S. Homozygous Missense Mutation in MED25 Segregates with Syndromic Intellectual Disability in a Large Consanguineous Family. *J. Med. Genet.* **2015**, *52* (2), 123–127. https://doi.org/10.1136/jmedgenet-2014-102793.

(9) Schiano, C.; Casamassimi, A.; Vietri, M. T.; Rienzo, M.; Napoli, C. The Roles of Mediator Complex in Cardiovascular Diseases. *Biochim. Biophys. Acta BBA - Gene Regul. Mech.* **2014**, *1839* (6), 444–451. https://doi.org/10.1016/j.bbagrm.2014.04.012.

(10) Zhu, Y.; Schluttenhoffer, C. M.; Wang, P.; Fu, F.; Thimmapuram, J.; Zhu, J.-K.; Lee, S. Y.; Yun, D.-J.; Mengiste, T. CYCLIN-DEPENDENT KINASE8 Differentially Regulates Plant Immunity to Fungal Pathogens through Kinase-Dependent and -Independent Functions in Arabidopsis. *Plant Cell* **2014**, *26* (10), 4149–4170.

(11) An, C.; Mou, Z. The Function of the Mediator Complex in Plant Immunity. *Plant Signal. Behav.* **2013**, *8* (3), e23182. https://doi.org/10.4161/psb.23182.

(12) Sela, D.; Conkright, J. J.; Chen, L.; Gilmore, J.; Washburn, M. P.; Florens, L.; Conaway, R. C.; Conaway, J. W. Role for Human Mediator Subunit MED25 in Recruitment of Mediator to Promoters by Endoplasmic Reticulum Stress-Responsive Transcription Factor ATF6α. *J. Biol. Chem.* **2013**, *288* (36), 26179–26187. https://doi.org/10.1074/jbc.M113.496968.

(13) Tazir, M.; Bellatache, M.; Nouioua, S.; Vallat, J.-M. Autosomal Recessive Charcot-Marie-Tooth Disease: From Genes to Phenotypes. *J. Peripher. Nerv. Syst.* **2013**, *18* (2), 113–129. https://doi.org/10.1111/jns5.12026.

(14) Han, E. H.; Rha, G. B.; Chi, Y.-I. MED25 Is a Mediator Component of HNF4α-Driven Transcription Leading to Insulin Secretion in Pancreatic Beta-Cells. *PLOS ONE* **2012**, *7* (8), e44007. https://doi.org/10.1371/journal.pone.0044007.

(15) Leal, A.; Huehne, K.; Bauer, F.; Sticht, H.; Berger, P.; Suter, U.; Morera, B.; Del Valle, G.; Lupski, J. R.; Ekici, A.; Pasutto, F.; Endele, S.; Barrantes, R.; Berghoff, C.; Berghoff, M.; Neundörfer, B.; Heuss, D.; Dorn, T.; Young, P.; Santolin, L.; Uhlmann, T.; Meisterernst, M.; Sereda, M.; Zu Horste, G. M.; Nave, K.-A.; Reis, A.; Rautenstrauss, B. Identification of the Variant Ala335Val of MED25 as Responsible for CMT2B2: Molecular Data, Functional Studies of the SH3 Recognition Motif and Correlation between Wild-Type MED25 and PMP22 RNA

Levels in CMT1A Animal Models. *neurogenetics* **2009**, *10* (4), 275–287. https://doi.org/10.1007/s10048-009-0183-3.

(16) Bäckström, S.; Elfving, N.; Nilsson, R.; Wingsle, G.; Björklund, S. Purification of a Plant Mediator from Arabidopsis Thaliana Identifies PFT1 as the Med25 Subunit. *Mol. Cell* **2007**, *26* (5), 717–729. https://doi.org/10.1016/j.molcel.2007.05.007.

(17) Takagi, Y.; Kornberg, R. D. Mediator as a General Transcription Factor. *J. Biol. Chem.* **2006**, *281* (1), 80–89. https://doi.org/10.1074/jbc.M508253200.

(18) Myers, L. C.; Kornberg, R. D. Mediator of Transcriptional Regulation. *Annu. Rev. Biochem.* **2000**, *69* (1), 729–749. https://doi.org/10.1146/annurev.biochem.69.1.729.

(19) Tomomori-Sato, C.; Sato, S.; Parmely, T. J.; Banks, C. A. S.; Sorokina, I.; Florens, L.; Zybailov, B.; Washburn, M. P.; Brower, C. S.; Conaway, R. C.; Conaway, J. W. A Mammalian Mediator Subunit That Shares Properties with Saccharomyces Cerevisiae Mediator Subunit Cse2*. *J. Biol. Chem.* **2004**, *279* (7), 5846–5851. https://doi.org/10.1074/jbc.M312523200.

(20) Luo, D.; Sun, W.; Cai, J.; Hu, G.; Zhang, D.; Zhang, X.; Larkin, R. M.; Zhang, J.; Yang, C.; Ye, Z.; Wang, T. SlBBX20 Attenuates JA Signalling and Regulates Resistance to *Botrytis Cinerea* by Inhibiting SlMED25 in Tomato. *Plant Biotechnol. J.* **2023**, *21* (4), 792–805. https://doi.org/10.1111/pbi.13997.

(21) Saunders, J.; Sikder, K.; Phillips, E.; Ishwar, A.; Mothy, D.; Margulies, K. B.; Choi, J. C. Med25 Limits Master Regulators That Govern Adipogenesis. *Int. J. Mol. Sci.* **2023**, *24* (7), 6155. https://doi.org/10.3390/ijms24076155.

(22) Rovnak, J.; Quackenbush, S. L. Exploitation of the Mediator Complex by Viruses. *PLOS Pathog.* **2022**, *18* (4), e1010422. https://doi.org/10.1371/journal.ppat.1010422.

(23) Wang, H.; Li, S.; Li, Y.; Xu, Y.; Wang, Y.; Zhang, R.; Sun, W.; Chen, Q.; Wang, X.; Li, C.; Zhao, J. MED25 Connects Enhancer–Promoter Looping and MYC2-Dependent Activation of Jasmonate Signalling. *Nat. Plants* **2019**, *5* (6), 616–625. https://doi.org/10.1038/s41477-019-0441-9.

(24) Zhai, Q.; Li, L.; An, C.; Li, C. Conserved Function of Mediator in Regulating Nuclear Hormone Receptor Activation between Plants and Animals. *Plant Signal. Behav.* **2018**, *13* (5), e1403709. https://doi.org/10.1080/15592324.2017.1403709.

(25) Liu, J.; Zhang, T.; Jia, J.; Sun, J. The Wheat Mediator Subunit TaMED25 Interacts with the Transcription Factor TaEIL1 to Negatively Regulate Disease Resistance against Powdery Mildew. *Plant Physiol.* **2016**, *170* (3), 1799–1816.

(26) Wang, C.; Du, X.; Mou, Z. The Mediator Complex Subunits MED14, MED15, and MED16 Are Involved in Defense Signaling Crosstalk in Arabidopsis. *Front. Plant Sci.* **2016**, *7*. https://doi.org/10.3389/fpls.2016.01947.

(27) Aguilar, X.; Blomberg, J.; Brännström, K.; Olofsson, A.; Schleucher, J.; Björklund, S. Interaction Studies of the Human and Arabidopsis Thaliana Med25-ACID Proteins with the Herpes Simplex Virus VP16- and Plant-Specific Dreb2a Transcription Factors. *PLoS ONE* **2014**, *9* (5), e98575. https://doi.org/10.1371/journal.pone.0098575.

(28) Borggrefe, T.; Yue, X. Interactions between Subunits of the Mediator Complex with Gene-Specific Transcription Factors. *Semin. Cell Dev. Biol.* **2011**, *22* (7), 759–768. https://doi.org/10.1016/j.semcdb.2011.07.022.

(29) Nakamura, Y.; Yamamoto, K.; He, X.; Otsuki, B.; Kim, Y.; Murao, H.; Soeda, T.; Tsumaki, N.; Deng, J. M.; Zhang, Z.; Behringer, R. R.; Crombrugghe, B. D.; Postlethwait, J. H.; Warman, M. L.; Nakamura, T.; Akiyama, H. Wwp2 Is Essential for Palatogenesis Mediated by the Interaction between Sox9 and Mediator Subunit 25. *Nat. Commun.* **2011**, *2* (1), 251. https://doi.org/10.1038/ncomms1242.

(30) Rana, R.; Surapureddi, S.; Kam, W.; Ferguson, S.; Goldstein, J. A. Med25 Is Required for RNA Polymerase II Recruitment to Specific Promoters, Thus Regulating Xenobiotic and Lipid Metabolism in Human Liver. *Mol. Cell. Biol.* **2011**, *31* (3), 466–481. https://doi.org/10.1128/MCB.00847-10.

(31) Yang, M.; Hay, J.; Ruyechan, W. T. Varicella-Zoster Virus IE62 Protein Utilizes the Human Mediator Complex in Promoter Activation. *J. Virol.* **2008**, *82* (24), 12154–12163. https://doi.org/10.1128/JVI.01693-08.

(32) Eletsky, A.; Ruyechan, W. T.; Xiao, R.; Acton, T. B.; Montelione, G. T.; Szyperski, T. Solution NMR Structure of MED25(391–543) Comprising the Activator-Interacting Domain (ACID) of Human Mediator Subunit 25. *J. Struct. Funct. Genomics* **2011**, *12* (3), 159–166. https://doi.org/10.1007/s10969-011-9115-1.

(33) Bontems, F.; Verger, A.; Dewitte, F.; Lens, Z.; Baert, J.-L.; Ferreira, E.; Launoit, Y. de; Sizun, C.; Guittet, E.; Villeret, V.; Monté, D. NMR Structure of the Human Mediator MED25 ACID Domain. *J. Struct. Biol.* **2011**, *174* (1), 245–251. https://doi.org/10.1016/j.jsb.2010.10.011.

(34) Vojnic, E.; Mourão, A.; Seizl, M.; Simon, B.; Wenzeck, L.; Larivière, L.; Baumli, S.; Baumgart, K.; Meisterernst, M.; Sattler, M.; Cramer, P. Structure and VP16 Binding of the Mediator Med25 Activator Interaction Domain. *Nat. Struct. Mol. Biol.* **2011**, *18* (4), 404–409. https://doi.org/10.1038/nsmb.1997.

(35) Lee, H.-K.; Park, U.-H.; Kim, E.-J.; Um, S.-J. MED25 Is Distinct from TRAP220/MED1 in Cooperating with CBP for Retinoid Receptor Activation. *EMBO J.* **2007**, *26* (15), 3545–3557. https://doi.org/10.1038/sj.emboj.7601797.

(36) Landrieu, I.; Verger, A.; Baert, J.-L.; Rucktooa, P.; Cantrelle, F.-X.; Dewitte, F.; Ferreira, E.; Lens, Z.; Villeret, V.; Monté, D. Characterization of ERM Transactivation Domain Binding to the ACID/PTOV Domain of the Mediator Subunit MED25. *Nucleic Acids Res.* **2015**, *43* (14), 7110–7121. https://doi.org/10.1093/nar/gkv650.

(37) Verger, A.; Baert, J.-L.; Verreman, K.; Dewitte, F.; Ferreira, E.; Lens, Z.; De Launoit, Y.; Villeret, V.; Monté, D. The Mediator Complex Subunit MED25 Is Targeted by the N-Terminal Transactivation Domain of the PEA3 Group Members. *Nucleic Acids Res.* **2013**, *41* (9), 4847–4859. https://doi.org/10.1093/nar/gkt199.

(38) Haze, K.; Yoshida, H.; Yanagi, H.; Yura, T.; Mori, K. Mammalian Transcription Factor ATF6 Is Synthesized as a Transmembrane Protein and Activated by Proteolysis in Response to Endoplasmic Reticulum Stress. *Mol. Biol. Cell* **1999**, *10* (11), 3787–3799. https://doi.org/10.1091/mbc.10.11.3787.

(39) Henderson, A. R.; Henley, M. J.; Foster, N. J.; Peiffer, A. L.; Beyersdorf, M. S.; Stanford, K. D.; Sturlis, S. M.; Linhares, B. M.; Hill, Z. B.; Wells, J. A.; Cierpicki, T.; Brooks, C. L.; Fierke, C. A.; Mapp, A. K. Conservation of Coactivator Engagement Mechanism Enables Small-Molecule Allosteric Modulators. *Proc. Natl. Acad. Sci.* **2018**, *115* (36), 8960–8965. https://doi.org/10.1073/pnas.1806202115.

(40) Dong, J.; Basse, V.; Bierre, M.; Peres de Oliveira, A.; Vidalain, P.-O.; Sibille, P.; Tangy, F.; Galloux, M.; Eleouet, J.-F.; Sizun, C.; Bajorek, M. Respiratory Syncytial Virus NS1 Protein Targets the Transactivator Binding Domain of MED25. *J. Mol. Biol.* **2022**, *434* (19), 167763. https://doi.org/10.1016/j.jmb.2022.167763.

(41) Van Royen, T.; Sedeyn, K.; Moschonas, G. D.; Toussaint, W.; Vuylsteke, M.; Van Haver, D.; Impens, F.; Eyckerman, S.; Lemmens, I.; Tavernier, J.; Schepens, B.; Saelens, X. An Unexpected Encounter: Respiratory Syncytial Virus Nonstructural Protein 1 Interacts with Mediator Subunit MED25. *J. Virol.* **2022**, *96* (19), e01297-22. https://doi.org/10.1128/jvi.01297-22.

(42) Nomoto, M.; Skelly, M. J.; Itaya, T.; Mori, T.; Suzuki, T.; Matsushita, T.; Tokizawa, M.; Kuwata, K.; Mori, H.; Yamamoto, Y. Y.; Higashiyama, T.; Tsukagoshi, H.; Spoel, S. H.; Tada, Y. Suppression of MYC Transcription Activators by the Immune Cofactor NPR1 Fine-Tunes Plant Immune Responses. *Cell Rep.* **2021**, *37* (11), 110125. https://doi.org/10.1016/j.celrep.2021.110125.

(43) Ueda, T.; Tamura, T.; Kawano, M.; Shiono, K.; Hobor, F.; Wilson, A. J.; Hamachi, I. Enhanced Suppression of a Protein–Protein Interaction in Cells Using Small-Molecule Covalent Inhibitors Based on an *N* -Acyl- *N* -Alkyl Sulfonamide Warhead. *J. Am. Chem. Soc.* **2021**, *143* (12), 4766–4774. https://doi.org/10.1021/jacs.1c00703.

(44) Zhai, Q.; Li, C. The Plant Mediator Complex and Its Role in Jasmonate Signaling. *J. Exp. Bot.* **2019**, *70* (13), 3415–3424. https://doi.org/10.1093/jxb/erz233.

(45) Lee, M.-S.; Lim, K.; Lee, M.-K.; Chi, S.-W. Structural Basis for the Interaction between P53 Transactivation Domain and the Mediator Subunit MED25. *Molecules* **2018**, *23* (10), 2726. https://doi.org/10.3390/molecules23102726.

(46) Li, X.; Yang, R.; Chen, H. The Arabidopsis Thaliana Mediator Subunit MED8 Regulates Plant Immunity to Botrytis Cinerea through Interacting with the Basic Helix-Loop-Helix (BHLH) Transcription Factor FAMA. *PLOS ONE* **2018**, *13* (3), e0193458. https://doi.org/10.1371/journal.pone.0193458.

(47) Xie, F.; Li, B. X.; Kassenbrock, A.; Xue, C.; Wang, X.; Qian, D. Z.; Sears, R. C.; Xiao, X. Identification of a Potent Inhibitor of CREB-Mediated Gene Transcription with Efficacious in Vivo Anticancer Activity. *J. Med. Chem.* **2015**, *58* (12), 5075–5087. https://doi.org/10.1021/acs.jmedchem.5b00468.

(48) Shi, Z.; Yang, W.; Goldstein, J. A.; Zhang, S.-Y. Med25 Is Required for Estrogen Receptor Alpha (ERα)-Mediated Regulation of Human CYP2C9 Expression. *Biochem. Pharmacol.* **2014**, *90* (4), 425–431. https://doi.org/10.1016/j.bcp.2014.06.016.

(49) Kazan, K.; Manners, J. M. MYC2: The Master in Action. *Mol. Plant* **2013**, *6* (3), 686–703. https://doi.org/10.1093/mp/sss128.

(50) Ou, B.; Yin, K.-Q.; Liu, S.-N.; Yang, Y.; Gu, T.; Wing Hui, J. M.; Zhang, L.; Miao, J.; Kondou, Y.; Matsui, M.; Gu, H.-Y.; Qu, L.-J. A High-Throughput Screening System for Arabidopsis Transcription Factors and Its Application to Med25-Dependent Transcriptional Regulation. *Mol. Plant* **2011**, *4* (3), 546–555. https://doi.org/10.1093/mp/ssr002.

(51) Yamamoto, S.; Eletsky, A.; Szyperski, T.; Hay, J.; Ruyechan, W. T. Analysis of the Varicella-Zoster Virus IE62 N-Terminal Acidic Transactivating Domain and Its Interaction with the Human Mediator Complex. *J. Virol.* **2009**, *83* (12), 6300–6305. https://doi.org/10.1128/JVI.00054-09.

(52) Currie, S. L.; Doane, J. J.; Evans, K. S.; Bhachech, N.; Madison, B. J.; Lau, D. K. W.; McIntosh, L. P.; Skalicky, J. J.; Clark, K. A.; Graves, B. J. ETV4 and AP1 Transcription Factors Form Multivalent Interactions with Three Sites on the MED25 Activator-Interacting Domain. *J. Mol. Biol.* **2017**, *429* (20), 2975–2995. https://doi.org/10.1016/j.jmb.2017.06.024.

(53) Cesa, L. C.; Mapp, A. K.; Gestwicki, J. E. Direct and Propagated Effects of Small Molecules on Protein–Protein Interaction Networks. *Front. Bioeng. Biotechnol.* **2015**, *3*. https://doi.org/10.3389/fbioe.2015.00119.

(54) Pirintsos, S.; Panagiotopoulos, A.; Bariotakis, M.; Daskalakis, V.; Lionis, C.; Sourvinos, G.; Karakasiliotis, I.; Kampa, M.; Castanas, E. From Traditional Ethnopharmacology to Modern Natural Drug Discovery: A Methodology Discussion and Specific Examples. *Mol. Basel Switz.* **2022**, *27* (13), 4060. https://doi.org/10.3390/molecules27134060.

(55) Atanasov, A. G.; Zotchev, S. B.; Dirsch, V. M.; Supuran, C. T. Natural Products in Drug Discovery: Advances and Opportunities. *Nat. Rev. Drug Discov.* **2021**, *20* (3), 200–216. https://doi.org/10.1038/s41573-020-00114-z.

(56) Zhang, L.; Song, J.; Kong, L.; Yuan, T.; Li, W.; Zhang, W.; Hou, B.; Lu, Y.; Du, G. The Strategies and Techniques of Drug Discovery from Natural Products. *Pharmacol. Ther.* **2020**, *216*, 107686. https://doi.org/10.1016/j.pharmthera.2020.107686.

(57) Lage, O. M.; Ramos, M. C.; Calisto, R.; Almeida, E.; Vasconcelos, V.; Vicente, F. Current Screening Methodologies in Drug Discovery for Selected Human Diseases. *Mar. Drugs* **2018**, *16* (8), 279. https://doi.org/10.3390/md16080279.

(58) Jeffery, H. M.; Weinzierl, R. O. J. Multivalent and Bidirectional Binding of Transcriptional Transactivation Domains to the MED25 Coactivator. *Biomolecules* **2020**, *10* (9), 1205. https://doi.org/10.3390/biom10091205.

(59) Mapp, A. K.; Pricer, R.; Sturlis, S. Targeting Transcription Is No Longer a Quixotic Quest. *Nat. Chem. Biol.* **2015**, *11* (12), 891–894. https://doi.org/10.1038/nchembio.1962.

(60) Kenanova, D. N.; Visser, E. J.; Virta, J. M.; Sijbesma, E.; Centorrino, F.; Vickery, H. R.; Zhong, M.; Neitz, R. J.; Brunsveld, L.; Ottmann, C.; Arkin, M. R. A Systematic Approach to the Discovery of Protein–Protein Interaction Stabilizers. *ACS Cent. Sci.* **2023**. https://doi.org/10.1021/acscentsci.2c01449.

(61) Henley, M. J.; Koehler, A. N. Advances in Targeting 'Undruggable' Transcription Factors with Small Molecules. *Nat. Rev. Drug Discov.* **2021**, *20* (9), 669–688. https://doi.org/10.1038/s41573-021-00199-0.

(62) Garlick, J. M.; Mapp, A. K. Selective Modulation of Dynamic Protein Complexes. *Cell Chem. Biol.* **2020**, *27* (8), 986–997. https://doi.org/10.1016/j.chembiol.2020.07.019.

(63) Choi, S.; Choi, K.-Y. Screening-Based Approaches to Identify Small Molecules That Inhibit Protein–Protein Interactions. *Expert Opin. Drug Discov.* **2017**, *12* (3), 293–303. https://doi.org/10.1080/17460441.2017.1280456.

(64) Pricer, R.; Gestwicki, J. E.; Mapp, A. K. From Fuzzy to Function: The New Frontier of Protein–Protein Interactions. *Acc. Chem. Res.* **2017**, *50* (3), 584–589. https://doi.org/10.1021/acs.accounts.6b00565.

(65) Modell, A. E.; Blosser, S. L.; Arora, P. S. Systematic Targeting of Protein–Protein Interactions. *Trends Pharmacol. Sci.* **2016**, *37* (8), 702–713. https://doi.org/10.1016/j.tips.2016.05.008.

(66) Boutureira, O.; Bernardes, G. J. L. Advances in Chemical Protein Modification. *Chem. Rev.* **2015**, *115* (5), 2174–2195. https://doi.org/10.1021/cr500399p.

(67) Jin, L.; Wang, W.; Fang, G. Targeting Protein-Protein Interaction by Small Molecules. *Annu. Rev. Pharmacol. Toxicol.* **2014**, *54* (1), 435–456. https://doi.org/10.1146/annurev-pharmtox-011613-140028.

(68) Thompson, A. D.; Dugan, A.; Gestwicki, J. E.; Mapp, A. K. Fine-Tuning Multiprotein Complexes Using Small Molecules. *ACS Chem. Biol.* **2012**, *7* (8), 1311–1320. https://doi.org/10.1021/cb300255p.

(69) Schulz, M. N.; Hubbard, R. E. Recent Progress in Fragment-Based Lead Discovery. *Curr. Opin. Pharmacol.* **2009**, *9* (5), 615–621. https://doi.org/10.1016/j.coph.2009.04.009.

(70) Sturlis, S. M. Targeting the Activator Interaction Domain of Mediator Subunit Med25.

(71) Henley, M. Mechanistic Analysis of Dynamic Transcriptional Protein- Protein Interactions.

(72) Garlick, J. M.; Sturlis, S. M.; Bruno, P. A.; Yates, J. A.; Peiffer, A. L.; Liu, Y.; Goo, L.; Bao, L.; De Salle, S. N.; Tamayo-Castillo, G.; Brooks, C. L.; Merajver, S. D.; Mapp, A. K. Norstictic Acid Is a Selective Allosteric Transcriptional Regulator. *J. Am. Chem. Soc.* **2021**, *143* (25), 9297–9302. https://doi.org/10.1021/jacs.1c03258.

(73) Stanford, K. D. Using Peptidomimetics to Dissect Activator-Coactivator Protein-Protein Interactions.

(74) Pattelli, O. N.; Valdivia, E. M.; Beyersdorf, M. S.; Regan, C. S.; Rivas, M.; Merajver, S. D.; Cierpicki, T.; Mapp, A. K. *A Lipopeptidomimetic of Transcriptional Activation Domains Selectively Disrupts Med25 PPIs*; preprint; Biochemistry, 2023. https://doi.org/10.1101/2023.03.24.534168.

(75) Erlanson, D. A.; Braisted, A. C.; Raphael, D. R.; Randal, M.; Stroud, R. M.; Gordon, E. M.; Wells, J. A. Site-Directed Ligand Discovery. *Proc. Natl. Acad. Sci.* **2000**, *97* (17), 9367–9372. https://doi.org/10.1073/pnas.97.17.9367.

(76) Erlanson, D. A.; Hansen, S. K. Making Drugs on Proteins: Site-Directed Ligand Discovery for Fragment-Based Lead Assembly. *Curr. Opin. Chem. Biol.* **2004**, *8* (4), 399–406. https://doi.org/10.1016/j.cbpa.2004.06.010.

(77) Wang, N.; Majmudar, C. Y.; Pomerantz, W. C.; Gagnon, J. K.; Sadowsky, J. D.; Meagher, J. L.; Johnson, T. K.; Stuckey, J. A.; Brooks, C. L. I.; Wells, J. A.; Mapp, A. K. Ordering a Dynamic Protein Via a Small-Molecule Stabilizer. *J. Am. Chem. Soc.* **2013**, *135* (9), 3363–3366. https://doi.org/10.1021/ja3122334.

(78) Henderson, A. R. Dissecting Transcriptional Coactivator Binding Networks To Enable Small Molecule Modulation.

(79) Prins, L. J.; Scrimin, P. Covalent Capture: Merging Covalent and Noncovalent Synthesis. *Angew. Chem. Int. Ed.* **2009**, *48* (13), 2288–2306. https://doi.org/10.1002/anie.200803583.

(80) Schürmann, M.; Janning, P.; Ziegler, S.; Waldmann, H. Small-Molecule Target Engagement in Cells. *Cell Chem. Biol.* **2016**, *23* (4), 435–441. https://doi.org/10.1016/j.chembiol.2016.03.008.

(81) Wang, J.; Li, H.; Xu, B. Biological Functions of Supramolecular Assemblies of Small Molecules in the Cellular Environment. *RSC Chem. Biol. 2* (2), 289–305. https://doi.org/10.1039/d0cb00219d.

(82) Zuo, X.; Zhao, Y.; Zhao, J.; Ouyang, Y.; Qian, W.; Hou, Y.; Yu, C.; Ren, X.; Zou, L.; Fang, J.; Lu, J. A Fluorescent Probe for Specifically Measuring the Overall Thioredoxin and Glutaredoxin Reducing Activity in Bacterial Cells. *The Analyst* **2022**, *147* (5), 834–840. https://doi.org/10.1039/D1AN01644J.

(83) Felber, J. G.; Zeisel, L.; Poczka, L.; Scholzen, K.; Busker, S.; Maier, M. S.; Theisen, U.; Brandstädter, C.; Becker, K.; Arnér, E. S. J.; Thorn-Seshold, J.; Thorn-Seshold, O. Selective, Modular Probes for Thioredoxins Enabled by Rational Tuning of a Unique Disulfide Structure Motif. *J. Am. Chem. Soc.* **2021**, *143* (23), 8791–8803. https://doi.org/10.1021/jacs.1c03234.

(84) Wang, M. O.; Piard, C. M.; Melchiorri, A.; Dreher, M. L.; Fisher, J. P. Evaluating Changes in Structure and Cytotoxicity during in Vitro Degradation of Three-Dimensional Printed Scaffolds. *Tissue Eng. Part A* **2015**, *21* (9–10), 1642–1653. https://doi.org/10.1089/ten.TEA.2014.0495.

(85) Bruns, R. F.; Watson, I. A. Rules for Identifying Potentially Reactive or Promiscuous Compounds. *J. Med. Chem.* **2012**, *55* (22), 9763–9772. https://doi.org/10.1021/jm301008n.

(86) Atkins, W. M. Biological Messiness vs. Biological Genius: Mechanistic Aspects and Roles of Protein Promiscuity. *J. Steroid Biochem. Mol. Biol.* **2015**, *151*, 3–11. https://doi.org/10.1016/j.jsbmb.2014.09.010.

(87) Gambini, L.; Baggio, C.; Udompholkul, P.; Jossart, J.; Salem, A. F.; Perry, J. J. P.; Pellecchia, M. Covalent Inhibitors of Protein–Protein Interactions Targeting Lysine, Tyrosine, or Histidine Residues. *J. Med. Chem.* **2019**, *62* (11), 5616–5627. https://doi.org/10.1021/acs.jmedchem.9b00561.

(88) Zheng, M.; Chen, F.-J.; Li, K.; Reja, R. M.; Haeffner, F.; Gao, J. Lysine-Targeted Reversible Covalent Ligand Discovery for Proteins via Phage Display. *J. Am. Chem. Soc.* **2022**, *144* (34), 15885–15893. https://doi.org/10.1021/jacs.2c07375.

(89) Berka, K.; Laskowski, R.; Riley, K. E.; Hobza, P.; Vondrášek, J. Representative Amino Acid Side Chain Interactions in Proteins. A Comparison of Highly Accurate Correlated Ab Initio Quantum Chemical and Empirical Potential Procedures. *J. Chem. Theory Comput.* **2009**, *5* (4), 982–992. https://doi.org/10.1021/ct800508v.

(90) Bischoff, R.; Schlüter, H. Amino Acids: Chemistry, Functionality and Selected Non-Enzymatic Post-Translational Modifications. *J. Proteomics* **2012**, *75* (8), 2275–2296. https://doi.org/10.1016/j.jprot.2012.01.041.

(91) Uranga, J.; Mujika, J. I.; Grande-Aztatzi, R.; Matxain, J. M. Oxidation of Acid, Base, and Amide Side-Chain Amino Acid Derivatives via Hydroxyl Radical. *J. Phys. Chem. B* **2018**, *122* (19), 4956–4971. https://doi.org/10.1021/acs.jpcb.7b12450.

(92) Allen, C. E.; Curran, P. R.; Brearley, A. S.; Boissel, V.; Sviridenko, L.; Press, N. J.; Stonehouse, J. P.; Armstrong, A. Efficient and Facile Synthesis of Acrylamide Libraries for Protein-Guided Tethering. *Org. Lett.* **2015**, *17* (3), 458–460. https://doi.org/10.1021/ol503486t.

(93) Orita, M.; Ohno, K.; Niimi, T. Two "Golden Ratio" Indices in Fragment-Based Drug Discovery. *Drug Discov. Today* **2009**, *14* (5–6), 321–328. https://doi.org/10.1016/j.drudis.2008.10.006.

(94) Wolter, M.; Valenti, D.; Cossar, P. J.; Levy, L. M.; Hristeva, S.; Genski, T.; Hoffmann, T.; Brunsveld, L.; Tzalis, D.; Ottmann, C. Fragment-Based Stabilizers of Protein–Protein Interactions through Imine-Based Tethering. *Angew. Chem. Int. Ed.* **2020**, *59* (48), 21520–21524. https://doi.org/10.1002/anie.202008585.

(95) Ibarra, A. A.; Bartlett, G. J.; Hegedüs, Z.; Dutt, S.; Hobor, F.; Horner, K. A.; Hetherington, K.; Spence, K.; Nelson, A.; Edwards, T. A.; Woolfson, D. N.; Sessions, R. B.; Wilson, A. J. Predicting and Experimentally Validating Hot-Spot Residues at Protein–Protein Interfaces. *ACS Chem. Biol.* **2019**, acschembio.9b00560. https://doi.org/10.1021/acschembio.9b00560.

(96) Gentile, D. R.; Rathinaswamy, M. K.; Jenkins, M. L.; Moss, S. M.; Siempelkamp, B. D.; Renslo, A. R.; Burke, J. E.; Shokat, K. M. Ras Binder Induces a Modified Switch-II Pocket in GTP and GDP States. *Cell Chem. Biol.* **2017**, *24* (12), 1455-1466.e14. https://doi.org/10.1016/j.chembiol.2017.08.025.

(97) Doak, B. C.; Norton, R. S.; Scanlon, M. J. The Ways and Means of Fragment-Based Drug Design. *Pharmacol. Ther.* **2016**, *167*, 28–37. https://doi.org/10.1016/j.pharmthera.2016.07.003.

(98) Corbi-Verge, C.; Kim, P. M. Motif Mediated Protein-Protein Interactions as Drug Targets. *Cell Commun. Signal.* **2016**, *14* (1), 8. https://doi.org/10.1186/s12964-016-0131-4.

(99) Cheng, S.-S.; Yang, G.-J.; Wang, W.; Leung, C.-H.; Ma, D.-L. The Design and Development of Covalent Protein-Protein Interaction Inhibitors for Cancer Treatment. *J. Hematol. Oncol.J Hematol Oncol* **2020**, *13* (1), 26. https://doi.org/10.1186/s13045-020-00850-0.

(100) Gao, K.; Oerlemans, R.; Groves, M. R. Theory and Applications of Differential Scanning Fluorimetry in Early-Stage Drug Discovery. *Biophys. Rev.* **2020**, *12* (1), 85–104. https://doi.org/10.1007/s12551-020-00619-2.

(101) Senisterra, G. A.; Finerty, P. J. High Throughput Methods of Assessing Protein Stability and Aggregation. *Mol. Biosyst.* **2009**, *5* (3), 217–223. https://doi.org/10.1039/b814377c.

(102) Niesen, F. H.; Berglund, H.; Vedadi, M. The Use of Differential Scanning Fluorimetry to Detect Ligand Interactions That Promote Protein Stability. *Nat. Protoc.* **2007**, *2* (9), 2212–2221. https://doi.org/10.1038/nprot.2007.321.

CHAPTER II Investigating the Role of Nipecotic Acid-based Fragments and Benzothiophene-based Fragments as Reversible Covalent Probes of Med25 AcID

Chapter2.1 Abstract

Identifying small molecule probes for dynamic coactivators has been a challenging and important goal for dissecting the role of coactivator protein-protein interactions (PPIs) in disease. The Mapp lab in conjunction with the Wells lab **have demonstrated how site-directed ligand discovery can be utilized for targeting dynamic loop regions of coactivator proteins.** In **Chapter 2** we report an analysis of several Tethering fragments discovered through a 2017 disulfide Tethering screen of the coactivator Med25. Through this work we found that lead fragment **5** composed of a benzothiophene moiety and a nipecotic acid group utilize both sub-features to form specific interactions with Med25 AcID displaying max tethering of 74%. Individually the benzothiophene or nipecotic acid moieties only Tethered 2-20%. Taken together, the results indicate that fragment **5** is an excellent starting point for the development of an irreversible Med25 modulator, as outlined in **Chapter 3.**

Chapter 2.2 Introduction

Disulfide Tethering has been used to study protein-small molecule[1–9]and protein-peptide binding[10–18]10–19 for a wide range of proteins of interest (POI)s[7,19–21] (**Figure 2.1A**) Tethering is a powerful method for doing so because it is a site-directed screening strategy such that one can target very specific regions within a protein for ligand discovery. In a site-directed disulfide Tethering screen, a POI containing a cysteine is incubated with a library of mixed disulfide fragment molecules. Fragments with innate affinity for a binding site within 5-10 Å away from a solvent-exposed cysteine will form a reversible covalent bond via disulfide exchange, forming a complex with detectable equilibrium concentration. In this way, hits can be identified through mass spectrometric (MS) analysis of each screening well.[19] This method can also be used in a high throughput manner allowing for rapid testing of large disulfide libraries. Disulfide fragments used in Tethering have two main components, a variable carboxylic "HEAD" for the interaction with the POI and a disulfide "TAIL" for the formation of a covalent bond with the cysteine in the POI (**Figure 2.1B**). By using this site-directed ligand discovery method, the Mapp lab has identified several ligands that

Fragment 1-10

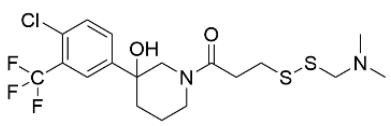

Scheme 2.2 Structure of Fragment 1-10. *Fragment* ***1-10*** *discovered in a disulfide Tethering screen against master coactivator GACKIX.[20] The first crystal structure of ligand bound KIX was identified using this fragment.* ***PDB: 4I90***

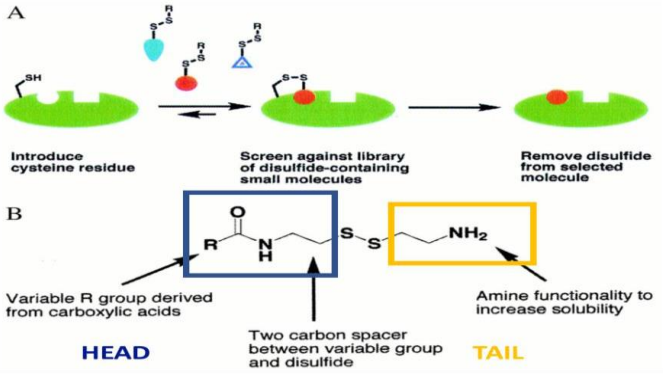

Figure 2.1 Disulfide Fragments and Cysteine Tethering. ***(A)*** *Tethering: A site-directed ligand discovery method utilizing disulfide fragments as reversible probes.* ***(B)*** *The disulfide fragments are made of two major regions, the* ***HEAD*** *fragment derived from a carboxylic acid, and responsible for binding noncovalently to the POI, and the amine* ***TAIL*** *that aids with solubility of the fragment. The two are connected by a disulfide bond that reacts with solvent exposed cysteines on the POI. Both the HEAD and TAIL fragments are considered in this dissertation. Figure adapted from Erlandson et al.*

are capable of binding to specific sites within transcriptional coactivators that alter the conformation and interaction networks of those proteins. For example, previous coworkers dissecting the structure and function of the master coactivator CBP identified a small molecule fragment that **targeted a dynamic loop** via engineered cysteine **L664C** in the KIX domain[20] (**Figure 2.2A**). This fragment **1-10** (**Scheme 2.1**), allosterically and orthosterically inhibited the KIX PPI networks and stabilized KIX sufficiently such that the first crystal structure of the protein was obtained.

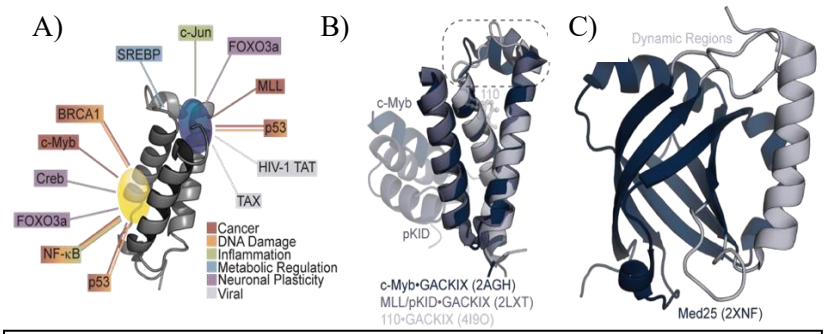

Figure 2.2 Dynamic Transcriptional Activators CBP KIX and Med25 AcID. ***(A)*** *The CBP GACKIX motif can bind over 10 different activators and these interactions are dysregulated in multiple diseases[9,14,22].* ***(B)*** *An overlay of NMR structures (2AGH and 2XLT) and the only crystal structure* ***(4I90)*** *of CBP GACKIX, with the dynamic loop region highlighted.* ***(C)*** *NMR structure of Med25 with the dynamic regions highlighted in gray.[23,24]*

More recently, the Mapp lab conducted a Tethering screen on the coactivator Med25, a sub stoichiometric subunit of the Mediator complex, in an effort to identify fragments capable of modifying Med25's activator-binding activities.[22,23] While the Med25 and CBP KIX exhibit disparate structures, they do share a few common features. Both have at least two binding sites that allosterically communicate and both contain dynamic loops that play a role in allostery. (**Figure 2.2B and 2.2C**) It is the **Ac**tivator **I**nteraction **D**omain (AcID) within Med25 that interacts with the transcription factors (TFs) VP16, [24–28] Ets-related activators ERM, ETV1, and ETV4, [29,30] cJun, [29,31] p53, [32] IE62, [33] RSV NR1, [34] and ATF6α [35,36] using the two binding surfaces either separately or simultaneously. (**Figure 2.3**). Dysregulation of these Med25-related

PPIs results in viral gene transcription, oncogenesis, and an altered ER stress response. Thus, it would be useful to have small molecule probes as starting points for therapeutic agents.

Previous attempts to target and disrupt Med25 PPIs using traditional screening methods have been largely unsuccessful, with only a single small-molecule inhibitor reported for Med25 PPIs.[22,37,38] Some recent natural products screens have identified natural products that can bind Med25 and inhibit related PPI activity; however their complicated structures make them challenging to chemically synthesize and thus difficult to use in SAR studies for probe development.

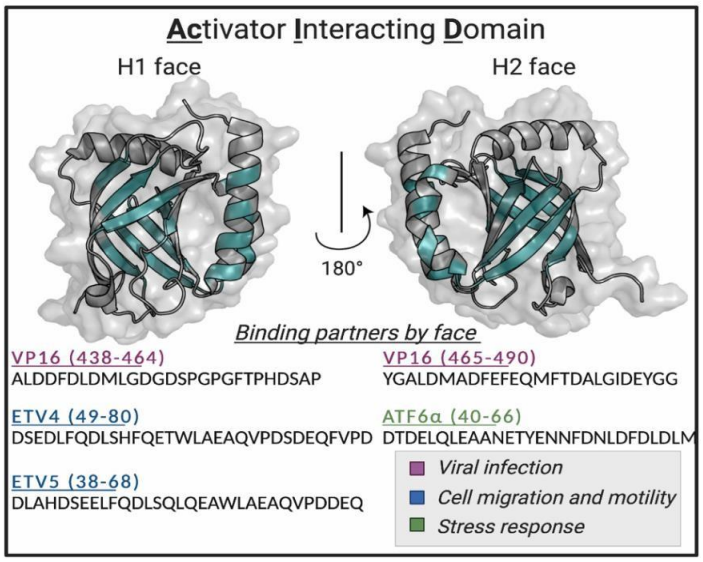

Figure 2.3 Med25 AcID and Transcriptional Activator Binding Partners. *Med25 Activator Interaction Domain (AcID) uses its H1 face to bind ETV4 and ETV5, its H2 face to bind ATF6α, and VP16 simultaneously binds both the H1 and H2 faces of AcID. Med25 AcID also displays a high degree of conformational dynamics indicated by the light blue regions above.*[25,37–39]

The binding surfaces within Med25 are much larger than typical binding pockets, approximately 900 A^2 [25,38–40], and lack significant topology for small molecule binding**. However, recent work from our lab found that the dynamic loops flanking the binding surfaces are critical for both the molecular recognition of activator binding partners and allosteric communication between the binding surfaces**[37,38] **(Figure 2.3**). Thus, Med25 AcID's **dynamic loops** were the focus of the Tethering screen.

Chapter 2.3 Results from a 2017 Tethering Screen against Med25 AcID

Prior work in the Mapp lab demonstrated that Med25 AcID has two solvent-exposed cysteines capable of reacting with electrophiles.[22,23] One of the cysteines (**C497**) is on the beta barrel core of the coactivator's **a**ctivator **b**inding **d**omain (ABD), adjacent to the dynamic loop on the H1 face. The second cysteine (**C506**) resides on a dynamic loop between the H1 and H2 faces, though both fragments are perfectly suited to target Med25 AcID's H1 face.[23] Thus, it was expected that a Tethering screen would identify ligands for one or both cysteines. In a 2017 Tethering screen conducted in collaboration with the Wells laboratory at UCSF, twenty-four small molecule fragments were identified as Med25 binders. (**Figures 2.4 and 2.5**)[22,23,41]

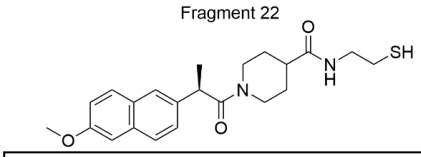

Scheme 2.2 Structure of Fragment 22. *Compound **22** identified from a 2017 Tethering Screen to bind to Med25 and recapitulate Med25 PPIs.[22]*

Previous studies with compound **22 (Scheme 2.2)** showed that when covalently bound to **C506** it recapitulates allosteric changes involved in native Med25 PPIs. More specifically, compound **22** lowers the off-rates of both ATF6α and VP16 with the H2 face of Med25.[22] A comparison of Med25 modulators obtained from the traditional disulfide Tethering screen, using

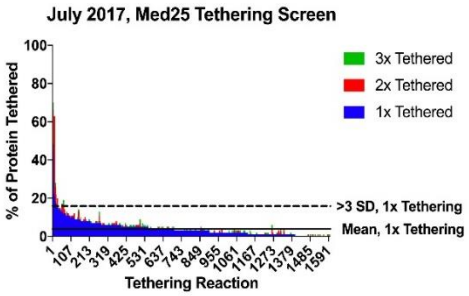

Figure 2.4 July 2017 wtMed25 Tethering Screen Results. *wTMed25AcID was subjected to a Tethering screen involving 1600 small molecule disulfide fragments. 100μM small molecule was assessed against 100μM Med25 allowing for a 1:1 binding ratio. The top 24 hit compounds were able to bind **16% or more** (+3SD). Blue(1x)- percent singly labeled species, Red(2x)- percent doubly*

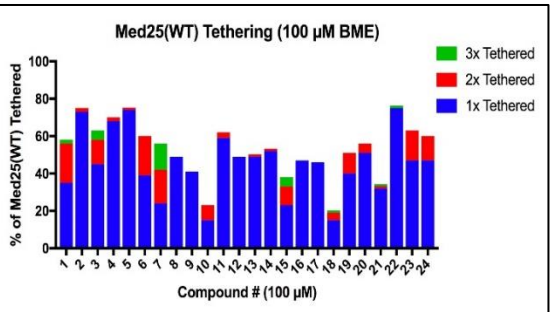

Figure 2.5 July 2017 wtMed25 Tethering Screen Hits. *The 24 hits identified from the 2017 wtMed25 Tethering Screen. **Compound 5** is shown to bind to AcID 74% once, but only 1% twice. **Compounds 22** and **5** appear to have the best single labeling ability which could be valuable to targeting wtMed25. Notably, some of the fragments here bind to Med25 AcID multiple times. Tethering screen was carried*

Med25 AcID as the POI and those obtained from an FP-Tethering screen using the Med25-ERM complex showed minimal overlap between the two hit groups.[23] These results emphasize the point that a molecule's ability to bind to a POI is not the only factor relevant to altering PPI activity. In other words, a molecule may Tether to one of the cysteines in Med25 AcID yet not affect the PPIs of interest, so choosing the best binding probe may not always result in the most biologically active probe. Rather, a molecule that can bind specifically to the POI and displays biological activity makes for the best modulator.

Examining fragment **22** in comparison to the other hit fragments from the tethering library (**Scheme 2.3**), a few notable patterns can be observed in structure and activity. First, the compound numbering scheme is in order of highest Med25 labeler **1** to lowest Med25 labeler **24**. Fragment had the ability to either singly tether (binding at a single Cysteine) or doubly tether (binding at both solvent exposed cysteines), however only the single labeling percentage is

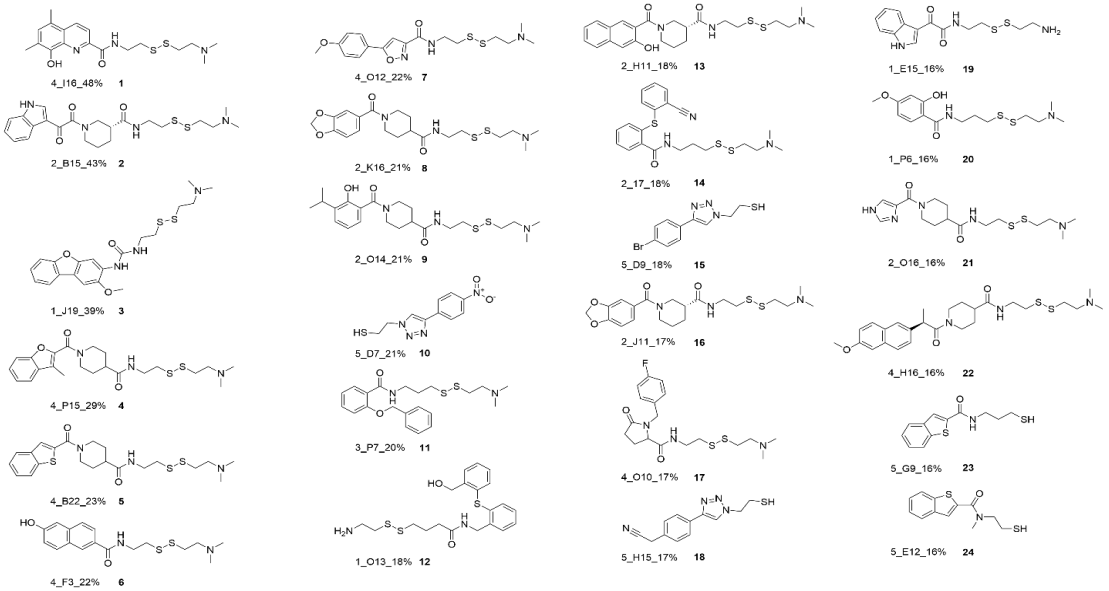

Scheme 2.3 Structure of Hits from 2017 Med25 Tethering Screen. *2017 Tethering Screening Results: Top 24 best labeling hit fragments are shown above. These compounds are numbered 1-24 based on Tethering Percentages (middle to bottom right of each molecule). Also, the plate well number and equilibrium Tethering percent (or percent of detected complex in solution at equilibrium or designated time points identified by MS) are noted below each fragment for reference. The screen was carried out by Dr. Nicholas Foster and Dr. Andrew Henderson. Additional cheminformatic analysis was carried out by Dr. Clint Regan to analyze trends within the HIT data set.*

shown in **Scheme 2.3** Of the hit fragments, 8 of them contain **the nipecotic acid or iso-nipecotic acid** substructures (**Scheme 2.3:** Compounds **2**, **4**, **5**, **8**, **9**, **16**, **21**, and **22**); however, many of the fragments within the inactive set also contained this feature. All the hits also contained **aromatic rings** and there was limited diversity among these aromatic moieties suggesting that these specific aromatic moieties are spatially arranged in a way that allows them to interact with Med25 AcID's H1 face after reversibly Tethering to one of the solvent exposed cysteines present. Additionally, the **benzothiophene** substructure was identified as a component of 3 of the hit fragments, appearing in compounds **5**, **23**, and **24** (**Scheme 2.3**) and only one other time within the entire Tethering library (**Scheme 2.4**). **Thus, the benzothiophene fragment appears to be enriched** within the active set while **the isonipecotic and (R)-nipecotic acid substructures may simply function as a chemical spacer to optimally position aromatic groups to enhance their ability to interact with Med25 AcID.**

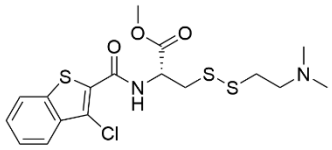

methyl *N*-(3-chlorobenzo[*b*]thiophene-2-carbonyl)-*S*-((2-(dimethylamino)ethyl)thio)-*L*-cysteinate

Scheme 2.4 Structure of methyl N-(3-chlorobenzo[b]thiophene-2-carbonyl)-S-((2-dimethylamino)ethyl)thio)-L-cysteinate. *The only other benzothiophene fragment within the disulfide library*

The hits from the Tethering screen have varying selectivity for **C497** and/or **C506**. In studies where **C506** was mutated to an alanine, several fragments displayed selective engagement with **C506** over **C497 as Tethering is drastically reduced or abolished under these conditions. (Figure 2.6) .** [22,23,41] Using the benzothiophene-based fragments for reference, compound **5** binds wild-type Med25 AcID (wtMed25 AcID) 23% at 1 mM β-mercaptoethanol (high stringency) and 75% at 0.1 mM β-mercaptoethanol (low stringency). Utilization of the Med25 **C506A** mutant, however, nearly abolishes this fragment's ability to tether, as seen by the decrease in single labeling percent of compound **5** to 1%, suggesting this fragment selectively binds **C506** over

C497. Compounds **23** and **24**, however, preferentially interact with **C506** but are still able to bind when Med25 **C506A** is used. The observed results suggest that compound **5** selectively targets **C506**, while compounds **23** and **24** interact with Med25 AcID with a lesser degree of specificity.

Since compound **5** singly labels Med25 AcID even under stringent Tethering conditions, displays an observable cysteine selectivity, and contains the enriched benzothiophene sub fragment, this study aims to further investigate the role that each of the composite sub fragments play in binding to Med25 AcID. Additionally, we sought to evaluate different TAIL moieties to

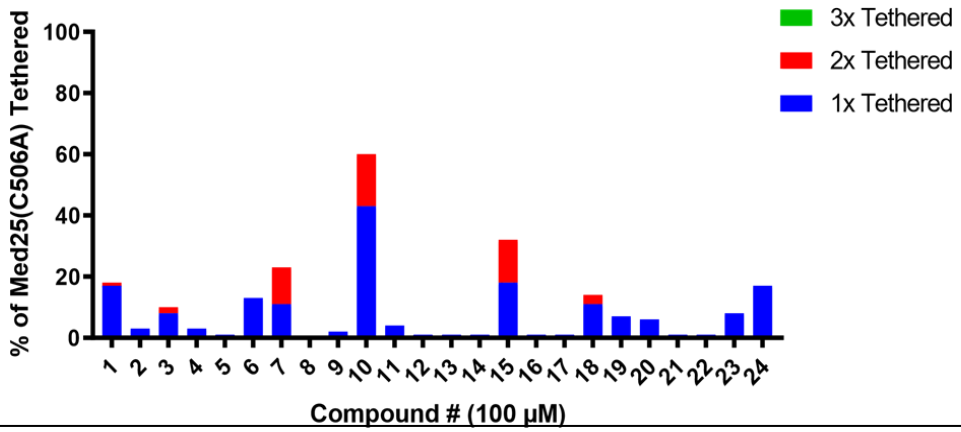

Figure 2.6 July 2017 Med25 C506A Tethering Screen Results. *Med25* ***C506*** *_ Screening Results: This mutation causes diminished binding as well abolished binding as seen in fragments (**5**, **8**, **12**, **13**,**16**, and **17**). Disulfide fragments unable to bind to Med25* ***C506A*** *selectively target C506. These data were obtained by Andrew Henderson and Nicholas Foster.*[22,23,41]

simplify the overall synthesis of the fragment molecules. To do this, we synthesized the respective disulfide analogs shown in **Scheme 2.5.**, then utilized single point Tethering (SPT) experiments to analyze the extent to which each Tethers to Med25 AcID, thus allowing a limited structure-activity relationship to emerge.

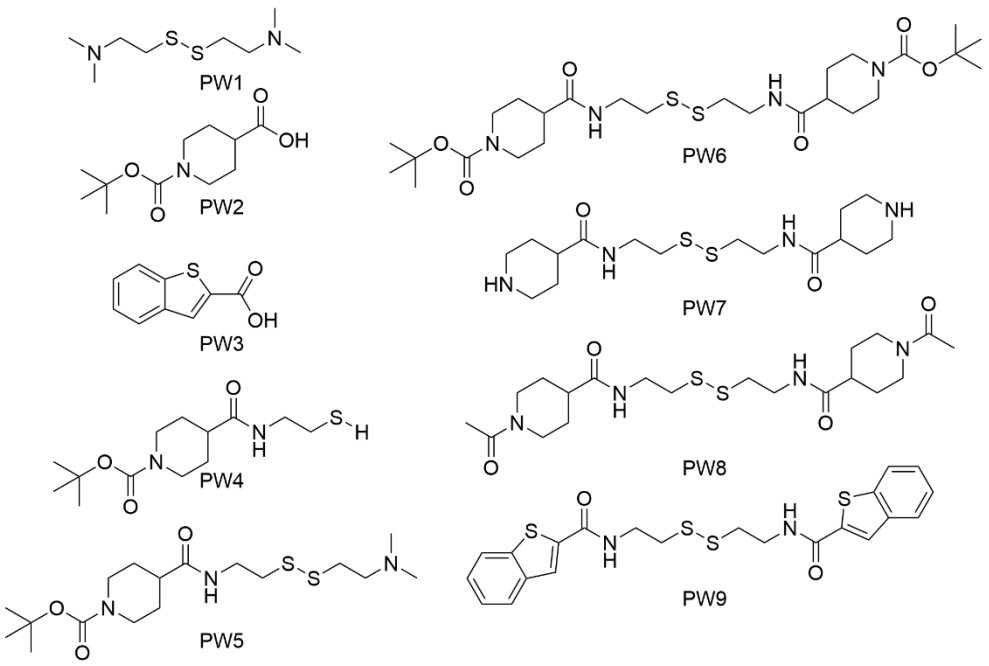

Scheme 2.5 Structures of Reversible Ligands Synthesized. *Reversible probes synthesized and used in Single Point Tethering Experiments (SPT)*

Chapter 2.4 Synthesis of Reversible Fragments

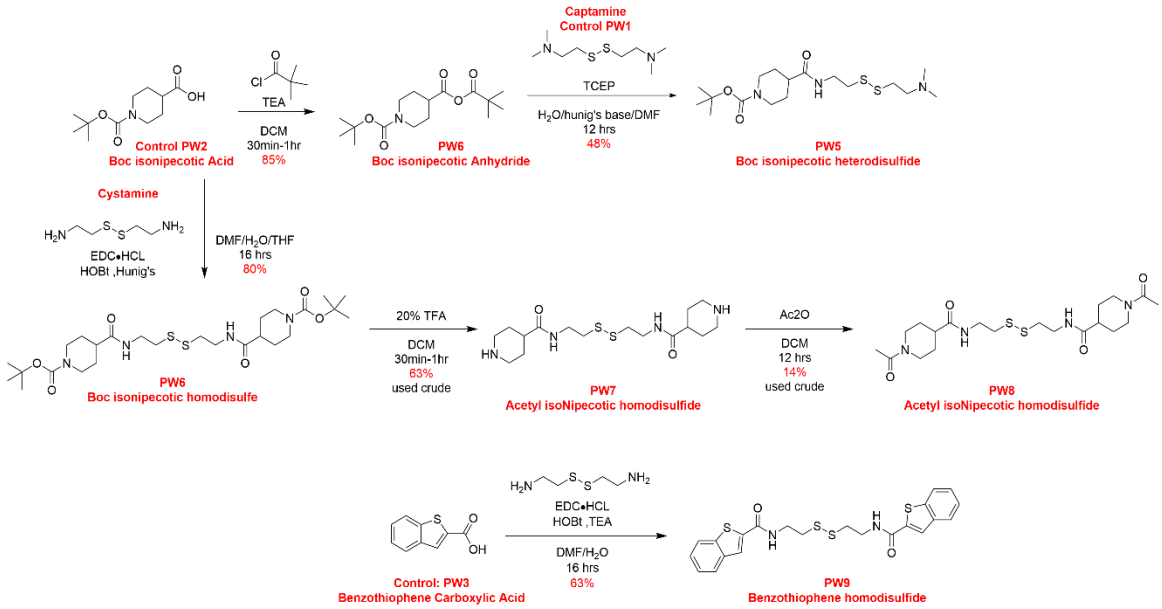

Scheme 2.6 Synthesis of Reversible Ligands. *Synthesis of Reversible Probes General carboxylic acids are transformed into disulfide or thiol probes through amide coupling with cystamine or cysteamine.*

Scheme 6 shows the synthetic scheme for the formation of reversible probes (**PW4**, **PW5**, **PW6**, **PW7**, **PW8**, and **PW9**)

We transformed Boc-isonipecotic acid into **a thiol**, a **homodisulfide** and a **heterodisulfide**. For the synthesis of Boc isoNipecotic thiol **PW4**, commercially available Boc-isonipecotic acid was converted into a mixed anhydride through treatment with pivaloyl chloride followed by the addition of β-mercaptoethylamine to yield **PW4** (46%). For **PW6**, commercially available Boc-isonipecotic acid was treated with cystamine using general amide coupling conditions to form Boc isoNipecotic homodisulfide **PW6** (48%). **PW6** was then converted into Boc isoNipecotic heterodisulfide **PW5** (48%) through a disulfide exchange reaction with 2,2′-dithiobis[N,Ndimethylethanamine] (Captamine) and tris(2-chloroethyl) phosphate (TCEP). Compound **PW6** was additionally converted into isoNipecotic homodimer **PW7** (63%) using 20% trifluoroacetic acid (TFA) in DCM. Compound **PW7** was then converted into compound **PW8** (14%) through treatment of the free amine with acetic anhydride and Hünig's base. Finally, compound **PW9** (63%) was made by taking the commercially available benzothiophene carboxylic acid and converting it into a mixed anhydride through treatment of pivaloyl chloride. Following pivonylation, cystamine was added and the reaction was subjected to general amide coupling conditions resulting in homodisulfide **PW9** (63%).

Chapter 2.5 Single Point Tethering Experiments

With the molecules in hand, single point Tethering (SPT) experiments were performed to assess the interaction of each fragment with Med25 AcID. For these experiments, Med25 was incubated with five equivalents of small molecule fragment and either 1 mM or 0.1 mM β-mercaptoethanol (BME) in Med25 storage buffer (10 mM phosphate, 50 mM NaCl, 10% v/v glycerol, 0.001% v/v NP-40, pH 6.8). At various time points, the reaction mixtures were evaluated using qTOF-MS to identify the extent of small molecule-protein complexation. The

addition of BME initiates the disulfide exchange experiment. BME can also reversibly compete with the small molecule. By evaluating both 1 mM or 0.1 mM concentrations of BME we can assess the stringency of the experiment as weaker small molecule probes can be ruled out as they are more easily reduced from Med25 AcID and therefore less likely to form substantial amounts of a favorable equilibrium complex.

Chapter 2.5aTethering Controls

SPT Experiments of Controls Molecules (**Figure 2.7**):

Captamine **PW1**, Boc isonipecotic acid **PW2**, and Benzothiophene carboxylic acid **PW3**

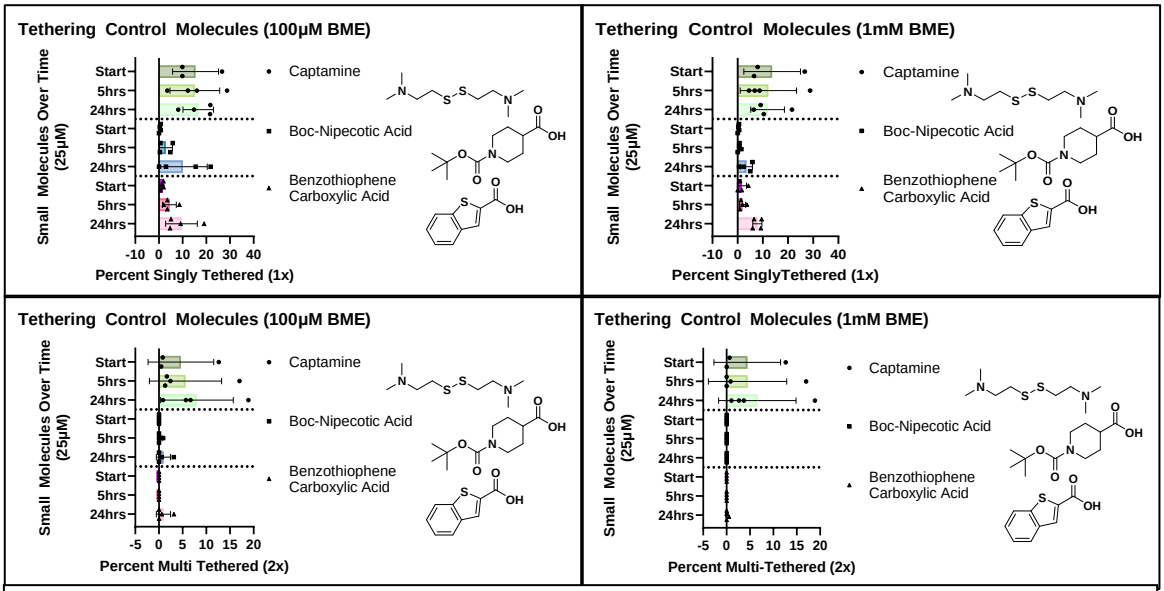

Figure 2.7 SPT of Control Molecules. *Tethering percentages of the control molecules under less stringent* ***(left)*** *and more stringent* ***(right)*** *reaction conditions. The top displays the single labeling results while the bottom displays the multi-labeled results. Maximum observed tethering: 25% (0.1mM) and (10% 1mM). The bar graphs represent 3 independent experiments with indicated percent error (SD).*

Initially we assessed captamine as a positive control capable of disulfide Tethering as well as two negative controls that were anticipated to interact with Med25 AcID non-specifically and/or noncovalently. When five equivalents of **PW1** were incubated with Med25 AcID, this fragment Tethered both of Med25's solvent-exposed cysteines. Additionally, this fragment is analogous to the Tail portion of typical disulfide probes and can sometimes be seen as one of the

major equilibrium species detected by MS-analysis of a Tethering reaction. As can be seen in **Figure 2.7**, captamine quickly labels Med25 AcID with a detectable concentration present at the start of the reaction, roughly 15% single-labeled, 5% double-labeled regardless of the reaction stringency. (t=0 hours). At equilibrium, the percentage of detectable captamine-Med25 slightly increases, but not to a significant amount as the start and 24 hours data points are within error of each other.

The negative controls Boc-isonipecotic acid **PW2** and benzothiophene carboxylic acid **PW3** were not expected to form a covalent bond with Med25 due to lack of a thiol-reactive moiety in their structures. Unexpectedly, some degree of Med25 single labeling was observed, albeit limited. However, neither of these negative controls showed significant double labeling under either BME concentration. While the identification of a MS adduct generally represents the formation of a covalent bond, under the reaction conditions it is unlikely that either of these carboxylic acids are meaningfully engaging with Med25 AcID, and thus further studies will need to be carried out to determine if the observed binding is real or an artifact.

Chapter 2.5b Tethering TAIL Fragments

Boc-isonipecotic thiol **PW4,** Boc-isonipecotic heterodisulfide **PW5**, Boc-isonipecotic homodisulfide **PW6**

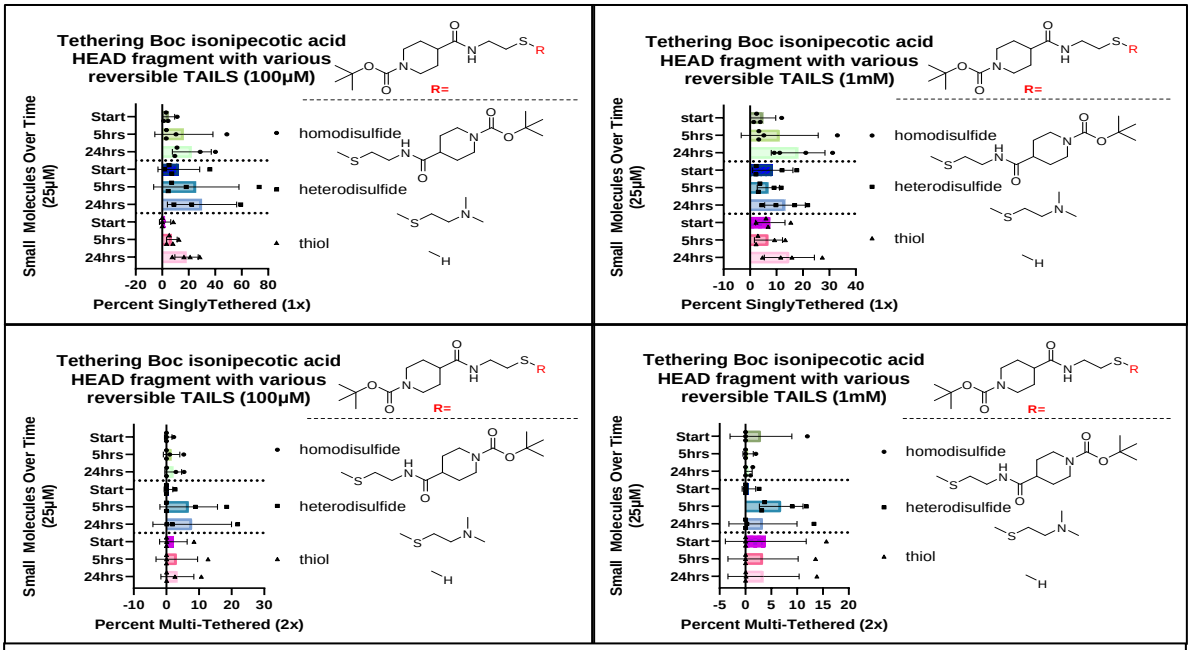

Figure 2.8 SPT Analysis of TAIL Fragments. *Tethering percentages of the TAIL molecules under less stringent* ***(left)*** *and more stringent* ***(right)*** *reaction conditions. The top displays the single labeling results while the bottom displays the multi-labeled results. The bar graphs represent 3 independent experiments with indicated percent error (SD).*

Figure 2.8 shows the percentage of small molecule observed singly or doubly Tethered to Med25 AcID at various time points under less stringent (left, 0.1 mM BME) or more stringent (right, 1mM BME) detected by MS analysis. The top displays the single-Tethering percentages while the bottom displays the percentages of double-labeled species detected at equilibrium. Next, we compared the how the structural differences between compounds **PW4**, **PW5**, and **PW6**, that differ only in the reversible TAIL, affect the probe's ability to bind Med25 AcID. Under ideal conditions, it would be expected that the equilibrium Tethering percentages would be identical among the three fragments since the HEAD portion of the disulfide fragments remain the same and complexation is dependent on the HEAD fragment's innate binding affinity for a POI. However, the starting molecules display different solubilities and may involve alterations in the redox conditions. Under the experimental conditions each fragment singly labeled Med25 with the Boc-isonipecotic HEAD fragment roughly 30-50% under less stringent

conditions whereas Tethering was reduced to 30 % with added stringency (**Figure2.8**). At both BME concentrations these molecules all bind to Med25 more effectively than the controls. This Boc-isonipecotic HEAD fragment is also capable of double-labeling as shown by the bottom of **Figure 2.8**. Interestingly, when the Boc-Nipecotic Acid fragment is a heterodisulfide PW5 the highest percentage of doubled labeled Med25 could be observed, with a maximum of 6% at 1 mM BME. However, both the Boc-nipecotic acid homodimer **PW6** and thiol **PW4** constructs did not Tether more than 3% at either concentration. Equilibrium percentages for **PW4**, **PW5**, and **PW6** all vary within error but suggest that the boc-nipecotic acid HEAD fragment binds to both of Med25 AcID's cysteine's, one more specifically than the other.

Chapter 2.5c Tethering HEAD Fragments

Boc isoNipecotic Acetyl Bromide **PW 6,** isoNipecotic Acetyl Bromide **PW7**, Acetyl isoNipecotic Acetyl Bromide **PW8** and Benzothiophene Acetyl Bromide **PW9**:

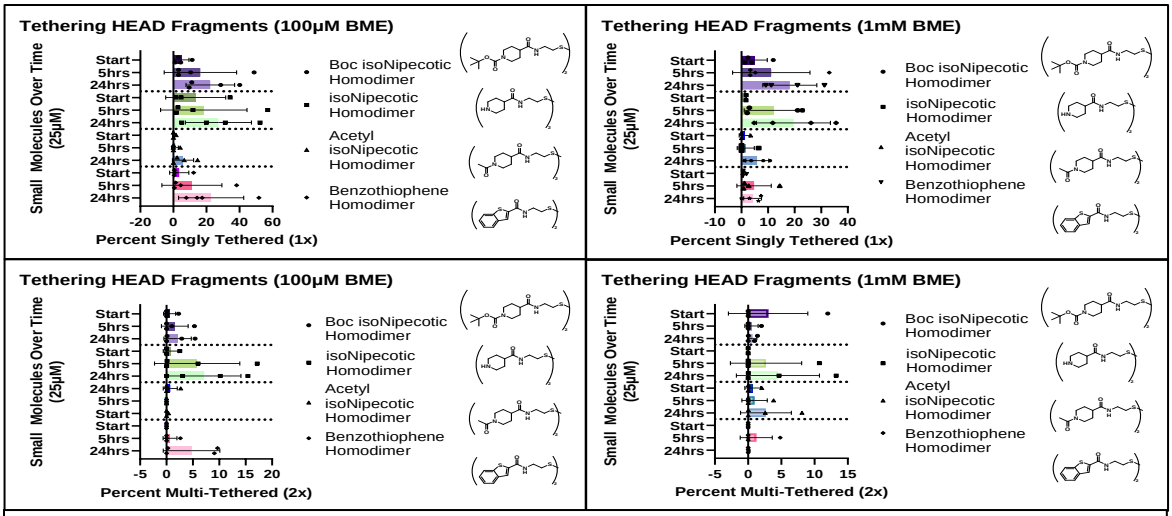

Figure 2.9 SPT Analysis of HEAD Fragments. ***Figure 2.9*** *shows the percentage of small molecule observed singly or doubly Tethered to Med25 AcID at various time points under less stringent (left, 0.1 mM BME) or more stringent (right, 1mM BME) detected by MS analysis. The bar graphs represent 3 independent experiments with indicated percent error (SD).*

Since the Boc-nipecotic homodimer **PW6** labeled Med25AcID relatively well (25-30%), the analogous, unprotected **PW7** and acetyl protected **PW8** molecules were also tested. In addition to these, the simplest benzothiophene substrate **PW9** was also considered. (**Figure 2.9**) Each of these molecules were synthesized as homodisulfides and compared to the homodisulfide **PW6**. It was hypothesized that the hydrophobic nature of the Boc group within fragment **PW6** added to the interaction of the subgroup, increasing its residence time on Med25 AcID. It was also hypothesized that **PW7** may bind poorly due to its overall positive charge which should repel positively charged Med25. Interestingly, **PW6** and **PW7** both singly label Med25 to a similar extent under both concentrations of BME at roughly 20%. On the other hand, **PW8** is barely able to bind at all under either condition with a maximum of 6% at both BME concentrations. Another finding to mention, **PW9** seems to singly label Med25 20% over time under the less stringent conditions; however, this labeling is reduced to about 5% when BME is at 1mM. Regarding the double labeling data, only isonipecotic acid shows apparent double labeling, suggesting the removal of the Boc group decreases cysteine selectivity.

Chapter 2.6 Conclusions and Future Directions

The results from the single point Tethering experiments provided useful insight for the development of compound **5** and its analogs as useful probes for Med25 PPIs. For the first time I demonstrated that having a mixed disulfide as the Tethering moiety is not required; both a thiol or a homodisulfide are sufficient, as each species **PW4**, **PW5**, and **PW6** showed similar Tethering. The results also suggest that nipecotic acid functions as more than just a spacer, as this moiety is capable of Tethering to Med25 AcID in substantial amounts. Additionally, the benzothiophene fragment alone is capable of labeling Med25 in significant amounts as demonstrated by **PW9**, yet the combination of both pieces significantly increased this fragments tetherability. When comparing **PW6**, **PW7**, and **PW8**, to compound **5**, we can see that the N-

substitution affects the fragments binding. Having an aromatic substituent such as the benzothiophene in compound **5** offers the best binding ability and best selectivity. Changing the aromatic substituent to a Boc protecting group decreases the binding of the fragment, but having either a free amine or an acetyl substituent decreases the binding more significantly and increases nonspecific binding as tethering of both of Med25 AcID's cysteines is observed. Thus, moving forwards, I decided to further investigate the two Boc-isonipecotic acid and benzothiophene carboxylic acid substructures, along with the composite full fragment compound **5**. However, these reversible probes would not survive within a cellular experiment. By converting these reversible probes into irreversible thiol reactive moieties, these fragments can be further developed into mechanistic and therapeutic probes to investigate Med25 and its PPI networks. Towards this end, in **Chapter 3** we transform these fragments and various analogs into irreversible ligands and evaluate their ability to bind to Med25 AcID.

Chapter 2.7 Methods

General Procedures:

13C and 1H NMR spectra were recorded on a Varian MR400, a Varian Vnmrs 600MHz, or a Bruker Ascend 500 magnetic resonance spectrometer, as noted. Proton chemical shifts are referenced to CHCl3 (δ 7.26ppm) in CDCl3 solutions, CD3OD (δ 3.31) in CD3OD solutions, and DMSO δ 2.5). Carbon chemical shifts are referenced to δ 77.16ppm in CDCl3 solutions, δ 49.09 ppm in CD3OD solutions, and δ 39.53 ppm in DMSO.

High Resolution Mass Spectra were recorded with a (TOF, QTOF) using either positive or negative mode electrospray ionization (ESI)

Products were purified by flash chromatography using indicated solvent systems. Column chromatography was performed manually.

Purchase and Synthesis of Probes

Control Molecules 2,2'-disulfanediylbis(ethan-1-amine) **PW1**, 1-(tert-butoxycarbonyl)piperidine-4-carboxylic acid **PW2**, and benzo[b]thiophene-2-carboxylic acid **PW3** were used as purchased from commercial vendor Sigma Aldrich.

Silica gel, Pivonyl Chloride, Hunig's base, K2CO3, HOBt, Cystamine, Cysteamine, BME, TCEP, CH_2Cl_2, and DMF were all purchased from commercial vendors (Sigma Aldrich or Toronto Chemical)

Experimental

Synthesis of tert-butyl 4-((2-mercaptoethyl)carbamoyl)piperidine-1-carboxylate

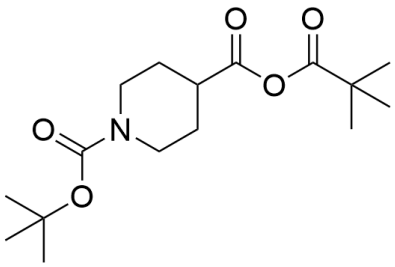

Boc nipecotic mixed Anhydride

To a round bottom flask charged with a stir bar was added Boc nipecotic acid (control **PW2**) (1.0 g, 4.36 mmol), in THF (21.80 mL). Dropwise Hünig's base (0.91 mL) was added, and the reaction mixture was cooled to -5 °C pivaloyl chloride (0.64 mL) was added dropwise to the reaction mixture. The reaction was allowed to stir at room temperature for 1 hour. When the reaction was judged to be complete, the reaction mixture was extracted into CH_2Cl_2, washed

with saturated $NaHCO_3$, brine, dried with anhydrous Na_2SO_4, filtered and concentrated under reduced pressure to give Boc anhydride (1.21 g, 88 %) as a white solid as previously described.

PW4 (Boc isonipecotic thiol

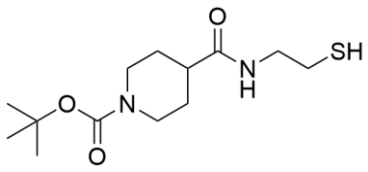

To a round bottom flask charged with a stir bar was added Boc nipecotic anhydride (1.21g, 3.85 mmol) and 3-aminopropane-1-thiol (356.79 mg, 4.62 mmol in CH_2Cl_2 (20.00 mL) and the reaction mixture was let stir at room temperature overnight. When the reaction was judged to be complete, the reaction mixture was poured into a separatory funnel and extracted into CH_2Cl_2 (15mL x3), washed with saturated $NaHCO_3$ (15 mL) then brine (15 mL), and dried over anhydrous $MgSO_4$, filtered, then concentrated under reduced pressure to give a clear-yellow oil. (950 mg, 86%). The crude fragment **PW4** was then used for SPT experiments.

^{1}H NMR (599 MHz, MeOD) δ 3.99 (dt, *J* = 13.4, 4.1 Hz, 2H), 2.93 (bs, 3H), 2.73 (tt, *J* = 10.8, 4.2 Hz, 1H), 1.95 (dd, *J* = 13.6, 3.9 Hz, 2H), 1.59 (dtdd, *J* = 13.4, 11.3, 4.4, 2.0 Hz, 2H), 1.46 (s, 9H), 1.26 (d, *J* = 1.8 Hz, 9H).

^{13}C NMR (151 MHz, MeOD) δ 176.22, 155.03, 79.69, 48.16, 42.66, 42.33, 28.30, 27.85, 27.26.

Synthesis of tert-butyl 4-((2-((2-(dimethylamino)ethyl)disulfaneyl)ethyl)carbamoyl)piperidine-1-carboxylate **PW5 (**Boc isonipecotic heterodisulfide)

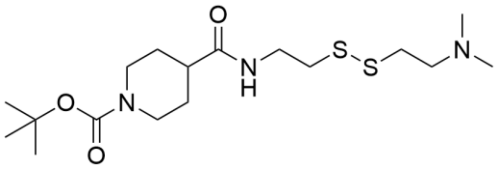

To a round bottom flask charged with a stir bar was added Boc isoNipecotic Homodimer **PW6** (200mg, 0.0348mmol), Captamine (734mg, 3.479mmol), and TCEP (10.03mg, 0.035mmol) was added to a mixture of DMF (1.2 mL) and H_2O (1.2 mL). Hünig's base (1.2 mL) was added dropwise (DMF/H_2O/ Hünig (0.1M)) and the reaction was stirred at room temperature overnight. When the reaction was judged to be complete, ice water was added to the reaction mixture followed by acidification of the solution to pH 7. The crude mixture was then extracted into CH_2Cl_2 (10mL) washed with $NaHCO_3$ (10mL) then brine (10mL), dried over anhydrous $MgSO_4$, filtered, and concentrated under reduced pressure. The crude was subsequently purified by flash chromatography (1% CH2Cl2:MeOH) to give an off white solid (129.7 mg, 48%) The purified fragment **PW5** was then used for SPT experiments.

1H NMR (599 MHz, cdcl3) δ 6.51 – 6.44 (m, 1H), 4.12 (s, 2H), 3.56 (q, J = 6.3 Hz, 2H), 3.41 (d, *J* = 1.2 Hz, 6H), 2.81 (t, J = 6.4 Hz, 2H), 2.73 (s, 3H), 2.30 (tt, J = 11.6, 3.8 Hz, 1H), 1.80 (d, J = 13.1 Hz, 2H), 1.62 (qt, J = 12.5, 5.9 Hz, 2H), 1.44 (d, J = 1.2 Hz, 9H), 1.29 – 1.26 (m, 1H), 1.24 (s, 2H)

Synthesis of di-tert-butyl 4,4'-(((disulfanediylbis(ethane-2,1-diyl))bis(azanediyl))bis(carbonyl))bis(piperidine-1-carboxylate) **PW6**,

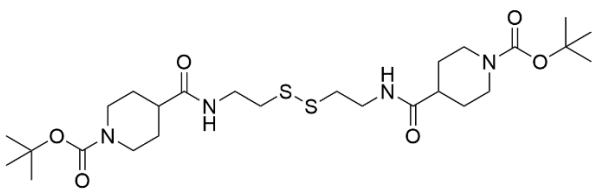

To a round bottom flask charged with a stir bar was added Boc isonipecotic acid (1.0 g, 4.35 mmol), 1-hydroxybenzotriazole hydrate (HOBt) (1.06 g, 7.85 mmol), N-(3-dimethylaminopropyl)-N'ethylcarbodiimide hydrochloride EDCI·HCL (4.181 g, 21.81 mmol), 2,2'-disulfanediylbis(ethan-1-amine) (cystamine) (492 mg, 2.18 mmol), and Hünig's base (3.04 mL) in DMF (21.8 mL). This mixture was stirred overnight at room temperature, When the reaction was judged to be complete, the reaction mixture was diluted over ice H_2O (15mL) and extracted into ethyl acetate (15mL). The organic extracts were washed with brine, dried over anhydrous Na_2SO_4, filtered, and concentrated under reduced pressure. The crude was subsequently purified by flash chromatography (70% ethyl acetate: hexanes). to give an off white solid. The purified fragment **PW6** was then used for SPT experiments. (1.1145 g, 85 %)

^{1}H NMR (599 MHz, DMSO) δ 7.95 (t, *J* = 5.6 Hz, 2H), 3.88 (d, *J* = 13.1 Hz, 4H), 3.31 – 3.24 (m, 4H), 2.71 (t, *J* = 6.7 Hz, 4H), 2.51 – 2.47 (m, 4H), 2.47 – 2.44 (m, 2H), 2.23 (tt, *J* = 11.5, 3.7 Hz, 2H), 1.63 – 1.56 (m, 4H), 1.34 (s, 18H).

^{13}C NMR (151 MHz, DMSO) δ 173.21, 152.93, 77.69, 47.41, 40.05, 39.52, 37.48, 27.20.

Synthesis of N,N'-(disulfanediylbis(ethane-2,1-diyl))bis(piperidine-4-carboxamide) **PW7**,

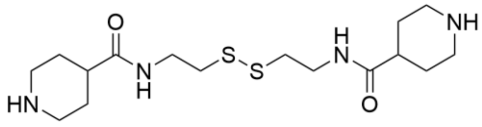

To a round bottom flask charged with a stir bar was added Homodisulfide **PW6** (200 mg, 0.348 mmol) in CH_2Cl_2 (2.8mL). TFA was then added dropwise (0.7 mL), and the mixture was stirred for 30 minutes to an hour at room temperature. When the reaction was judged to be complete, cold ether (5mL) was added and **PW7** precipitated out of solution. Excess solvent and TFA were evaporated with N_2 (g). This fragment was used as crude for preparation of **PW8** and SPT experiments. (82.58 mg, 63 %)

^{1}H NMR (599 MHz, DMSO) δ 8.26 (s, 2H), 8.06 (t, *J* = 5.6 Hz, 2H), 3.29 (q, *J* = 6.4 Hz, 4H), 3.23 (dd, *J* = 9.7, 6.2 Hz, 4H), 2.94 (s, 2H), 2.88 – 2.79 (m, 4H), 2.72 (t, *J* = 6.7 Hz, 4H), 1.70 – 1.60 (m, 2H).

Synthesis of N,N'-(disulfanediylbis(ethane-2,1-diyl))bis(1-acetylpiperidine-4-carboxamide)

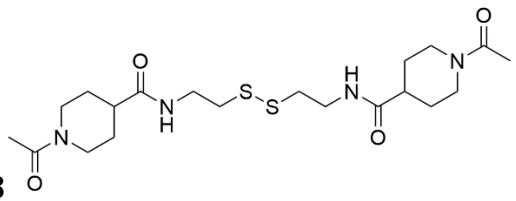

PW8

To a round bottom flask charged with a stir bar was added Homodisulfide **PW7** (23mg, 0.061 mmol) in CH_2Cl_2 (1 mL). Hünig's base (0.1 mL) was added dropwise, and the reaction was cooled to 0° C and acetic anhydride (0.5mL) was added dropwise to the reaction mixture and stirred overnight. When the reaction was judged to be complete, the crude reaction mixture was extracted into CH_2Cl_2 x3. The combined organic layers were then washed with brine, dried over anhydrous $MgSO_4$, and concentrated. The crude **PW8** was used for SPT experiments. (4mg, 14%)

^{1}H NMR (599 MHz, DMSO) δ 7.99 (t, *J* = 5.6 Hz, 2H), 3.25 (q, *J* = 6.4 Hz, 4H), 2.70 (t, *J* = 6.7 Hz, 4H), 1.91 (s, 6H), 1.82 – 1.79 (m, 4H), 1.67 – 1.55 (m, 4H), 1.41 (qd, *J* = 12.3, 4.4 Hz, 2H).

Synthesis of N,N'-(disulfanediylbis(ethane-2,1-diyl))bis(benzo[b]thiophene-2-carboxamide) **PW9**.

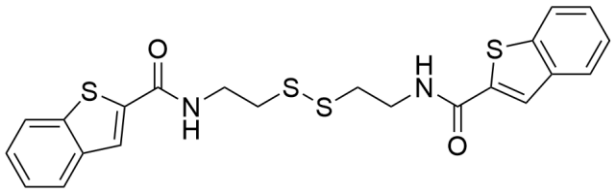

To a round bottom flask charged with a stir bar was added benzothiophene carboxylic acid (1.0 g, 5.61 mmol), 1-hydroxybenzotriazole hydrate (HOBt) (1.36 mg, 7.85 mmol), N-(3-dimethylaminopropyl)-N'ethylcarbodiimide hydrochloride EDCI·HCL (1.936 g, 10.10 mmol), 2,2'-disulfanediylbis(ethan-1-amine) (cystamine) (436 mg, 2.10 mmol), and triethylamine (0.6 mL) in DMF (43 mL) and H_2O (2.6 mL). This mixture was stirred overnight at room temperature. When the reaction was judged to be complete, the reaction mixture was diluted over ethyl acetate (150 mL) then washed with H_2O (25 mL). The combined organic layers were then washed with brine, dried over anhydrous Na_2SO_4, filtered, and concentrated under reduced pressure. The crude was subsequently purified by flash chromatography (gradient 30-70% ethyl acetate: hexanes) to give an off a reddish brown solid (1.670 mg, 63 %) The purified fragment **PW9** was then used for SPT experiments.

^{1}H NMR (599 MHz, DMSO) δ 8.91 (t, *J* = 5.6 Hz, 2H), 8.02 (d, *J* = 0.8 Hz, 2H), 7.97 (dq, *J* = 8.3, 0.9 Hz, 2H), 7.92 – 7.87 (m, 2H), 7.45 – 7.36 (m, 4H), 3.58 – 3.52 (m, 4H), 2.95 (s, 8H).

Protein Expression and Purification

WT Med25 was expressed and purified from heat-shock competent Rosetta pLysS cells (Novagen), in Terrific Broth (TB) containing 0.1 mg/mL ampicillin and 0.034 mg/mL chloramphenicol, using previously described conditions.20,27 Cells were grown at 37 °C to an optical density (OD600nm) of 0.8. Temperature was reduced to 18°C and protein expression was induced upon addition of IPTG to a final concentration of 0.5 mM. Post-induction, cells were incubated for 16 hours at 18°C.

Cells were pelleted via centrifugation at 6000xg for 20 mins at 4°C. Cell pellets were stored at 80°C prior to purification. The harvested pellet was thawed on ice and resuspended in 20 mL of lysis buffer (50 mM phosphate, 300 mM sodium chloride, 10 mM imidazole, pH 6.8). Cells were then lysed by sonication on ice and cellular lysates were cleared by centrifugation at 9500 rpm for 20 min at 4°C. The supernatant lysate was then added to 750µL Ni-NTA beads (Qiagen) and incubated for 1 hour at 4°C. The resin was pelleted by centrifugation at 2500 rpm for 2 min at 4°C and washed with wash buffer (50 mM phosphate, 300 mM sodium chloride, 30 mM imidazole, pH 6.8) a total of five times. Protein was then eluted with 2 mL of elution buffer (50 mM phosphate, 300 mM sodium chloride, 400 mM imidazole, pH 6.8) a total of three times. Eluent was then pooled and purified by cation exchange FPLC (Source 15S, GE Healthcare) using a gradient of Buffer B (50 mM phosphate, 100 mM NaCl, 1 mM DTT, pH 6.8) in Buffer A (50 mM phosphate, 1 mM DTT). The FPLC purified protein was then dialyzed into storage buffer (10 mM phosphate, 50 mM NaCl, 10% v/v glycerol, 0.001% v/v NP-40, pH 6.8) overnight, concentrated, aliquoted, and stored at -80°C. Final protein was greater than 90% pure as determined by Coomassie stained polyacrylamide gel. Protein concentration was determined by UV-Vis spectroscopy using an extinction coefficient, $\varepsilon = 22{,}460\ M^{-1}\ cm^{-1}$.24,27

Single Point Tethering Experiments

Med25 AcID was incubated with 5 equivalents of Small Molecule fragment in storage buffer (10 mM phosphate, 50 mM NaCl, 10% v/v glycerol, 0.001% v/v NP-40, pH 6.8) in a 100µL solution. Order of addition (Buffer, Protein, Small Molecule). When ready to start the reaction, add either 0.1mM or 1mM BME to initiate the disulfide exchange reaction. Mass spectrometry analysis of covalent adducts of wtMed25 was performed on 2µL samples of each 100µL SPT solution. Samples were incubated for 30 minutes, 5 hours, and 24 hours at room temperature. Analysis was conducted by mass spectrometry using an Agilent QToF LC/MS equipped with a Poroshell 300SB C8 reverse-phased column with a gradient of 5-100% acetonitrile with 0.1% formic acid in water with 0.1% formic acid over five minutes. Analysis of data was completed using the Agilent Qualitative Analysis Program with background subtraction and deconvolution settings for an intact protein of 16,000- 40,000 Da.

Total abundances that correspond to masses of tethered species and common adducts were compared to untethered Med25 or BME tethered Med25 fragments to detect equilibrium percentages.

Chapter 2.8 References

(1) Ueda, T.; Tamura, T.; Kawano, M.; Shiono, K.; Hobor, F.; Wilson, A. J.; Hamachi, I. Enhanced Suppression of a Protein–Protein Interaction in Cells Using Small-Molecule Covalent Inhibitors Based on an N -Acyl- N -Alkyl Sulfonamide Warhead. J. Am. Chem. Soc. 2021, 143 (12), 4766– 4774. https://doi.org/10.1021/jacs.1c00703.

(2) Thompson, A. D.; Dugan, A.; Gestwicki, J. E.; Mapp, A. K. Fine-Tuning Multiprotein Complexes Using Small Molecules. ACS Chem. Biol. 2012, 7 (8), 1311–1320. https://doi.org/10.1021/cb300255p.

(3) Mapp, A. K.; Ansari, A. Z.; Ptashne, M.; Dervan, P. B. Activation of Gene Expression by Small Molecule Transcription Factors. Proc. Natl. Acad. Sci. 2000, 97 (8), 3930–3935. https://doi.org/10.1073/pnas.97.8.3930.

(4) Lodge, J. M. Discovery of Small Molecules to Dissect the Individual Roles of GACKIXActivator Complexes.

(5) Ikeda, K.; Maezawa, Y.; Yonezawa, T.; Shimizu, Y.; Tashiro, T.; Kanai, S.; Sugaya, N.; Masuda, Y.; Inoue, N.; Niimi, T.; Masuya, K.; Mizuguchi, K.; Furuya, T.; Osawa, M. DLiP-PPI

Library: An Integrated Chemical Database of Small-to-Medium-Sized Molecules Targeting Protein–Protein Interactions. Front. Chem. 2023, 10, 1090643. https://doi.org/10.3389/fchem.2022.1090643.
(6) Allen, C. E.; Curran, P. R.; Brearley, A. S.; Boissel, V.; Sviridenko, L.; Press, N. J.; Stonehouse, J. P.; Armstrong, A. Efficient and Facile Synthesis of Acrylamide Libraries for Protein-Guided Tethering. Org. Lett. 2015, 17 (3), 458–460. https://doi.org/10.1021/ol503486t.
(7) Doak, B. C.; Norton, R. S.; Scanlon, M. J. The Ways and Means of Fragment-Based Drug Design. Pharmacol. Ther. 2016, 167, 28–37. https://doi.org/10.1016/j.pharmthera.2016.07.003.
(8) Erlanson, D. A.; Hansen, S. K. Making Drugs on Proteins: Site-Directed Ligand Discovery for Fragment-Based Lead Assembly. Curr. Opin. Chem. Biol. 2004, 8 (4), 399–406. https://doi.org/10.1016/j.cbpa.2004.06.010.
(9) Magee, T. V. Progress in Discovery of Small-Molecule Modulators of Protein–Protein Interactions via Fragment Screening. Bioorg. Med. Chem. Lett. 2015, 25 (12), 2461–2468. https://doi.org/10.1016/j.bmcl.2015.04.089.
(10) Modell, A. E.; Marrone, F. I.; Panigrahi, N. R.; Zhang, Y.; Arora, P. S. Peptide Tethering: Pocket-Directed Fragment Screening for Peptidomimetic Inhibitor Discovery. J. Am. Chem. Soc. 2022, 144 (3), 1198–1204. https://doi.org/10.1021/jacs.1c09666.
(11) Wang, H.; Dawber, R. S.; Zhang, P.; Walko, M.; Wilson, A. J.; Wang, X. Peptide-Based Inhibitors of Protein–Protein Interactions: Biophysical, Structural and Cellular Consequences of Introducing a Constraint. Chem. Sci. 2021, 12 (17), 5977–5993. https://doi.org/10.1039/D1SC00165E.
(12) Cesa, L. C.; Mapp, A. K.; Gestwicki, J. E. Direct and Propagated Effects of Small Molecules on Protein–Protein Interaction Networks. Front. Bioeng. Biotechnol. 2015, 3. https://doi.org/10.3389/fbioe.2015.00119.
(13) Dugan, A.; Pricer, R.; Katz, M.; Mapp, A. K. TRIC: Capturing the Direct Cellular Targets of Promoter-Bound Transcriptional Activators. Protein Sci. 2016, 25 (8), 1371–1377. https://doi.org/10.1002/pro.2951.
(14) Krishnamurthy, M.; Dugan, A.; Nwokoye, A.; Fung, Y.-H.; Lancia, J. K.; Majmudar, C. Y.; Mapp, A. K. Caught in the Act: Covalent Cross-Linking Captures Activator–Coactivator Interactions in Vivo. ACS Chem. Biol. 2011, 6 (12), 1321–1326. https://doi.org/10.1021/cb200308e.
(15) Bates, C. A.; Pomerantz, W. C.; Mapp, A. K. Transcriptional Tools: Small Molecules for Modulating CBP KIX-Dependent Transcriptional Activators. Biopolymers 2011, 95 (1), 17–23. https://doi.org/10.1002/bip.21548.
(16) Buhrlage, S. J.; Bates, C. A.; Rowe, S. P.; Minter, A. R.; Brennan, B. B.; Majmudar, C. Y.; Wemmer, D. E.; Al-Hashimi, H.; Mapp, A. K. Amphipathic Small Molecules Mimic the Binding Mode and Function of Endogenous Transcription Factors. ACS Chem. Biol. 2009, 4 (5), 335–344. https://doi.org/10.1021/cb900028j.
(17) Casey, R. J.; Desaulniers, J.-P.; Hojfeldt, J. W.; Mapp, A. K. Expanding the Repertoire of Small Molecule Transcriptional Activation Domains. Bioorg. Med. Chem. 2009, 17 (3), 1034–1043. https://doi.org/10.1016/j.bmc.2008.02.045.
(18) Mapp, A.; Romesberg, F. E. Editorial Overview. Curr. Opin. Chem. Biol. 2008, 12 (4), 387– 388. https://doi.org/10.1016/j.cbpa.2008.08.003.
(19) Mapp, A. K.; Ansari, A. Z.; Ptashne, M.; Dervan, P. B. Activation of Gene Expression by Small Molecule Transcription Factors. Proc. Natl. Acad. Sci. 2000, 97 (8), 3930–3935. https://doi.org/10.1073/pnas.97.8.3930.

(20) Erlanson, D. A.; Braisted, A. C.; Raphael, D. R.; Randal, M.; Stroud, R. M.; Gordon, E. M.; Wells, J. A. Site-Directed Ligand Discovery. Proc. Natl. Acad. Sci. 2000, 97 (17), 9367–9372.
https://doi.org/10.1073/pnas.97.17.9367.
(21) Erlanson, D. A.; Wells, J. A.; Braisted, A. C. Tethering: Fragment-Based Drug Discovery. Annu. Rev. Biophys. Biomol. Struct. 2004, 33 (1), 199–223. https://doi.org/10.1146/annurev.biophys.33.110502.140409.
(22) Wang, N.; Majmudar, C. Y.; Pomerantz, W. C.; Gagnon, J. K.; Sadowsky, J. D.; Meagher, J. L.;
Johnson, T. K.; Stuckey, J. A.; Brooks, C. L. I.; Wells, J. A.; Mapp, A. K. Ordering a Dynamic Protein Via a Small-Molecule Stabilizer. J. Am. Chem. Soc. 2013, 135 (9), 3363–3366. https://doi.org/10.1021/ja3122334.
(23) Wang, N.; Majmudar, C. Y.; Pomerantz, W. C.; Gagnon, J. K.; Sadowsky, J. D.; Meagher, J. L.; Johnson, T. K.; Stuckey, J. A.; Brooks, C. L.; Wells, J. A.; Mapp, A. K. Ordering a Dynamic Protein Via a Small-Molecule Stabilizer. J. Am. Chem. Soc. 2013, 135 (9), 3363–3366. https://doi.org/10.1021/ja3122334.
(24) Henderson, A. R.; Henley, M. J.; Foster, N. J.; Peiffer, A. L.; Beyersdorf, M. S.; Stanford, K. D.; Sturlis, S. M.; Linhares, B. M.; Hill, Z. B.; Wells, J. A.; Cierpicki, T.; Brooks, C. L.; Fierke, C. A.;
Mapp, A. K. Conservation of Coactivator Engagement Mechanism Enables Small-Molecule Allosteric Modulators. Proc. Natl. Acad. Sci. 2018, 115 (36), 8960–8965. https://doi.org/10.1073/pnas.1806202115.
(25) Henderson, A. R. Dissecting Transcriptional Coactivator Binding Networks To Enable Small Molecule Modulation.
(26) Milbradt, A. G.; Kulkarni, M.; Yi, T.; Takeuchi, K.; Sun, Z.-Y. J.; Luna, R. E.; Selenko, P.; Näär, A. M.; Wagner, G. Structure of the VP16 Transactivator Target in the Mediator. Nat. Struct. Mol. Biol. 2011, 18 (4), 410–415. https://doi.org/10.1038/nsmb.1999.
(27) Vojnic, E.; Mourão, A.; Seizl, M.; Simon, B.; Wenzeck, L.; Larivière, L.; Baumli, S.; Baumgart,
K.; Meisterernst, M.; Sattler, M.; Cramer, P. Structure and VP16 Binding of the Mediator Med25 Activator Interaction Domain. Nat. Struct. Mol. Biol. 2011, 18 (4), 404–409. https://doi.org/10.1038/nsmb.1997.
(28) Verger, A.; Baert, J.-L.; Verreman, K.; Dewitte, F.; Ferreira, E.; Lens, Z.; De Launoit, Y.; Villeret, V.; Monté, D. The Mediator Complex Subunit MED25 Is Targeted by the N-Terminal Transactivation Domain of the PEA3 Group Members. Nucleic Acids Res. 2013, 41 (9), 4847–4859. https://doi.org/10.1093/nar/gkt199.
(29) Landrieu, I.; Verger, A.; Baert, J.-L.; Rucktooa, P.; Cantrelle, F.-X.; Dewitte, F.; Ferreira, E.;
Lens, Z.; Villeret, V.; Monté, D. Characterization of ERM Transactivation Domain Binding to the ACID/PTOV Domain of the Mediator Subunit MED25. Nucleic Acids Res. 2015, 43 (14), 7110–7121. https://doi.org/10.1093/nar/gkv650.
(30) Lee, M.-S.; Lim, K.; Lee, M.-K.; Chi, S.-W. Structural Basis for the Interaction between P53 Transactivation Domain and the Mediator Subunit MED25. Molecules 2018, 23 (10), 2726. https://doi.org/10.3390/molecules23102726.
(31) Yamamoto, S.; Eletsky, A.; Szyperski, T.; Hay, J.; Ruyechan, W. T. Analysis of the VaricellaZoster Virus IE62 N-Terminal Acidic Transactivating Domain and Its Interaction with

the Human Mediator Complex. J. Virol. 2009, 83 (12), 6300–6305. https://doi.org/10.1128/JVI.00054-09.
(32) Van Royen, T.; Sedeyn, K.; Moschonas, G. D.; Toussaint, W.; Vuylsteke, M.; Van Haver, D.; Impens, F.; Eyckerman, S.; Lemmens, I.; Tavernier, J.; Schepens, B.; Saelens, X. An Unexpected Encounter: Respiratory Syncytial Virus Nonstructural Protein 1 Interacts with Mediator Subunit MED25. J. Virol. 2022, 96 (19), e01297-22. https://doi.org/10.1128/jvi.01297-22.
(33) Haze, K.; Yoshida, H.; Yanagi, H.; Yura, T.; Mori, K. Mammalian Transcription Factor ATF6 Is Synthesized as a Transmembrane Protein and Activated by Proteolysis in Response to Endoplasmic Reticulum Stress. Mol. Biol. Cell 1999, 10 (11), 3787–3799. https://doi.org/10.1091/mbc.10.11.3787.
(34) Han, E. H.; Rha, G. B.; Chi, Y.-I. MED25 Is a Mediator Component of HNF4α-Driven Transcription Leading to Insulin Secretion in Pancreatic Beta-Cells. PLOS ONE 2012, 7 (8), e44007. https://doi.org/10.1371/journal.pone.0044007.
(35) Henley, M. J.; Linhares, B. M.; Morgan, B. S.; Cierpicki, T.; Fierke, C. A.; Mapp, A. K. Unexpected Specificity within Dynamic Transcriptional Protein–Protein Complexes. Proc. Natl. Acad. Sci. U. S. A. 2020, 117 (44), 27346–27353.
(36) Garlick, J. M.; Sturlis, S. M.; Bruno, P. A.; Yates, J. A.; Peiffer, A. L.; Liu, Y.; Goo, L.; Bao, L.; De Salle, S. N.; Tamayo-Castillo, G.; Brooks, C. L.; Merajver, S. D.; Mapp, A. K. Norstictic Acid Is a Selective Allosteric Transcriptional Regulator. J. Am. Chem. Soc. 2021, 143 (25), 9297–9302. https://doi.org/10.1021/jacs.1c03258.
(37) Pattelli, O. N.; Valdivia, E. M.; Beyersdorf, M. S.; Regan, C. S.; Rivas, M.; Merajver, S. D.;
Cierpicki, T.; Mapp, A. K. A Lipopeptidomimetic of Transcriptional Activation Domains Selectively
Disrupts Med25 PPIs; preprint; Biochemistry, 2023. https://doi.org/10.1101/2023.03.24.5341

CHAPTER III: Irreversible Ligands of Med25 AcID

Chapter 3.1 Abstract

Med25, a coactivator protein relevant to transcription, uses its Activator Interaction Domain (AcID) to form protein-protein interactions (PPIs) with transcriptional activator proteins that regulate transcriptional activity.[1–15] It is of great value to identify small molecule probes that target Med25 AcID's binding surfaces as these molecules can be transformed into therapeutics.[16–18,18–29] Here we demonstrate that benzothiophene-based ligands discovered through disulfide Tethering[30,31] can be transformed into irreversible probes that target Med25 AcID. We show that both (R)- and (S)-benzothiophene nipecotic acetyl bromides not only irreversibly bind to Med25 AcID but also shift the melting temperature of Med25 AcID, suggesting that these two compounds stabilize particular Med25 AcID conformations. Future efforts will examine the effect of the conformational stabilization on Med25 PPI networks.

Chapter 3.2 Introduction

Med25 of the Mediator complex found within higher order eukaryotes has important roles in regulating species-specific transcriptional processes.[30–32] Med25 uses its **A**ctivator **B**inding **D**omain (ABD) AcID (**Ac**tivator ***I***nteracting **D**omain) to form key protein-protein interactions (PPIs) at cell programmed times to regulate these transcriptional mechanisms. Dysfunction of Med25 AcID PPIs can lead to viral progression, unregulated stress response, and various cancer progress. Therefore, identifying small molecule modulators that can be transformed into therapeutics would be of great value.

In **Chapter 2**, we dissected compound **5**, previously identified in a site-directed disulfide Tethering screen, into its subunits isonipecotic acid and benzothiophene carboxylic acid for a structure-binding analysis experiment. (**Figure 3.1**) We demonstrated that even the simple sub fragments Tether to Med25 AcID, suggesting that each moiety contributes to the affinity of compound **5** for the protein. Additionally, Boc-nipecotic acid was shown to have similar Tetherability as isonipecotic acid suggesting that the hydrophobic interactions from the Boc group may also add to overall ligand binding. Disulfide fragments and other reversible ligands, while excellent tools for exploring in vitro space, do not function well within the reducing cellular environment. [33–38,38–4] By converting these small molecule "HEAD" fragments into thiol reactive analogs, irreversible probes can be made.[29,33–38] By transforming these

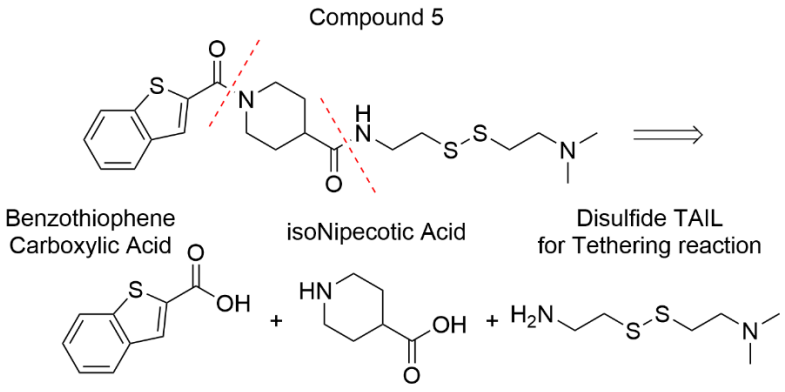

Figure 3.1 Dissecting Fragment 5 into Constituent Fragments. *Compound **5** identified from a July 2017 Tethering Screen of the Wells disulfide fragment library broken down into its constituent fragments. Screen performed by Dr. Nick Foster and Dr. Andrew Henderson.[30] Compound **5** can be synthesized by combining benzothiophene carboxylic acid, isonipecotic acid, and the disulfide tail drawn above which could come from a disulfide exchange of cystamine and captamine.*

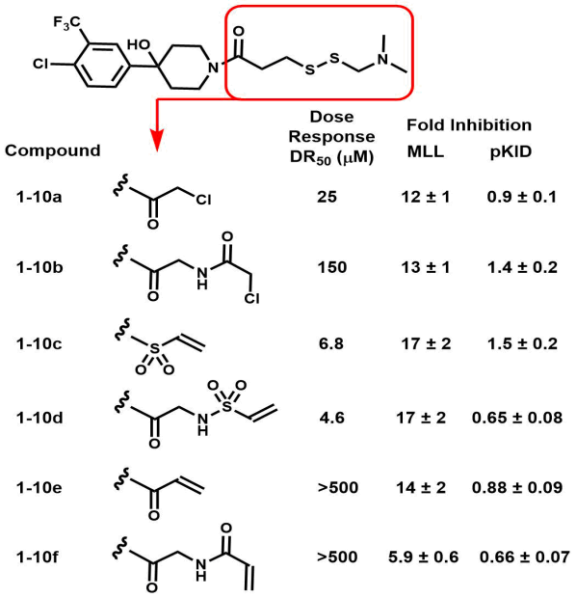

Compound	Dose Response DR_{50} (μM)	Fold Inhibition MLL	Fold Inhibition pKID
1-10a	25	12 ± 1	0.9 ± 0.1
1-10b	150	13 ± 1	1.4 ± 0.2
1-10c	6.8	17 ± 2	1.5 ± 0.2
1-10d	4.6	17 ± 2	0.65 ± 0.08
1-10e	>500	14 ± 2	0.88 ± 0.09
1-10f	>500	5.9 ± 0.6	0.66 ± 0.07

Figure 3.2 Replacing the Disulfide TAIL with thiol reactive TAILs. *Fragment **1-10** was isolated from a Tethering screen of CBP/p300 KIX.[27] Replacement of the disulfide moiety with the thiophiles shown produced irreversible modulators of KIX. These modifiers are both orthosteric (MLL) and allosteric (pKID) modulators, with **1-10d** being the most potent and effective.*

fragments in this way, ligands will be irreversibly bound to their targets allowing us to properly correlate downstream effects to small molecule-protein complex formation.

Recently, the Mapp Lab has shown that irreversible probes can be used to modulate activator-coactivator PPIs. In one example involving the master coactivator CBP/KIX, a coactivator responsible for a wide variety of cellular processes, the top fragment found from a Tethering screen performed in collaboration with the Wells Lab was modified with four different thiol reactive "TAILS" resulting in both orthosteric and allosteric modifications of PPIs.[27,31] For example, compound **1-10d** inhibits MLL but enhances the binding of pKID while **1-10c** exhibits modest inhibition of pKID with only a change in linker length. Additionally, simply changing the "TAIL" from a vinyl sulfonamide **1-10d** to an α-chloroacetamide **1-10a** allows for the same allosteric trends, at a lower efficacy. (**Figure 3.2**)

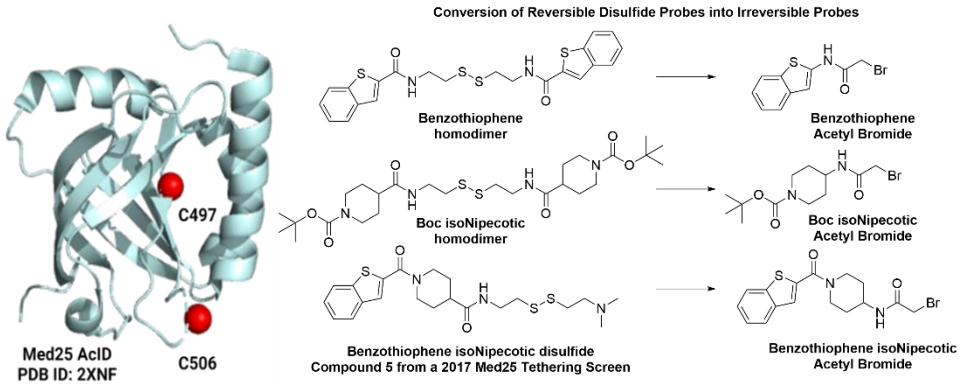

Figure 3.3 Transforming Reversible Ligands into Irreversible Ligands that Target Med25 AcID. *Med25 AcID has two solvent-exposed cysteines,* ***C497*** *and* ***C506****. Disulfide-containing ligands modify* ***C506****. Conversion of the disulfide moiety to an α-bromoacetemide group is proposed to create irreversible ligands.*

In **Chapter 3**, we explore how the **reversible covalent probes** produced in **Chapter 2** can be **transformed into irreversible probes and how they engage Med25 AcID** (**Figure 3.3)** we elected to investigate how the benzothiophene isonipecotic fragment and related analogs react with Med25 AcID when coupled to bromoacetyl bromide as a reactive and irreversible thiophiles. The complete suite of molecules utilized for this study is shown in **Scheme 3.1.**

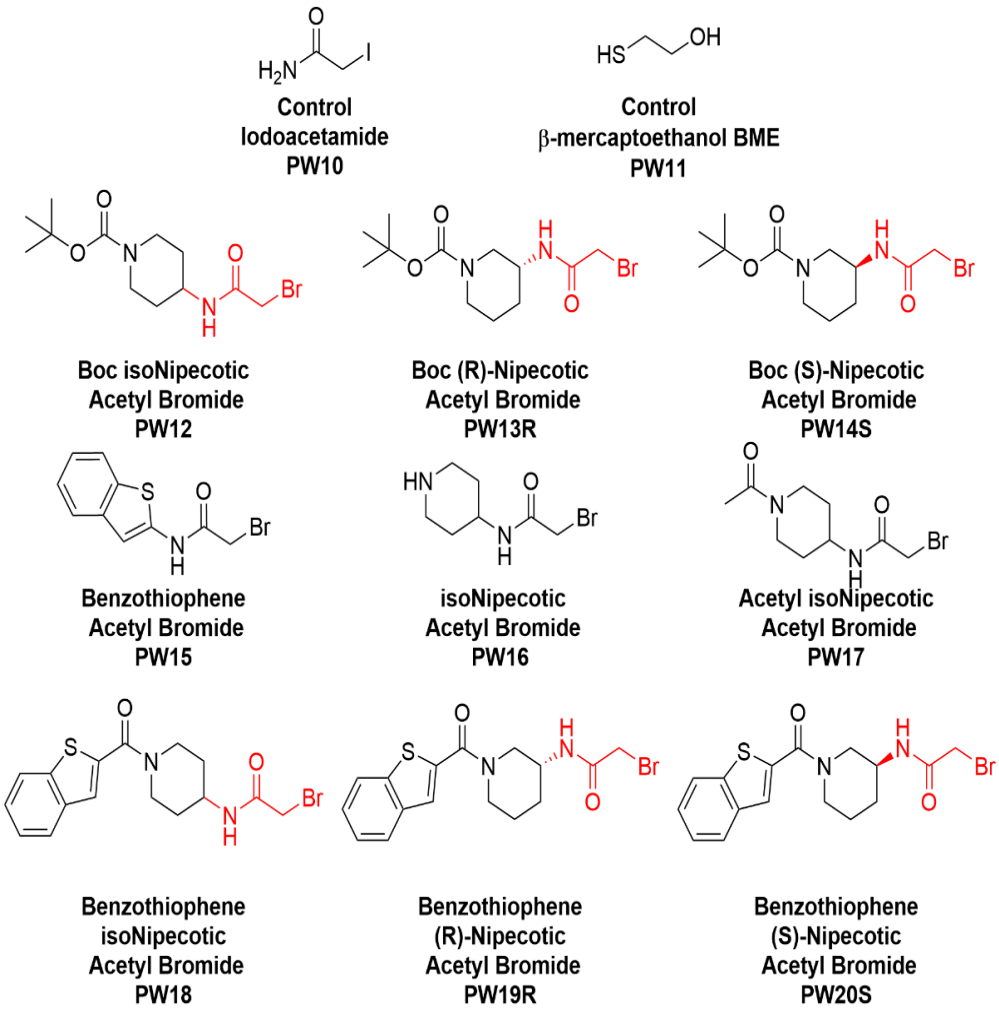

Scheme 3.1 Structures of Irreversible Ligands Synthesized.
Structures of Irreversible compounds used for SPA Experiments.

Chapter 3.3 Synthesis of Irreversible Probes

Chapter 3.3a Synthesis of Nipecotic-based Irreversibles

Formation of Boc isoNipecotic Acetyl Bromide **PW12**, Boc (R)-Nipecotic Acetyl Bromide **PW13R**, and Boc (S)-Nipecotic Acetyl Bromide **PW14S**

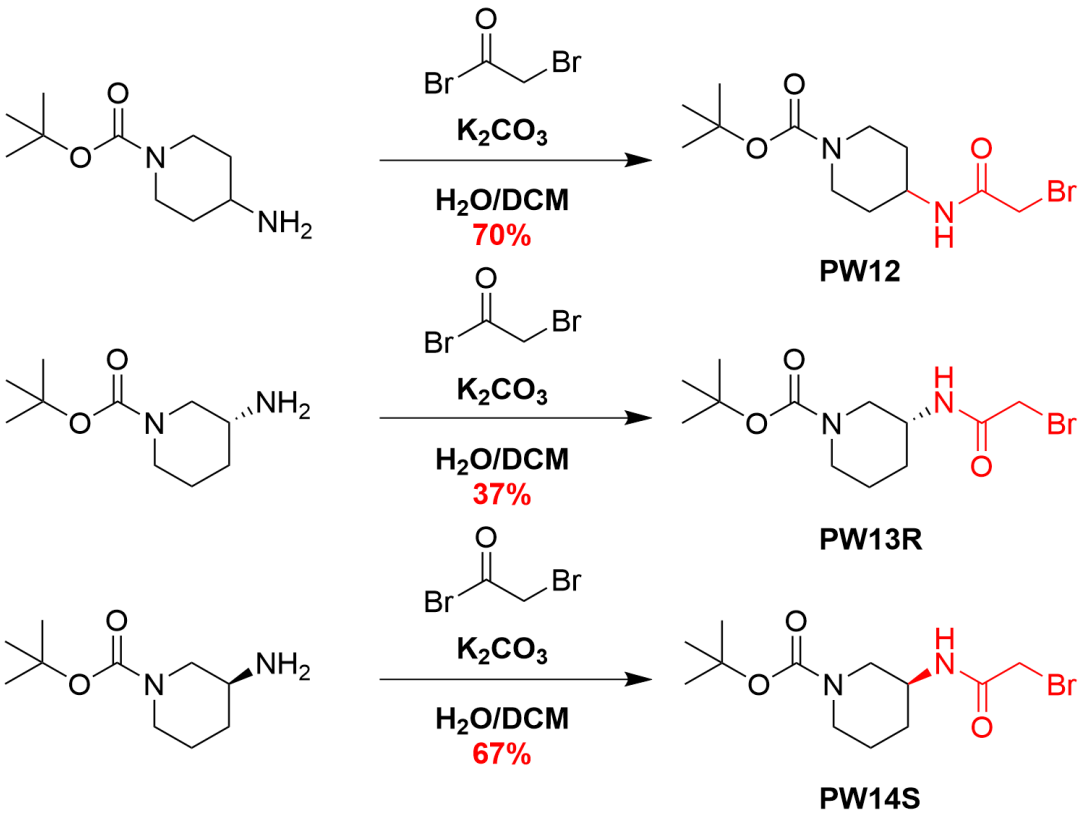

Scheme 3.2 Synthesis of BocNipecotic-Based Irreversible Ligands. *Synthetic scheme for the preparation of nipecotic acid-based modulators.*

The synthesis of the molecules proceeded in a straightforward. The Boc-nipecotic amines in **Scheme 3.2** were dissolved in DCM and combined with K_2CO_3 dissolved in water. Then bromoacetyl bromide was added to the reaction mixture to convert the corresponding amines into Boc-isonipecotic acetyl bromide **PW12** (tert-butyl 4-(2-bromoacetamido)piperidine-1-carboxylate) (70%), Boc-(R)-nipecotic acetyl bromide **PW13R** (tert-butyl (R)-3-(2-bromoacetamido)piperidine-1-carboxylate) (37%), and Boc-(S)-nipecotic acetyl bromide **PW14S** (tert-butyl (S)-3-(2-bromoacetamido)piperidine-1-carboxylate) (87%).

Chapter 3.3b Synthesis of Benzothiophene based Irreversibles

Formation of Benzothiophene Acetyl Bromide **PW15**, Benzothiophene isoNipecotic Acetyl Bromide **PW18**, Benzothiophene (R)-Nipecotic Acetyl Bromide **PW19R**, and Benzothiophene (S)-Nipecotic Acetyl Bromide **PW20S**.

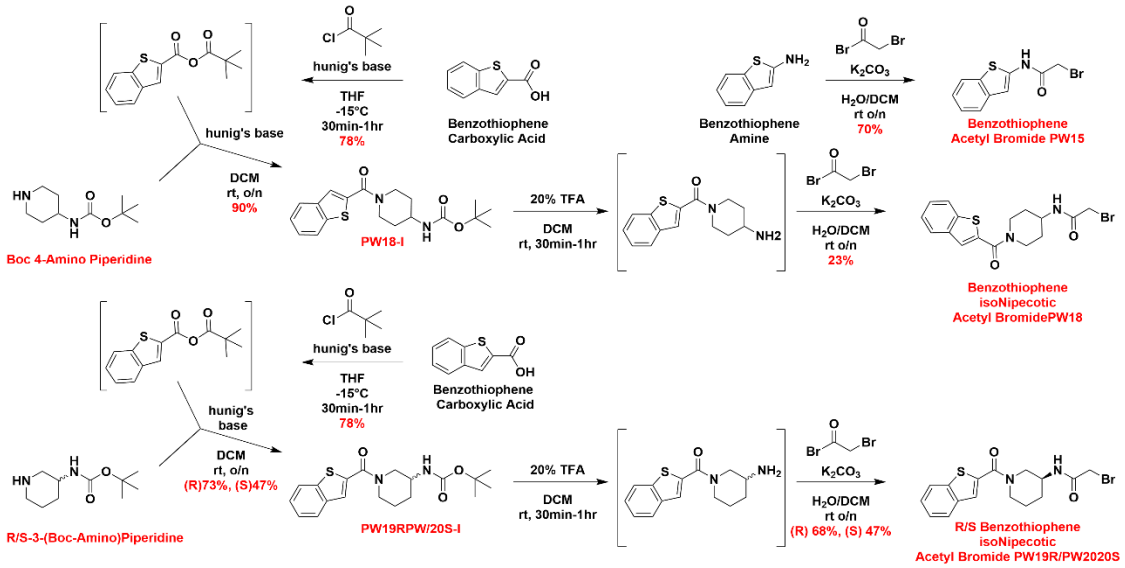

Scheme 3.3 Synthesis of Benzothiophene-based Irreversible Ligands.
Synthesis of benzothiophene-based irreversible ligands.

Scheme 3.3 shows the synthesis of Benzothiophene Acetyl Bromide (N-(benzo[b]thiophen-2-yl)-2-bromoacetamide), **PW15**, Benzothiophene isoNipecotic Acetyl Bromide **PW18** (N-(1-(benzo[b]thiophene-2-carbonyl)piperidin-4-yl)-2-bromoacetamide), Benzothiophene (R)-Nipecotic Acetyl Bromide **PW19R** ((R)-N-(1-(benzo[b]thiophene-2-carbonyl)piperidin-3-yl)-2-bromoacetamide) and Benzothiophene (S)-Nipecotic Acetyl Bromide ((S)-N-(1-(benzo[b]thiophene-2-carbonyl)piperidin-3-yl)-2-bromoacetamide) **PW20S** .

Benzo[b]thiophen-2-amine was converted into **PW15** through treatment with K_2CO_3 and bromo acetyl bromide in DCM/H_2O (19%).

Benzothiophene-Nipecotic Acetyl Bromides derivatives **PW18**, **PW19R**, and **PW20S** were made by first converting benzothiophene carboxylic acid into a mixed anhydride by

treatment with pivaloyl chloride. Then addition of Boc-Amino-Piperidine derivatives and TEA to the solution results in the formation of intermediates **PW18-I**, **PW19R-I**, and **PW20S-I.** Deboc protection of each intermediate followed by treatment with K_2CO_3 and bromoacetyl bromide in DCM/ H_2O led to the formation of each benzothiophene nipecotic acetyl bromide fragments. Benzothiophene isoNipecotic Acetyl Bromide **PW18** N-(1-(benzo[b]thiophene-2-carbonyl)piperidin-4-yl)-2-bromoacetamide (5%), Benzothiophene (R)-Nipecotic Acetyl Bromide **PW19R** ((R)-N-(1-(benzo[b]thiophene-2-carbonyl)piperidin-3-yl)-2-bromoacetamide) (14%), and Benzothiophene (S)-Nipecotic Acetyl Bromide **PW20S** Benzothiophene (S)-Nipecotic Acetyl Bromide ((S)-N-(1-(benzo[b]thiophene-2-carbonyl)piperidin-3-yl)-2-bromoacetamide) (37%).

Chapter 3.3c Synthesis of Nipecotic-derived Irreversibles

Formation of isoNipecotic Acetyl Bromide **PW16** and Acetyl Nipecotic Acetyl Bromide **PW17**

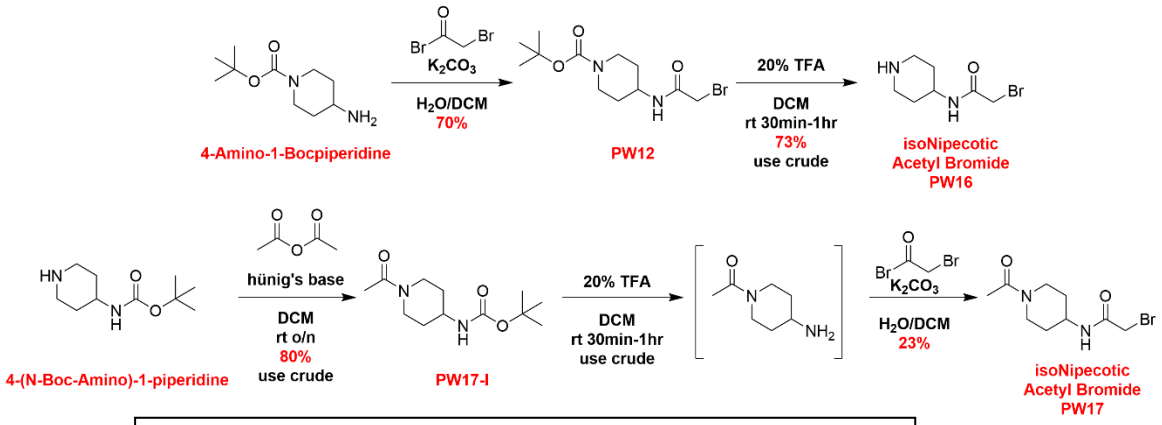

Scheme 3.4 Synthesis of isoNipecotic-Based Ligands. *Synthetic scheme for the preparation of isonipecotic acid-based irreversible modulators*

For the preparation of **PW16, PW12** was synthesized as described above then subjected to 20% TFA in DCM for 30min- 1hr to form isoNipecotic Acetyl Bromide **PW16** 2-bromo-N-(piperidin-4-yl)acetamide (73%)

For the preparation of **PW17**,4-Amino-1-Bocpiperidine was first transformed into isoNipecotic Anhydride **17I** through treatment with acetic anhydride and hünig's base in DCM. K_2CO3 and bromoacetyl bromide in a DCM/H_2O mixture followed removal of the Boc protecting group with TFA. The resulting intermediate **PW17-I** was then subjected to 20% TFA in DCM for a BOC deprotection followed by treatment with K_2CO_3 and bromoacetyl bromide in DCM/H_2O resulting in the formation of Acetyl isoNipecotic Acetyl Bromide **PW17** (N-(1-acetylpiperidin-4-yl)-2-bromoacetamide) (27%) (**Scheme 3.4**)

Chapter 3.3d Notes on Synthesis

While general amide coupling conditions are able to form the desired products, whenever the pivaloyl anhydride was formed, the reactions proceeded with higher yields and generally had less side products. However without an aromatic ring anhydrides compounds can be tricky to identify as they quickly hydrolize with any available nucleophile. Thus its better to use these fragments crude and choose a future step to purify your compound rather than allowing these fragments to react with water or silica.. Additionally, its important to remember that the thiols or disulfides used all have very pungent odors, so using bleach to neutralize the effects is a must. Some of thse fragmes also are sensitve to oxidation. Thus storing them out of light and under N2 (g) can help preserve the compound for longer periods. If these compounds have reacted with oxidizers, NMRs may show combinations of redox products.

Another thing of note, the nipecotic derivatives tend to have rather complicated spectra. Each of the piperidine ring nitrogens tend to to be diaseteotopic appearing at different chemical shifts in several solvents. These fragments are more soluble in MeOD than CDCl3, however the residual solvent peak in MeOD and water interfere with compound signals especially when using lower purity or less concentrated samples. Also, if the concentration of sample is high enough, you can see multiple rotomers within both the 13C spectra and the 1H spectra at various ratios. These peaks take an odd shape in that they appear slightly broader and each major peak will have a small partner or shoulder.

Additionally, I had trouble with samples with free amines getting stuck in my aqueous layer during work ups and other hits to yields came during the purification steps resulting in challenges obtaining clear 13C spectra for all samples.

Last, once you've found a fragment of interest, try to create a synthesis that allows you to make the most of it in the least amount of steps. If you aim to add a diversification step to explore SAR, try to have the diversification step as one of the last ones so you can make several probes that branch off from one step.

Chapter 3.4 Single Point Alkylation Experiments

Chapter 3.4a SPA Introduction

Alkylation differs from tethering in that an irreversible bond is formed between a small molecule and a POI, thus when the ligand binds it stays bound blocking that site from further interactions. To study the Med25-related PPIs of interest, it would be useful to have Small Molecule-Med25 complexes to compare to unbound Med25. To identify conditions where Med25 is 50% bound or higher for use in future biological assays, we utilize Single Point Alkylation (SPA) experiments where we test small molecules at two constant concentrations **(high 250µM, low 25 µM**) against Med25 AcID. We can see differences in alkylation by

examining the total abundance of Med25 related species at equilibrium. With higher small molecule concentrations, higher alkylation should be observed, however since drug fragments are typically administered in low micromolar to high nanomolar concentrations, better probes would alkylate well even at low small molecule concentrations. Additionally, using higher concentrations allows us to investigate single alkylation (binding to either **C497 OR C506**) versus multi-alkylation events (binding to both **C497 AND C506**). Since Med25 has two solvent exposed cysteines capable of reacting with thiophiles, it would be useful to identify a small molecule probe that preferentially binds to one cysteine, as a probe like this could be used against wtMed25 in cellular experiments without further development.

Chapter 3.4b SPA Experiment 1

In each of the following SPA experiments, Med25 (25 μM) was added to Med25 storage buffer solution (10 mM phosphate, 50 mM NaCl, 10% v/v glycerol, 0.001% v/v NP-40, pH 6.8) with **either 25 μM or 250 μM small molecule (2% DMSO)**, **1 mM DTT** to a volume of 100 μL. Samples (25 μL) were quenched with 10 μM of 1 mM BME and analyzed by q-tof mass spec at the indicated time points. Percentages of each species were calculated using the total abundance of all Med25 species as the denominator. (SPA Condition1)

Chapter 3.4b1 SPA of Control Molecules

SPA of Control Molecules Iodoacetamide **PW10** and β-mercaptoethanol **PW11**

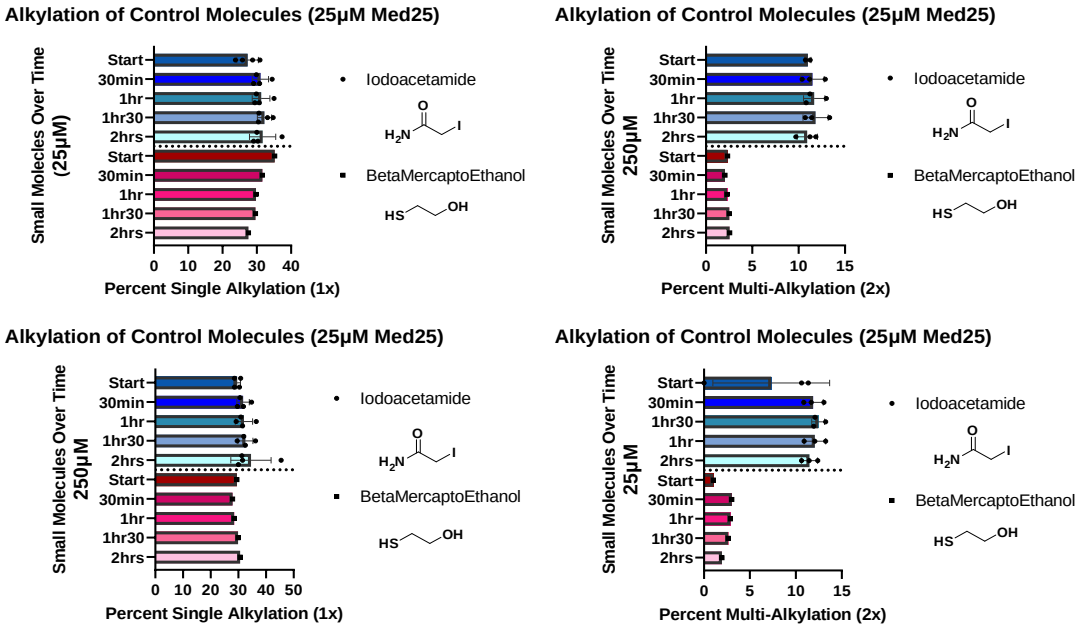

Figure 3.4 SPA of Control Molecules. *Data from single point alkylation experiments of control compounds Iodoacetamide **PW10** and Cystamine **PW11** with Med25. The upper panel shows the results of single alkylation **(left)** and double alkylation **(right)** over a 2-hour period at a 25 mM concentration of small molecule. The lower panel shows the results of single alkylation **(left)** and double alkylation **(right)** over a 2-hour period at a 250 mM concentration of small molecule. The Iodoacetamide bar graphs represent the average of 2-3 independent experiments with indicated error (SD). The β-mercaptoethanol bar graphs represent the data from a single experiment as this experiment was only performed once.*

Both iodoacetamide **PW10** and β-mecaptoethanol **PW11** were used as control molecules for this experiment. (**Figure 3.4**) Iodoacetamide is generally used to assess cysteine reactivity.[32,39–42] BME is likely binding in a reversible way; however, since BME was used to quench each reaction before MS analysis, this control allows us to evaluate any potential competition introduced by this step. Iodoacetamide can singly alkylate Med25 AcID roughly 30% under these conditions. Med25 AcID was doubly alkylated by **PW10** around 15%. BME, in contrast, can been seen alkylating once to the same percent as iodoacetamide; however, the maximum percent observed double labeling of **PW11** appears to be limited to about 3%. This shows that **PW10** is a stronger labeler than **PW11**, which is not unexpected. Also, since both fragments doubly labeled the protein, neither specifically targets either cysteine.

Thus, we were looking for fragments that could singly label Med25 greater than 15%. We want the small molecule fragment to have a higher affinity for the protein than BME and exhibit a similar reactivity to iodoacetamide. However, as stated above, **PW10** is very reactive towards many different targets, so the optimal fragment would perform somewhere in between the two control molecules.

Chapter 3.4b2 SPA of Boc Nipecotic-based Fragments:

Effects of Stereochemistry on Med25 AcID Alkylation: Boc isoNipecotic Acetyl Bromide Derivatives **PW12**, **PW13R**, **PW14S** (**Figure 3.5**)

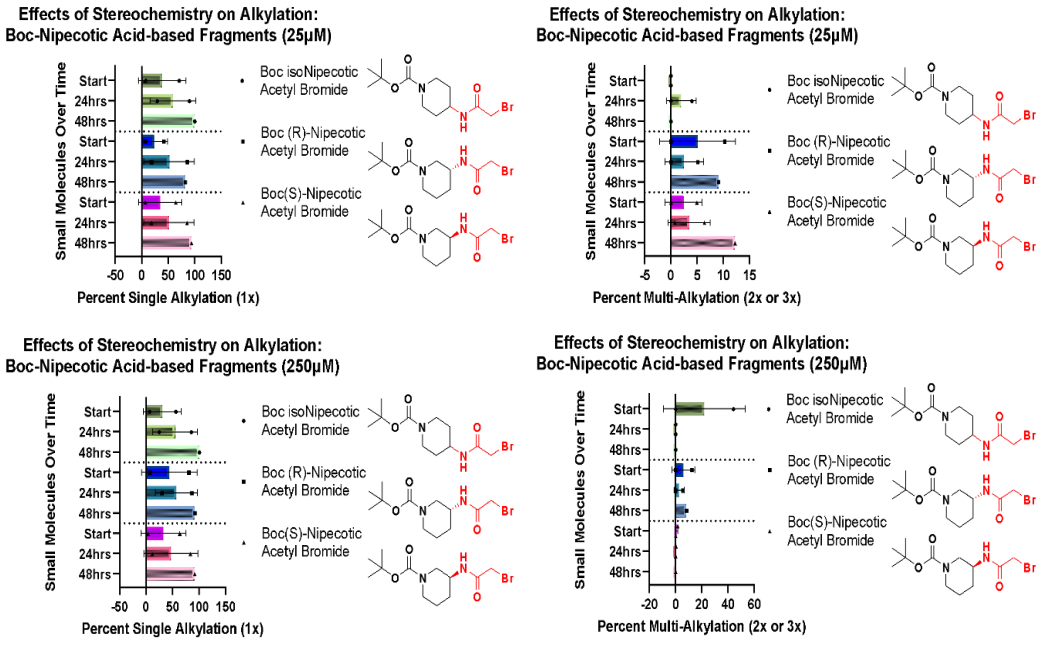

Figure 3.5 SPA1 of Boc Nipecotic-Based Irreversible Ligands. *Data from single point alkylation experiments of isonipecotic acetyl bromide* ***PW12,*** *Boc (R)-nipecotic acetyl bromide* ***PW13R,*** *and Boc (S)-nipecotic acetyl bromide* ***PW14S*** *Med25. The upper panel shows the results of single alkylation* ***(left)*** *and double alkylation* ***(right)*** *over a 48-hour period at a 25 mM concentration of small molecule. The lower panel shows the results of single alkylation* ***(left)*** *and double alkylation* ***(right)*** *over a 48-hour period at a 250 mM concentration of small molecule. The bar graphs represent the average of 2 independent experiments with indicated error (SD) for the start (0 hours) and 24-hour time points. The 48-hour data was only collected once.*

Boc isoNipecotic derivatives were able to Tether to Med25 AcID (**Figure 2.8 and 2.9 PW4-PW8**) and several hit fragments from the original screen contained the (R)-nipecotic acid moiety, we decided to investigate how stereochemistry affects alkylation. It is hypothesized that changes in stereochemistry will alter the binding activity of the fragment as a molecule's shape tends to play a pivotal role in molecular recognition.[43–49] With synthesized fragments Boc-isonipecotic acetyl bromide **PW12**, Boc-(R)-nipecotic acetyl bromide **PW13R**, and Boc (S)-nipecotic acetyl bromide **PW14S** in hand, we carried out single point alkylation reactions with Med25 AcID to determine whether or not a molecules stereochemistry alter its ability to bind to a POI.

Compounds **PW12**, **PW13R** and **PW14S** singly alkylate Med25 to roughly the same extent (**Figure 3.5**). Based on data from the original Tethering screen and follow up experiments, the assumption is that this occurs at **C506**. At the beginning of the experiment (t=0), these fragments alkylated Med25 on average 38%, 24%, and 35%, at smaller concentrations of small molecule and 30%, 43%, and 33% at higher concentrations of small molecule, respectively. These percentages were all within error of each other. Over time (~48hrs), each fragment can fully alkylate Med25 AcID at both concentrations of small molecule. Under these conditions, both **PW13R** and **PW14S**, seem to bind less specifically than **PW12**, as they can doubly alkylate Med25 ~10% when only 25 μM small molecule is added. However, when 250 μM of small molecule is added, this value drops to about 7% for both **PW13R** and **PW14S**, but **PW12** can be seen multi-alkylating Med25 roughly 20%. This suggests that the two compounds may have similar innate affinity to Med25 AcID.

Chapter 3.4b3 SPA of Benzothiophene-Based Fragments

Alkylation of benzothiophene-based fragments **PW15**, **PW19R** and **PW20S**

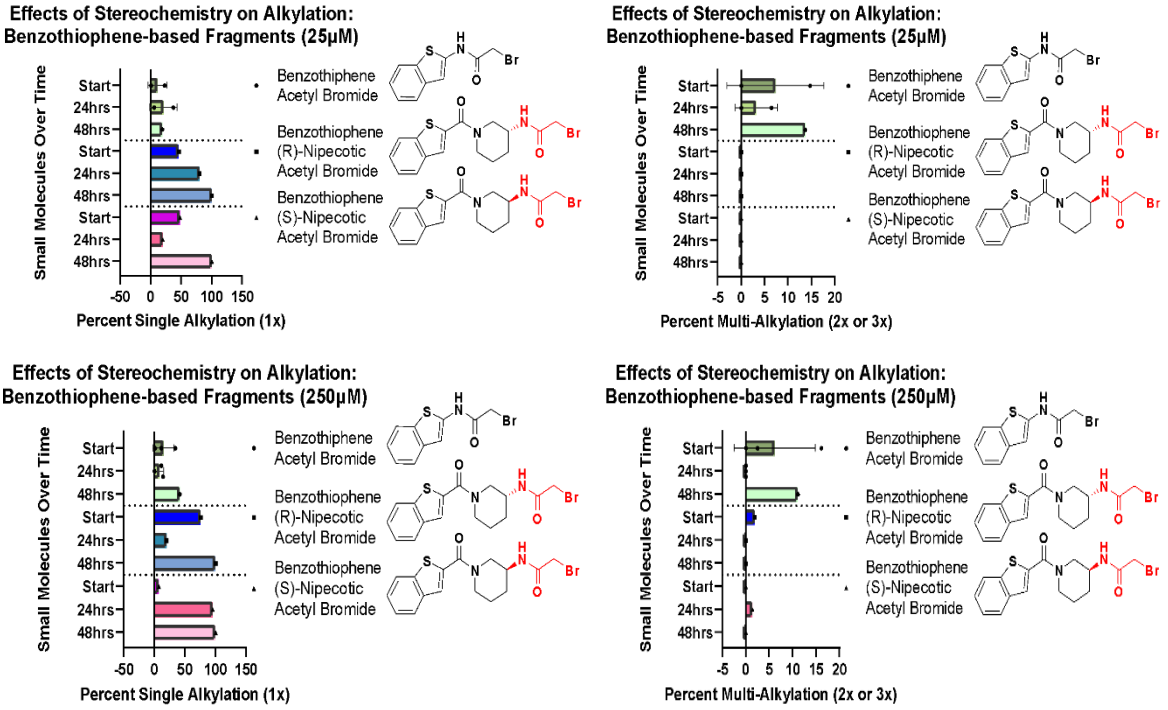

Figure 3.6 SPA1 of Benzothiophene-Based Irreversible Ligands. *Data from single point alkylation experiments of benzothiophene-based compounds benzothiophene acetyl bromide **PW15**, benzothiophene (R)-nipecotic acetyl bromide **PW19R**, and benzothiophene (S)-nipecotic acetyl bromide **PW20S** with Med25. The upper panel shows the results of single alkylation **(left)** and double alkylation **(right)** over a 48-hour period at a 25 mM concentration of small molecule. The lower panel shows the results of single alkylation **(left)** and double alkylation **(right)** over a 48-hour period at a 250 mM concentration of small molecule. The bar graphs represent the average of 2 independent experiments with indicated error (SD) for the start (0 hours) and 24-hour time points. The 48-hour data was only collected once.*

Next, we synthesized benzothiophene acetyl bromide **PW15**, benzothiophene (R)-nipecotic acetyl bromide **PW19R**, and benzothiophene (S)-nipecotic acetyl bromide **PW20S** to determine how each of these moieties react with Med25 AcID on their own. Compound **PW15** resembles two of the fragments from the original Tethering screen **23** and **24** but contains a flipped amide bond necessary to form the irreversible probe. Both **PW19R** and **PW20S** resemble compound **5** from **Chapter 2**, but with a replacement of the isonipecotic acid fragment with its two regioisomers. This allows us to evaluate how the benzothiophene fragment and its placement on the molecule affect alkylation.

Figure 3.6 shows Benzothiophene acetyl bromide **PW15** is initially able to singly alkylate Med25 about 12% -15% at both concentrations tested, much less than any of the Boc Nipecotic-based derivatives (**Figure 3.5**), while the new enantiomers **PW19R** and **PW20S** perform better, initially binding around 47% when added at 25 μM, and roughly 75% when added at 250 μM. While the data shown suggests that **PW20S** may engage with Med25 more slowly than **PW19R** due to an observed smaller alkylation percentage at the start of the experiment, these two fragments were only tested at these concentrations once. Comparing this result to (**Figure 3.5**), it's likely that the two enantiomers **PW19R** and **PW20S** may have similar affinity regarding Med25 AcID (**Figure 3.6)**. Using both concentrations of small molecule, both enantiomers **PW19R** and **PW20S** can singly alkylate Med25 100% after 48 hours.

An irregular data point occurs with both enantiomers **PW19R** and **PW20S** as it can be observed that the 24-hour time points appear to show lower alkylation percents than at the start of the reaction. This may be explained by precipitation of the small molecule-protein complex out of solution over time, or inconsistencies occurring in the analysis of the qTOF-MS data. (**Figure 3.5 left**)

Interestingly, **PW15** can be seen double-labeling Med25 at both concentrations, roughly 11%. This is most comparable to the double-labeling results of **PW10** iodoacetamide control **(Figure 3.3) PW13R** and **PW14S (Figure 3.5)**. The other two benzothiophene-based fragments then in **Figure 3.6**, **PW19R** and **PW20S,** showed limited double alkylation suggesting they selectively target one of Med25 AcID's cysteines, most likely C506. These results suggest that in the case of these two fragments stereochemistry may alter the speed of alkylation and cysteine selectivity of this irreversible reaction, but not binding affinity. This exemplifies how sub fragments can be grown into larger more potent fragments **(From PW15 to compound 5)** and

how altering stereochemistry of connected sub fragments can also identify new similar performing irreversible probes**. (From compound 5 to PW19R or PW20 S (Scheme 3.5)**

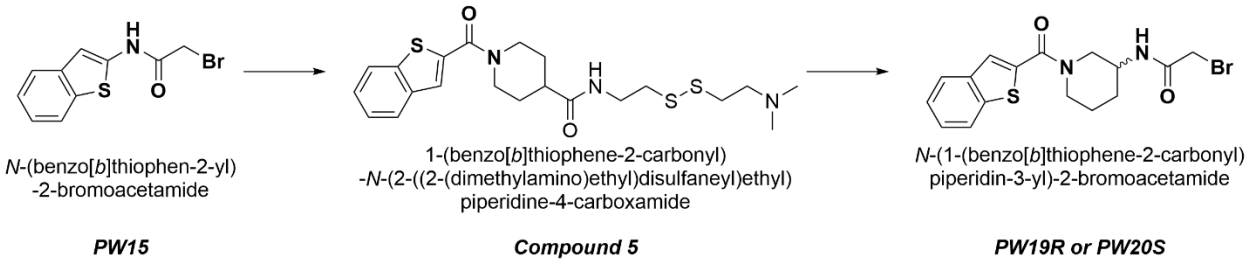

Scheme3.5 Compound 5 dissected and stereochemically altered. *A schematic that shows how compounds discovered from a reversible Tethering screen can be dissected and stereochemically modified to create irreversible probes.*

Chapter 3.4b4 SPA of Head Sub-fragments

Choosing different alkylation conditions:

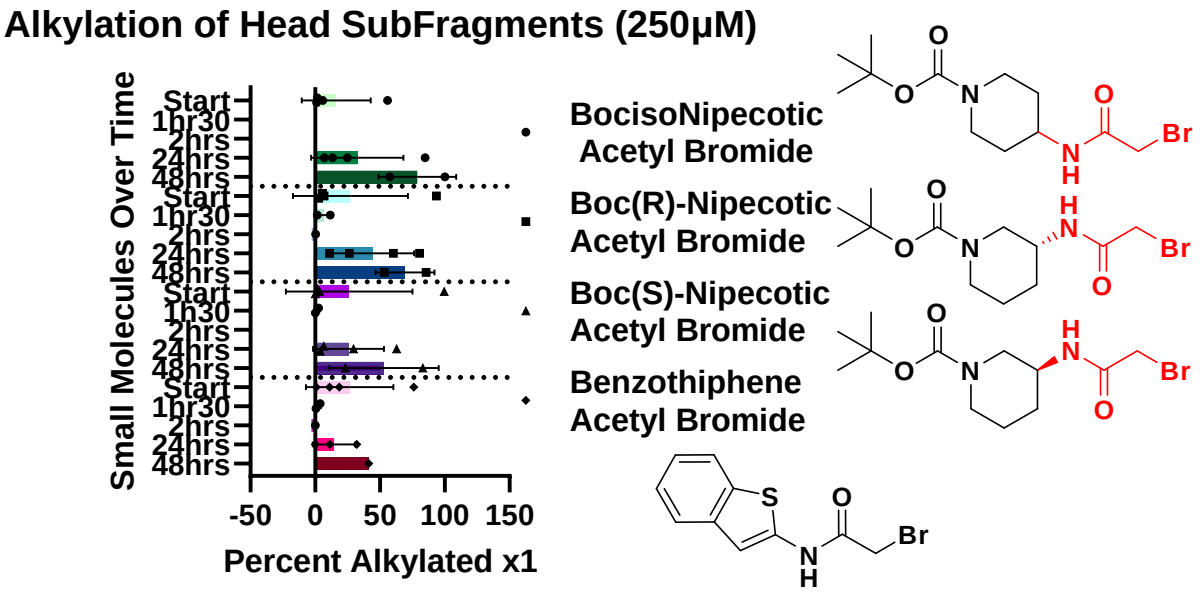

Figure 3.7 SPA of Sub-fragments over 48 hours. *Data from single point alkylation experiments of HEAD sub fragment compounds Boc isonipecotic acetyl bromide* ***PW12*** *Boc (R)-nipecotic acetyl bromide* ***PW13R****, Boc (S)-nipecotic acetyl bromide* ***PW14S****, and benzothiophene acetyl bromide* ***PW15*** *with Med25 over 48 hours. The bar graphs represent the average of 2 or 4 independent experiments with indicated error (SD) for the start (0 hours), 1hour 30 min, and 24-hour time points. The 2 hour and 48-hour data were only collected once.*

When initially running this experiment, there were a few time points considered between the start of the experiment (t=0) and 48 hours after. With that in mind, the potential for the Med25-Small Molecule complex to precipitate out of solution, and the consideration that the

alkylation results under these conditions did not display any significant differences in affinity for Med25 AcID we decided to rerun the alkylation experiments over shorter time points. (Figures 3.8-3.12)

Chapter 3.4c SPA Experiment 2

SPA Conditions 2: For these experiments, Med25 (**25 µM**) was added to Med25 Storage buffer solution (10 mM phosphate, 50 mM NaCl, 10% v/v glycerol, 0.001% v/v NP-40, pH 6.8) with **either 25 µM or 250 µM small molecule (2% DMSO)**, **1 mM DTT** to a volume of 100 µL. Since these experiments were focused on capturing alkylated Med25 AcID over 2 hours, 2**0 µL samples were quenched with 10 µM of 1 mM BME** and analyzed by q-tof MS at various time points. Percentages of each species were calculated using total abundance as a base line for comparison.

Chapter3.4c1 SPA of Boc Nipecotic-based Fragments

SPA Analysis of **PW12**, **PW13R**, and **PW14S**

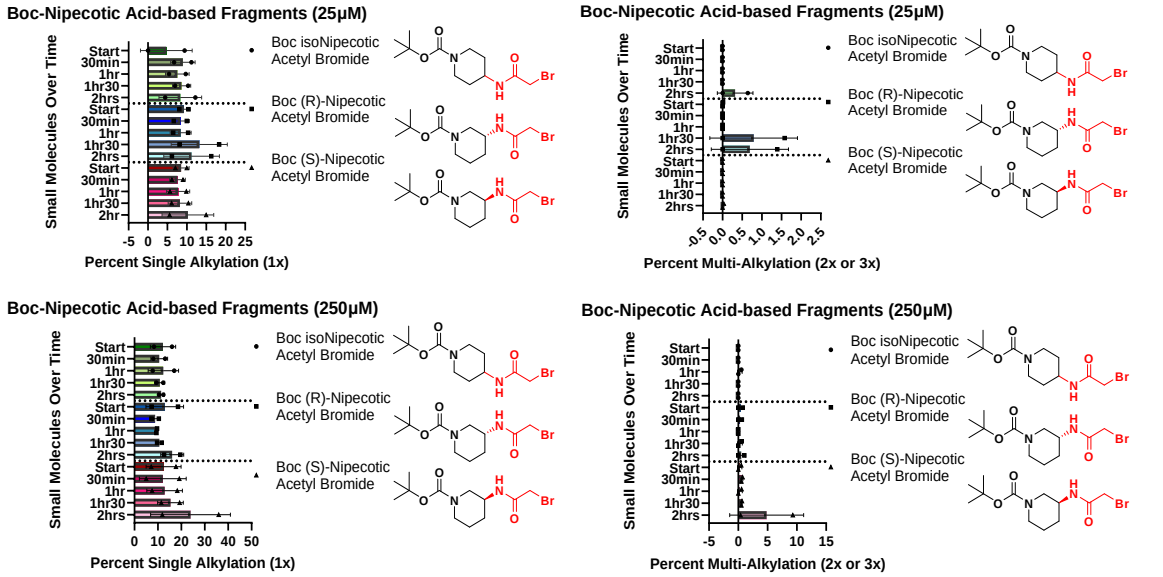

Figure 3.8 SPA2 of Boc Nipecotic-Based Irreversible Ligands. *Data from single point alkylation experiments of Boc isonipecotic acetyl bromide **PW12**,Boc (R)- nipecotic acetyl bromide **PW13R**, and Boc (S)-nipecotic acetyl bromide **PW14S** with Med25. The upper panel shows the results of single alkylation **(left)** and double alkylation **(right)** over a 2-hour period at a 25 mM concentration of small molecule. The lower panel shows the results of single alkylation **(left)** and double alkylation **(right)** over a 2-hour period at a 250 mM concentration of small molecule. The bar graphs represent the average of 2 or 3 independent experiments with indicated error (SD).*

Chapter 3.4c2 SPA HEAD Sub-Fragments

At this point, we also decided to test isonipecotic acid acetyl bromide **PW16**, and acetyl isonipecotic acetyl bromide **PW17** which were synthesized following **Scheme 3.4.** We wanted to see if the N-substitution binding trend (Best: Aromatic > Boc > H > Ac: Worst) we observed in the Tethering interactions from **Chapter 2** would be consistent with these new irreversible probes. Thus, with **PW16** and **PW17** in hand we performed Single Point Alkylation Experiments as described above. Here (Figure 3.9) it is valuable to note that each of these fragments poorly singly alkylated Med25 at both concentrations tested (max alkylation %: 8% at 25 μM and 16% at 250 μM). These values are similar to the boc-nipecotic-based fragments in **Figure 3.5.**

Additionally, both fragments **PW16** and **PW17** display the ability to alkylate both cysteines suggesting these fragments interact with Med25 in a nonspecific way. The data also suggests that **PW16** consisting of a free amine is the most nonspecific binder out of the molecules tested. Interestingly, over shorter time points, it becomes more challenging to point out significant binding differences between these fragments which suggests they may not react with Med25 AcID as quickly as iodoacetamide. Though they do bind in a comparable way to PW15 when low stringency conditions are used. At higher BME concentrations however, PW15 almost exclusively doubly alkylates Med25. This observation suggests this fragment may have a special affinity for Med25 and it would be interesting to consider how this fragment functionally alters Med25 function as a double labeler.

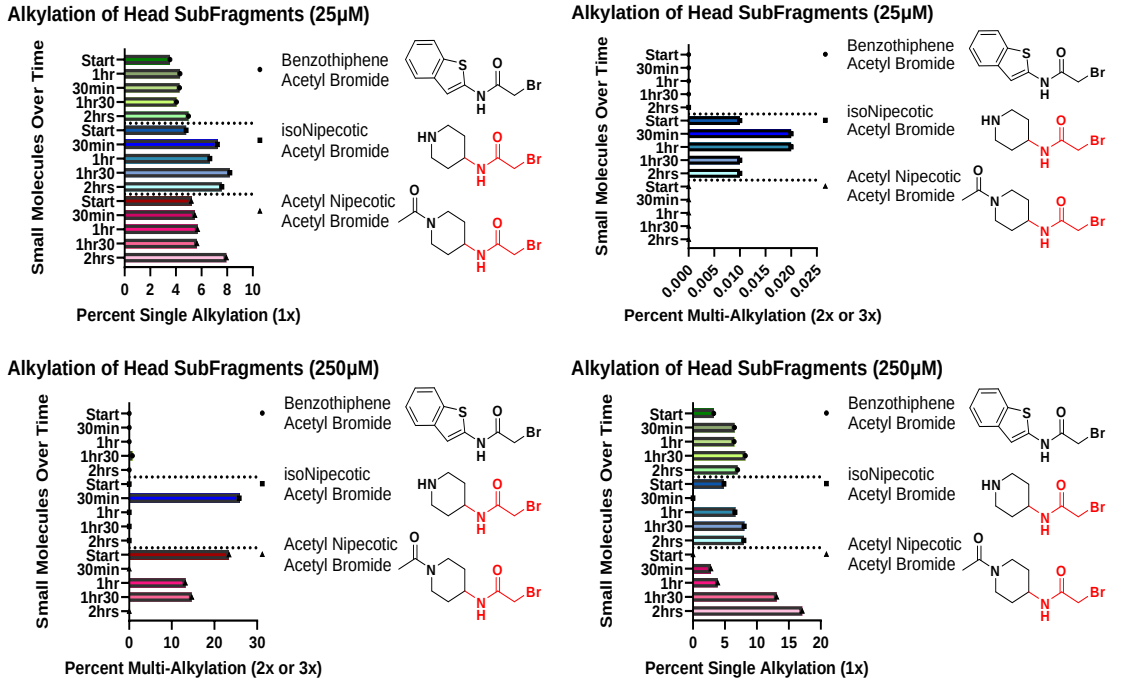

Figure 3.9 SPA2 of Head Sub-fragment Irreversible Ligands. *Data from single point alkylation experiments of HEAD sub fragments benzothiophene acetyl bromide **PW15**, isonipecotic acetyl bromide **PW16**, and acetyl nipecotic acetyl bromide **PW17** with Med25. The upper panel shows the results of single alkylation **(left)** and double alkylation **(right)** over a 2-hour period at a 25 mM concentration of small molecule. The lower panel shows the results of single alkylation **(left)** and double alkylation **(right)** over a 2-hour period at a 250 mM concentration of small molecule. The bar graphs represent one independent experiment.*

Chapter 3.4d SPA Experiment 3

Given that the 2-hour alkylation results SPA Conditions 2 did not result in significant alkylation with the various Head fragments, we decided to explore alternate reaction conditions (12.5 µM Med25 and with 25 µM or 250 µM Small Molecule in 1mM DTT over 2 hours SPA Conditions 3) with the hope of seeing similar trends with higher percent alkylation. Compound **PW18** Benzothiophene isoNipecotic Acetyl Bromide synthesized according to **Scheme 3.4** was used as a comparison against **PW19R** and **PW20S** to further test the hypothesis that the addition of a new stereocenter would not greatly affect the sub fragment's ability to bind Med25 AcID. The following figures 3.10-3.12 display fragments **PW12-PW20S** under the new reaction conditions.

Chapter 3.4d1 SPA of Boc Nipecotic-Based Fragments

SPA of Boc Nipecotic Based Fragments **PW12**, **PW13R**, and **PW14S**

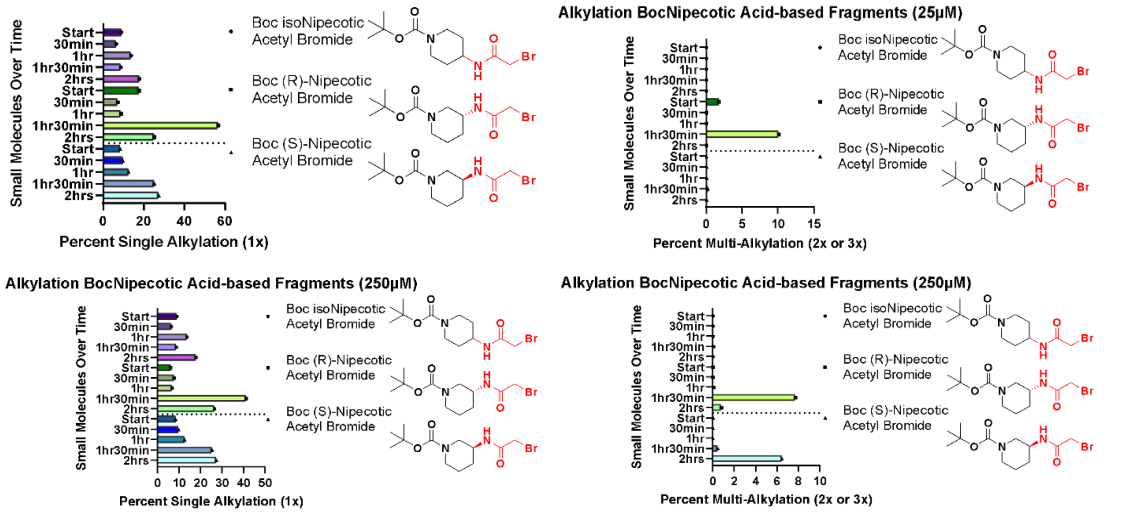

Figure 3.10 SPA3 of Boc Nipecotic-based Irreversible Ligands. *Data from single point alkylation experiments of Boc Nipecotic-based sub fragments Boc isonipecotic acetyl bromide* ***PW12****, Boc (R)-nipecotic acetyl bromide* ***PW13R****, and Boc (S)-nipecotic acetyl bromide* ***PW14S*** *with Med25. The upper panel shows the results of single alkylation* ***(left)*** *and double alkylation* ***(right)*** *over a 2-hour period at a 25 mM concentration of small molecule. The lower panel shows the results of single alkylation* ***(left)*** *and double alkylation* ***(right)*** *over a 2-hour period*

Chapter 3.4d2 SPA of HEAD Sub-Fragments

SPA of Head Sub-fragments **PW15**, **PW16**, and **PW17**

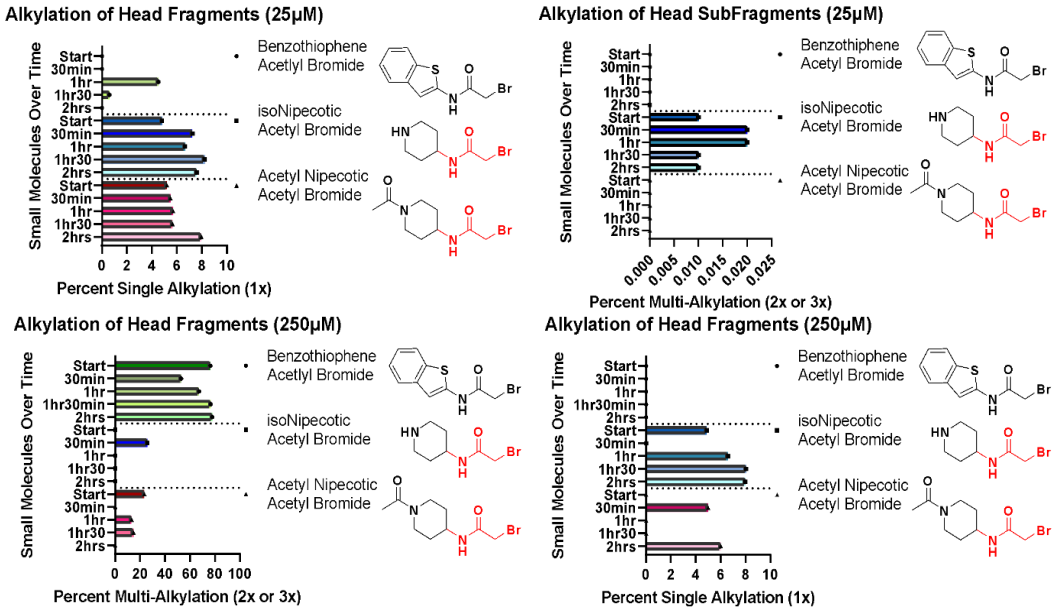

Figure 3.11 SPA3 of Head Sub-fragment Irreversible Ligands. *Data from single point alkylation experiments of HEAD sub fragments benzothiophene acetyl bromide **PW 15**, isonipecotic acetyl bromide **PW16**, and acetyl nipecotic acetyl bromide **PW17** with Med25. The upper panel shows the results of single alkylation **(left)** and double alkylation **(right**) over a 2-hour period at a 25 mM concentration of small molecule. The lower panel shows the results of single alkylation **(left)** and double alkylation **(right)** over a*

Chapter 3.4d3 SPA of Benzothiophene Based Fragments

SPA of Benzothiophene based fragments **PW18**, **PW19R**, and **PW20S**

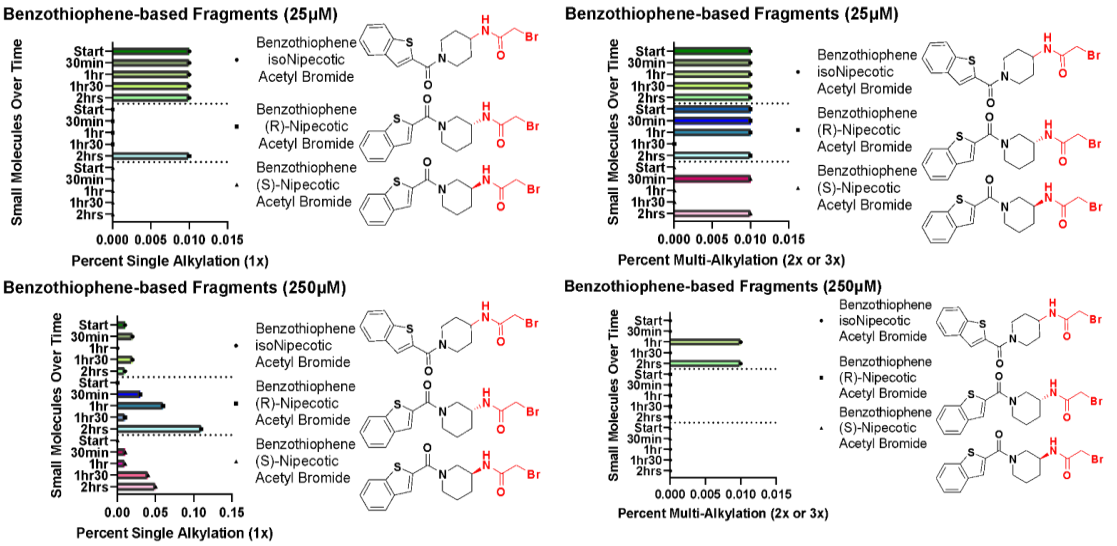

Figure 3.12 SPA3 of Benzothiophene-Based Irreversible Ligands. *Data from single point alkylation experiments of benzothiophene-based fragments benzothiophene isonipecotic acetyl bromide* ***PW 18****, benzothiophene (R)-nipecotic acetyl bromide* ***PW19R****, and benzothiophene (S)-nipecotic acetyl bromide* ***PW20S*** *with Med25. The upper panel shows the results of single alkylation* ***(left)*** *and double alkylation* ***(right)*** *over a 2-hour period at a 25 mM concentration of small molecule. The lower panel shows the results of single alkylation* ***(left)*** *and double alkylation* ***(right)*** *over a 2-hour period at a 250 mM concentration of small molecule. The bar graphs represent one independent experiment.*

Chatper3.4e Summary of SPA Experiments

In summary, the benzothiophene nipecotic acid-based fragments **PW18**, **PW19R**, and **PW20S** performed the best as the highest labeling fragments and displayed selectivity for one cysteine over the other as shown by these fragments' abilities to singly alkylate Med25 AcID 100% after 48 hours. This was consistent at all Med25 AcID concentrations tested. It is hypothesized that these fragments bind irreversibly to C506, based on the Tethering studies described in **Chapter 2** where Med25 AcID **C506A** was used and the benzothiophene isonipecotic heterodisulfide, compound **5** displayed diminished alkylation percentages due to this mutation suggesting cysteine selectivity. Similar Tethering and mutational analysis studies can be done to test this hypothesis. After the benzothiophene nipecotic acid-based fragments, the boc nipecotic acid-based derivatives **PW12**, **PW13R**, and **PW14S** showed significant alkylation to Med25 AcID

(60-70%) over 2 days. The simple benzothiophene fragment **PW15** binds both cysteines in reasonable amounts despite the fragment's concentration, suggesting this fragment alone is likely too nonspecific to be considered as a viable probe Finally, both **PW16** and **PW17** performed the worst in this experiment binding the least and relatively nonspecifically. These results correlate with the Single Point Tethering experiment results. Also, the concentration of protein and small molecules affect the results of the experiment. With too much of either, precipitation occurs and with too little of either significant alkylation cannot be detected, so it is important to choose adequate reaction conditions to assess any differences in binding. Last, alkylation generally occurs in a quick manner and since this is an irreversible process once the small molecule binds to a cysteine on the protein, that cysteine remains bound. In the case of this experiment, only considering shorter time points (0-2hrs) would likely have led us to switching our focus to analyzing a different HIT fragment, but the longer time points (24-48hrs) better display these molecules' significance.

Chapter 3.5 Investigating Protein Thermostability

With these results each compound can covalently and irreversibly bind to Med25 in a time dependent manner. One may think, a ligand capable of binding at a higher equilibrium concentration over a set period would indicate this ligand is important for targeting that protein's PPIs. Unfortunately, ligand binding which suggests protein stabilization, does not always correlate to PPI modulation. It has been previously cited that a ligand garnering affinity for a protein of interest may or may not affect its PPIs. For example, compound **5** has been previously tested in an FP-Tethering screen against Med25-ERM interactions. In this study this fragment was not identified as an inhibitor of this interaction. [32] Also, compound **22** was able to induce allosteric activity similar to ERM even though it was only the 22nd best Med25 AcID binder.[30]

This can be due to compounds being toxic and thus dangerous to develop further[50–53], identification promiscuous scaffolds[54–58], or even the compound simply being too small to effectively orthosterically inhibit the interaction.

To determine if any of these fragments alter Med25's stability we explored Differential Scanning Fluorimetry (DSF)which allows us to monitor how a ligand affects the conformation and resulting stability of a protein-ligand complex through changes in protein melting temperature (T_m). This method uses a hydrophobic dye that binds to a protein of interest's hydrophobic regions as it unfolds due based on temperature changes. Thus, we can compare the melting temperatures of unlabeled Med25 AcID and small molecule bound Med25 Acid to see if this complexation results in stabilization of Med25 through changes in T_m. Generally, the melting temperature can either be increased or decreased, however both imply protein conformation stabilization. For Med25 AcID a decrease in T_m is typically observed.

Med25 was incubated with varying amounts of small molecules for 24 hours then subjected to DSF experiments. Compounds decreased the Tm and the absolute value of the change in melting temperature was plotted.

Condition	Tma	SD
Med25_DTT	71.5	0.36

Condition	Tma	SD
2x	71.4	0.44
5x	70.9	0.2
10x	70.27	0.4
20x	69.67	0.06

Condition	Tma	SD
2x	70.77	0.06
5x	68.3	0.1
10x	66	0
20x	61.37	0.91

Condition	Tma	SD
2x	71.33	0.42
5x	68.97	0.38
10x	67.47	0.21
20x	65.03	0.65

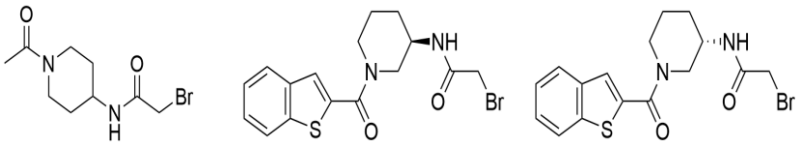

Figure 3.13 PW17, PW19R and PW20S alter Med25's Meling temperature*. Changes in Med25 melting temperature due to small molecule complexation. Acetyl isoNipecotic Acetyl Bromide* ***PW17 (left)*** *moderately stabilizes Med25 AcID while Benzothiophene (R)-Nipecotic Acetyl Bromide* ***PW19R (middle)****, and Benzothiophene (S)-Nipecotic Acetyl Bromide* ***PW20S (right)*** *stabilize Med25 >3 standard deviations of the mean.*

Condition	Tma	SD
Med25_DTT	71.53	0.25

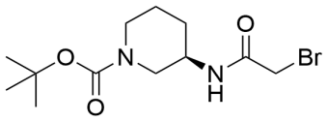

Condition	Tma	SD
2x	71.5	0.1
5x	71	0.53
10x	70.47	0.29
20x	69.57	0.75

Figure 3.14 PW14R alters Med2DSF Results and Med25 Thermostability5's Melting temperature. *Boc (R)-Nipecotic Acetyl Bromide* ***PW13R*** *is a moderate stabilizer of Med25 AcID.*

Results

Through DSF we identified 2 fragments that alter Med25 AcID's Tm greater than 3 standard deviations of the mean. This suggests these fragments stabilize a particular conformation of Med25 that could alter the protein's ability to mediate PPIs. In comparison we show two other fragments tested that were not able to cause the same stabilization. Figure 3.14 shows how increasing ligand concentrations decrease Med25's melting point. As fragments capable of decreasing the melting point by greater than 3 standard deviations of the mean, **PW19R** and **PW20S** have been shown to be thermostabilizers of Med25 AcID. This suggests that we have captured a particular Med25 conformation, that may alter related PPI activity. Thus,

it would be useful to further test these probes using functional assays such as Fluorescence Polarization (FP)

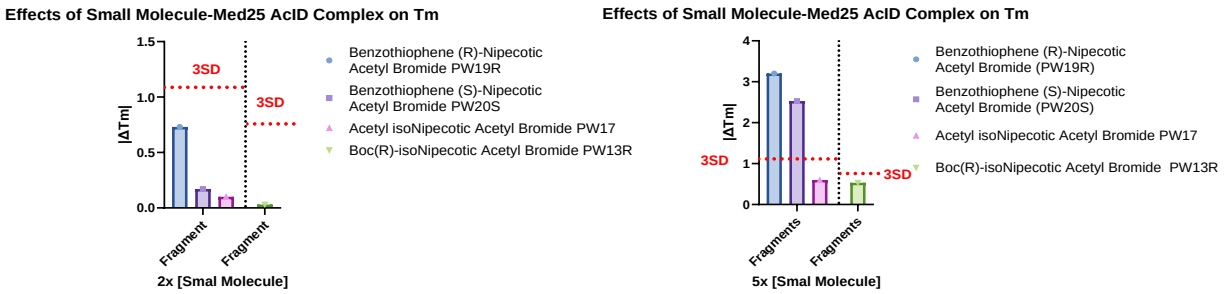

Figure 3.15 DSF Results and Med25 Thermostability. ***Figure 3.15*** *shows the absolute value of the ΔTm when* ***2x*** *small molecule or* ***5x*** *small molecule is incubated with Med25 AcID over 24. Small molecule complexation results in decreases in Med25 Melting Temperature. The ΔTm was not plotted for 10x or 20x small molecule concentrations to focus on single labeling events. (****PW19R (blue), PW20S (purple), PW17 (pink) PW13R (green)****) These plots show the average of 3 individual experimental replicates with the indicated error (SD).*

Chapter 3.6 Discussion and Conclusion

R-Benzothiophene nipecotic acetyl bromide and S-benzothiophene nipecotic acetyl bromide both alter Med25's melting temperature by more than 3 standard deviations of the mean suggesting they stabilize the Med25 AcID conformation. Interestingly, when compound 5 was evaluated as a potential inhibitor of Med25-ERM PPIs, this fragment did not display significant inhibition activity[30] When considering irreversible analogues **PW19R** and **PW20S**, it was shown that these fragments act as stabilizers of Med25 AcID by quickly singly binding Med25 100% and decreasing Med25's melting temperature by greater than 3 standard deviations of the mean. The differences of note are as follows. First, to create the irreversible probe, the amide most closely connected to Med25 AcID's cysteine(s) must be reversed for synthetic feasibility. Next, in **PW19R** and **PW20S** we have introduced a new stereocenter at the associated amide bond. Additionally, neither compound can be found within the original tethering library and thus neither has never been considered for inhibitory activity of Med25 PPIs. Since **PW19R** and **PW20S** are similar but notably different than compound **5** it is reasonable to hypothesize they

will also have differences in their biological activity. Thus, it would be useful to test these fragments against ERM as well as other Med25-related Activators for a thorough assessment of their biological use. Further studies can be done to investigate the role that these compounds play in Med25-PPI inhibition.

In conclusion, compound **5** from the list of ligands identified as Med25 binders from the Wells Tethering Library and its sub fragments were transformed into irreversible probes that target Med25 AcID. Two of the probes, R-Benzothiophene nipecotic acetyl bromide and S-benzothiophene nipecotic acetyl bromide suggest that both stabilize Med25 by shifting the Tm more than 3 SD units through DSF experiments. Further studies can be done to investigate if this stabilization results in disruption of Med25 AcID PPIs.

Chapter 3.7 Methods

General Procedures:

13C and 1H NMR spectra were recorded on a Varian MR400, a Varian Vnmrs 600MHz, or a Bruker Ascend 500 magnetic resonance spectrometer, as noted. Proton chemical shifts are referenced to CHCl3 (δ 7.26ppm) in CDCl3 solutions, CD3OD (δ 3.31) in CD3OD solutions, and DMSO δ 2.5). Carbon chemical shifts are referenced to δ 77.16ppm in CDCl3 solutions, δ 49.09 ppm in CD3OD solutions, and δ 39.53 ppm in DMSO and referenced in Appendix 2

High Resolution Mass Spectra were recorded with a (TOF, QTOF) using either positive or negative mode electrospray ionization (ESI)

Products were purified by flash chromatography using indicated solvent systems. Column chromatography was performed manually.

Purchase and Synthesis of Probes

Silica gel, 4-Amino-1-Boc piperidine, (R)-3-Amino-1-Boc piperidine, (S)-3-Amino-1- Boc piperidine, 4-(N-Boc amino)piperidine, (R)-3-(Boc Amino)Piperidine, (S)-3-(Boc Amino)Piperidine, Benzothiophene amine, Benzothiophene carboxylic acid, iodoacetamide, bromo acetyl bromide, β-mercaptoethanol (BME), Dithiolthreitol (DTT), pivaloyl chloride, hunig's base, sodium bicarbonate, trifluoroacetic acid (TFA) acetic anhydride, and DMSO were purchased from commercial vendors Sigma Aldrich or Toronto Chemical and used as received.

Control molecule Iodoacetamide **PW10** was used as purchased and dissolved in DMSO to create a 1mL 50mM stock solution. This stock was diluted to various other concentrations for use in SPA experiments.

Control molecule BME **PW11** was used as purchased and dissolved in Med25 buffer solution to create a 1mL solution of 10mM BME. This stock was diluted to various other concentrations and used for SPA experiments and for quenching of SPA experiments.

Formation of Irreversible Electrophiles

Synthesis of Boc-Nipecotic-derived alkylators (Boc isoNipecotic Acetyl Bromide PW12, **Boc (R)-Nipecotic Acetyl Bromide PW13R**, and **Boc (S)-Nipecotic Acetyl Bromide PW14S)**

Formation of Boc-iso Nipecotic Acetyl Bromide **PW12**

tert-butyl 4-(2-bromoacetamido)piperidine-1-carboxylate (80%)

To a round bottom flask charged with a stir bar was added 4-amino-1-Boc piperidine (1.0g, 4.9930 mmol) in CH_2Cl_2 (2.52 mL). This solution was combined with a solution of K_2CO_3 (1.0351g, 7.4895 mmol) in H_2O (2.33 mL) and cooled to 0° in an ice bath. Dropwise bromo acetyl bromide (436.29 µL, 4.9930 mmol) was added and the solution was allowed to stir at room temperature overnight. The crude product was extracted into CH_2Cl_2 (5 mL x3). The

combined organic layers were then washed with saturated $NaHCO_3$, brine, dried over anhydrous Na_2SO_4, and concentrated under reduced pressure and the residue was purified using flash chromatography (1% MeOH/CH2Cl2) to give **PW12** (1.2696 g crude, 79 %)

Synthesis of Boc-(R)-Nipecotic Acetyl Bromide **PW13R**

tert-butyl (R)-3-(2-bromoacetamido)piperidine-1-carboxylate (37%)

To a round bottom flask charged with a stir bar was added (R)-3-(Boc-amino) piperidine (505.4 mg, 2.52 mmol) in CH_2Cl_2 (1.25 mL). This solution was combined with a solution of K_2CO_3 (527.4 mg, 3.82 mmol) in H_2O (1.15 mL) and cooled to 0° in an ice bath. Dropwise bromo acetyl bromide (0.25 mL) was added and the solution was allowed to stir at room temperature overnight. The crude product was extracted into CH_2Cl_2 (5 mL x3). The combined organic layers were then washed with saturated $NaHCO_3$, brine, dried over anhydrous Na_2SO_4, and concentrated under reduced pressure and the residue was purified using flash chromatography (1% MeOH/CH2Cl2) to give **PW13R** as a bubble white solid (300mg, 37%)

Synthesis of Boc-(S)-Nipecotic Acetyl Bromide **PW14S**

tert-butyl (S)-3-(2-bromoacetamido)piperidine-1-carboxylate (67%)

To a round bottom flask charged with a stir bar was added (S)-3-(Boc-amino) piperidine (1.0g, 4.9930 mmol) in CH_2Cl_2 (2.52 mL). This solution was combined with a solution of K_2CO_3 (1.0351g, 7.4895 mmol) in water (2.33 mL) and cooled to 0° in an ice bath. Dropwise bromo acetyl bromide (436.29 µL, 4.9930 mmol) was added and the solution was allowed to stir at room temperature overnight. The crude product was extracted into CH_2Cl_2 (5 mL x3). The combined organic layers were then washed with saturated $NaHCO_3$, brine, dried over anhydrous

Na_2SO_4, and concentrated under reduced pressure and the residue was purified using flash chromatography (1% MeOH/CH2Cl2) to give **PW14S** as a bubble white solid, 973.3 mg, 67%)

Synthesis of Benzothiophene Acetyl Bromide **PW15**

N-(benzo[b]thiophen-2-yl)-2-bromoacetamide (70%)

To a round bottom flask charged with a stir bar was added benzothiophene amine (100 mg, 0.6710 mmol) in CH_2Cl_2 (388.89 µL). This solution was combined with a solution of K_2CO_3 (139mg, 1.0065 mmol) in H_2O (388.89 µL) and cooled to 0° in an ice bath. Dropwise bromo acetyl bromide (436.29 µL, 4.9930 mmol) was added and the solution was allowed to stir at room temperature overnight. The crude product was extracted into CH_2Cl_2 (5 mL x3). The combined organic layers were then washed with saturated $NaHCO_3$, brine, dried over anhydrous Na_2SO_4, and concentrated under reduced pressure and the residue was purified using flash chromatography (30%-70% ethyl acetate: hexanes) to give **PW15** (126 mg, 70%)

Formation of Nipecotic acid-derived alkylators

Synthesis of PW16 2-bromo-N-(piperidin-4-yl)acetamide

To a round bottom flask charged with a stir bar was added tert-butyl 4-(2-bromoacetamido)piperidine-1-carboxylate PW12 (55mg, mmol) to CH_2Cl_2 (1.71 mL). The reaction mixture was cooled to 0 °C, then dropwise was added TFA (0.34 mL, 4.48 mmol) and let stir 30 minutes to 1 hour. When the reaction was judged to be complete the solvent and excess TFA were evaporated using N_2 (g). The crude fragment **PW16** (27.63 mg, 73%) was used for SPA experiments.

Synthesis of Acetyl isonipecotic acetyl bromide **PW17**

N-(1-acetylpiperidin-4-yl)-2-bromoacetamide (27%)

To a round bottom flask charged with a stir bar was added tert-butyl piperidin-4-ylcarbamate (400 mg, 2 mmol) in CH_2Cl_2 (20 mL). Hünig's base (0.7 mL, 4.00 mmol the reaction mixture was then cooled to 0 °C in an ice bath. Dropwise acetic anhydride (0.19 mL, 2.00 mmol) was added, and the reaction stirred overnight. When the reaction was judged complete, the crude product was extracted into CH_2Cl_2 (15 mL x3). The combined organic layers were washed with saturated $NaHCO_3$, brine, died over Na2SO4, filtered, and concentrated under reduced pressure to yield intermediate **PW17-I** as a yellowish white solid. (605 mg, 80 %)

The crude product **PW17-I** (204 mg, 1.019 mmol) was dissolved in DCM (10 mL) and dropwise TFA (2.04 mL) was added, and the reaction was let stir for 30 min to 1 hour to produce the deprotected amine. The excess solvent and TFA was evaporated using N2 (g) and used as crude for the next step.

This intermediate free amine (1.019 mmol) was dissolved in DCM (0.69 mL) and mixed with a combined solution of $K2CO_3$ (313.00 mg, 2.26 mmol) in H_2O (0.75 mL). The reaction mixture was cooled to 0 °C with an ice bath and the reaction was let stir over night. When the reaction was judged to be complete, the reaction was quenched with saturated $NaHCO_3$ (5 mL) and extracted into DCM (5mL x3). The combined organic layers were then washed with NaHCO3 and brine, then dried with anhydrous Na_2SO_4, filtered, and concentrated under reduced pressure to obtain yellowish white solid, **PW17** (105mg, 27%) was then used for SPA experiments.

<u>Synthesis of Benzothiophene-Nipecotic acid-derived alkylators</u>

Synthesis of Benzothiophene isoNipecotic Acetyl Bromide **PW18**

N-(1-(benzo[b]thiophene-2-carbonyl)piperidin-4-yl)-2-bromoacetamide (23%)

To a round bottom flask charged with a stir bar was added a benzothiophene anhydride intermediate (350 mg, 1.33 mmol), tert-butyl piperidin-4-ylcarbamate (350 mg, 1.75 mmol) in CH_2Cl_2 (10 mL). Hünig's base (0.50 mL, 2.70 mmol) was then added, and the reaction mixture was allowed to stir overnight. When the reaction was judged complete the crude was extracted into CH_2Cl_2 (x3 10 mL). The combined organic layers were washed with $NaHCO_3$ (10 mL) and brine (10 mL), then dried over $MgSO_4$, filtered, and concentrated under reduced pressure to yield a white solid. The crude was then purified using flash chromatography (50% ethyl acetate: hexanes) to give intermediate **PW18-I** (420 mg, 90%).

To a round bottom flask charged with a stir bar was added **PW-18-I** (106 mg, 0.19 mmol) in CH_2Cl_2 (1.5 mL). The reaction mixture was cooled to 0 °C and dropwise TFA (0.3 mL, 3.93 mmol) was added, and the reaction mixture was let stir for 30 minutes to 1 hour to produce the deprotected intermediate. The excess solvent and TFA was evaporated using N_2 (g) and redissolved in CH_2Cl_2 (0.5mL) and used crude for the next step.

This intermediate free amine (0.19mmol) was dissolved in CH_2Cl_2 (0.5 mL) and mixed with a combined solution of K_2CO_3 (120 mg, 0.87 mmol) in H_2O (0.5 mL). The reaction mixture was cooled to 0 °C with an ice bath and the reaction was let stir over night. When the reaction was judged to be complete, the reaction was quenched with saturated $NaHCO_3$ (5 mL) and extracted into DCM (5mL x3). The combined organic layers were then washed with $NaHCO_3$ (5 mL) and brine (5mL), then dried with anhydrous Na_2SO_4, filtered, and concentrated under reduced pressure to obtain yellowish white solid. The crude was then purified using flash chromatography (100% DCM) to give **PW18** (26 mg, 23 %) was then used for SPA experiments.

Synthesis of Benzothiophene (R)-Nipecotic Acetyl Bromide **PW19R**

(R)-N-(1-(benzo[b]thiophene-2-carbonyl)piperidin-3-yl)-2-bromoacetamide (68%)

To a round bottom flask charged with a stir bar was added a benzothiophene anhydride intermediate (250mg, 0.95 mmol), tert-butyl (R)-piperidin-3-ylcarbamate (250mg, 1.248 mmol) in CH_2Cl_2 (10mL). Hünig's base (0.35 mL, 2.00 mmol) was then added, and the reaction mixture was allowed to stir overnight. When the reaction was judged complete the crude was extracted into CH_2Cl_2 (x3 10mL). The combined organic layers were washed with $NaHCO_3$ and brine, then dried over $MgSO_4$, filtered, and concentrated under reduced pressure to yield a white solid. The crude was then purified using flash chromatography (50% ethyl acetate: hexanes) to give intermediate **PW19-I** (250mg, 73%).

To a round bottom flask charged with a stir bar was added **PW19-I** (70 mg, 0.19 mmol) in CH_2Cl_2 (1.5 mL). The reaction mixture was cooled to 0 °C and dropwise TFA (0.3 mL, 3.93 mmol) was added, and the reaction mixture was let stir for 30 minutes to 1 hour to produce the deprotected intermediate. The excess solvent and TFA was evaporated using N_2 (g) and redissolved in CH_2Cl_2 (0.5mL) and used crude for the next step.

This intermediate free amine (0.19 mmol) was dissolved in CH_2Cl_2 (0.5 mL) and mixed with a combined solution of K_2CO_3 (120 mg, 0.87 mmol) in H_2O (0.5 mL). The reaction mixture was cooled to 0 °C with an ice bath and the reaction was let stir over night. When the reaction was judged to be complete, the reaction was quenched with saturated $NaHCO_3$ (5 mL) and extracted into CH_2Cl_2 (5mL x3). The combined organic layers were then washed with $NaHCO_3$ and brine, then dried with anhydrous Na_2SO_4, filtered, and concentrated under reduced pressure to obtain yellowish white solid. The crude was purified using flash chromatography (100%

CH_2Cl_2) to yield, **PW19R** (72 mg, 68%) and a white solid which was then used for SPA experiments.

Synthesis of Benzothiophene (S)-Nipecotic Acetyl Bromide **PW20S**

(S)-N-(1-(benzo[b]thiophene-2-carbonyl)piperidin-3-yl)-2-bromoacetamide (47%)

To a round bottom flask charged with a stir bar was added a benzothiophene anhydride intermediate (250mg, 0.95 mmol), tert-butyl (S)-piperidin-3-ylcarbamate (250mg, 1.248 mmol) in DCM (10mL). Hünig's base (0.35 mL, 2.00 mmol) was then added, and the reaction mixture was allowed to stir overnight. When the reaction was judged complete the crude was extracted into DCM (x3 10mL). The combined organic layers were washed with $NaHCO_3$ and brine, then dried over $MgSO_4$, filtered, and concentrated under reduced pressure to yield a white solid. The crude was then purified using flash chromatography (50% ethyl acetate: hexanes) (289 mg, 84%) to give intermediate **PW20S-I.**

To a round bottom flask charged with a stir bar was added **PW20S-I** (98 mg, 0.19 mmol) in DCM (1.5 mL). The reaction mixture was cooled to 0 °C and dropwise TFA (0.3 mL, 3.93 mmol) was added, and the reaction mixture was let stir for 30 minutes to 1 hour to produce the deprotected intermediate. The excess solvent and TFA was evaporated using N_2 (g) and redissolved in DCM (0.5mL) and used crude for the next step.

This intermediate free amine (0.19 mmol) was dissolved in DCM (0.5 mL) and mixed with a combined solution of K_2CO_3 (120 mg, 0.87 mmol) in H_2O (0.5 mL). The reaction mixture was cooled to 0 °C with an ice bath and the reaction was let stir over night. When the reaction was judged to be complete, the reaction was quenched with saturated NaHCO3 (5 mL) and extracted into DCM (5 mL x3). The combined organic layers were then washed with $NaHCO_3$

and brine, then dried with anhydrous Na_2SO_4, filtered, and concentrated under reduced pressure to obtain yellowish white solid. The crude was then purified using flash chromatography (100% CH_2Cl_2) **PW20S** (49 mg, 47%) to yield a white solid. **PW20S** was then used for SPA experiments.

Protein Expression and Purification

WT Med25 was expressed and purified from heat-shock competent Rosetta pLysS cells (Novagen), in Terrific Broth (TB) containing 0.1 mg/mL ampicillin and 0.034 mg/mL chloramphenicol, using previously described conditions.[30,59] Cells were grown at 37 °C to an optical density (OD_{600}nm) of 0.8. Temperature was reduced to 18°C and protein expression was induced upon addition of IPTG to a final concentration of 0.5 mM. Post-induction, cells were incubated 16 hours at 18°C. Cells were pelleted via centrifugation at 6000xg for 20 mins at 4°C. Cell pellets were stored at -80°C prior to purification. The harvested pellet was thawed on ice and resuspended in 20 mL of lysis buffer (50 mM phosphate, 300 mM sodium chloride, 10 mM imidazole, pH 6.8). Cells were then lysed by sonication on ice and cellular lysates were cleared by centrifugation at 9500 rpm for 20 min at 4°C. The supernatant lysate was then added to 750µL Ni-NTA beads (Qiagen) and incubated for 1 hour at 4°C. The resin was pelleted by centrifugation at 2500 rpm for 2 min at 4°C and washed with wash buffer (50 mM phosphate, 300 mM sodium chloride, 30 mM imidazole, pH 6.8) a total of five times. Protein was then eluted with 2 mL of elution buffer (50 mM phosphate, 300 mM sodium chloride, 400 mM imidazole, pH 6.8) a total of three times. Eluent was then pooled and purified by cation exchange FPLC (Source 15S, GE Healthcare) using a gradient of Buffer B (50 mM phosphate, 100 mM NaCl, 1 mM DTT, pH 6.8) in Buffer A (50 mM phosphate, 1 mM DTT). The FPLC purified protein was then dialyzed into storage buffer (10 mM phosphate, 50 mM NaCl, 10% v/v

glycerol, 0.001% v/v NP-40, pH 6.8) overnight, concentrated, aliquoted, and stored at -80°C. Final protein was greater than 90% pure as determined by Coomassie stained polyacrylamide gel. Protein concentration was determined by UV-Vis spectroscopy using an extinction coefficient, ε = 22,460 M-1 cm-1 .

Single Point Alkylation (SPA) Experiments

Med25 AcID (12.5 or 25 μM) was incubated with either 25μM or 250μM Small Molecule fragment and 1mM DTT in storage buffer (10 mM phosphate, 50 mM NaCl, 10% v/v glycerol, 0.001% v/v NP-40, pH 6.8) in a 100μL solution. Order of addition (Buffer, Protein, DTT, Small Molecule). The reaction begins upon addition of the small molecule fragment. At various time points, 20μL or 25μL samples of each SPA solution was quenched with 10μL of 10mM β-Mercaptoethanol. Mass spectrometry analysis of covalent adducts of wtMed25 was performed on 2μL samples of either 30μL or 35μL quenched SPA solution. Samples (25μL of 100 μL SPA solution) were incubated for 0 hours, 2 hour, 24 hours, and 48 hours at room temperature. Samples (20 μL of 100 μL SPA solution) were incubated for 0 hours, 30 minutes, 1 hour, 1 hour 30 minutes, 2 hours at room temperature. Analysis was conducted by mass spectrometry using an Agilent QToF LC/MS equipped with a Poroshell 300SB C8 reverse-phased column with a gradient of 5-100% acetonitrile with 0.1% formic acid in water with 0.1% formic acid over five minutes. Analysis of data was completed using the Agilent Qualitative Analysis Program with background subtraction and deconvolution settings for an intact protein of 16,000- 40,000 Da. Total abundances that correspond to masses of alkylated species and common adducts were compared to unalkylated Med25 or BME or DTT alkylated Med25 fragments to detect equilibrium percentages. When deciding on conditions, each experiment was done two to three times. Finally, the crude compounds used were only tested once as a proof of concept. Since their

SPA and SPT results were lower than the benzothiophene-based fragments we did not feel it was necessary to retest these fragments.

Chapter 3.8 References

(1) Currie, S. L.; Doane, J. J.; Evans, K. S.; Bhachech, N.; Madison, B. J.; Lau, D. K. W.; McIntosh, L. P.; Skalicky, J. J.; Clark, K. A.; Graves, B. J. ETV4 and AP1 Transcription Factors Form Multivalent Interactions with Three Sites on the MED25 Activator-Interacting Domain. *J. Mol. Biol.* **2017**, *429* (20), 2975–2995. https://doi.org/10.1016/j.jmb.2017.06.024.

(2) Eletsky, A.; Ruyechan, W. T.; Xiao, R.; Acton, T. B.; Montelione, G. T.; Szyperski, T. Solution NMR Structure of MED25(391–543) Comprising the Activator-Interacting Domain (ACID) of Human Mediator Subunit 25. *J. Struct. Funct. Genomics* **2011**, *12* (3), 159–166. https://doi.org/10.1007/s10969-011-9115-1.

(3) Milbradt, A. G.; Kulkarni, M.; Yi, T.; Takeuchi, K.; Sun, Z.-Y. J.; Luna, R. E.; Selenko, P.; Näär, A. M.; Wagner, G. Structure of the VP16 Transactivator Target in the Mediator. *Nat. Struct. Mol. Biol.* **2011**, *18* (4), 410–415. https://doi.org/10.1038/nsmb.1999.

(4) Nomoto, M.; Skelly, M. J.; Itaya, T.; Mori, T.; Suzuki, T.; Matsushita, T.; Tokizawa, M.; Kuwata, K.; Mori, H.; Yamamoto, Y. Y.; Higashiyama, T.; Tsukagoshi, H.; Spoel, S. H.; Tada, Y. Suppression of MYC Transcription Activators by the Immune Cofactor NPR1 Fine-Tunes Plant Immune Responses. *Cell Rep.* **2021**, *37* (11), 110125. https://doi.org/10.1016/j.celrep.2021.110125.

(5) Landrieu, I.; Verger, A.; Baert, J.-L.; Rucktooa, P.; Cantrelle, F.-X.; Dewitte, F.; Ferreira, E.; Lens, Z.; Villeret, V.; Monté, D. Characterization of ERM Transactivation Domain Binding to the ACID/PTOV Domain of the Mediator Subunit MED25. *Nucleic Acids Res.* **2015**, *43* (14), 7110–7121. https://doi.org/10.1093/nar/gkv650.

(6) Lee, H.-K.; Park, U.-H.; Kim, E.-J.; Um, S.-J. MED25 Is Distinct from TRAP220/MED1 in Cooperating with CBP for Retinoid Receptor Activation. *EMBO J.* **2007**, *26* (15), 3545–3557. https://doi.org/10.1038/sj.emboj.7601797.

(7) Lee, M.-S.; Lim, K.; Lee, M.-K.; Chi, S.-W. Structural Basis for the Interaction between P53 Transactivation Domain and the Mediator Subunit MED25. *Molecules* **2018**, *23* (10), 2726. https://doi.org/10.3390/molecules23102726.

(8) Yang, M.; Hay, J.; Ruyechan, W. T. Varicella-Zoster Virus IE62 Protein Utilizes the Human Mediator Complex in Promoter Activation. *J. Virol.* **2008**, *82* (24), 12154–12163. https://doi.org/10.1128/JVI.01693-08.

(9) Schiano, C.; Casamassimi, A.; Vietri, M. T.; Rienzo, M.; Napoli, C. The Roles of Mediator Complex in Cardiovascular Diseases. *Biochim. Biophys. Acta BBA - Gene Regul. Mech.* **2014**, *1839* (6), 444–451. https://doi.org/10.1016/j.bbagrm.2014.04.012.

(10) Napoli, C.; Schiano, C.; Soricelli, A. Increasing Evidence of Pathogenic Role of the Mediator (MED) Complex in the Development of Cardiovascular Diseases. *Biochimie* **2019**, *165*, 1–8. https://doi.org/10.1016/j.biochi.2019.06.014.

(11) Tazir, M.; Bellatache, M.; Nouioua, S.; Vallat, J.-M. Autosomal Recessive Charcot-Marie-Tooth Disease: From Genes to Phenotypes. *J. Peripher. Nerv. Syst.* **2013**, *18* (2), 113–129. https://doi.org/10.1111/jns5.12026.

(12) Han, E. H.; Rha, G. B.; Chi, Y.-I. MED25 Is a Mediator Component of HNF4α-Driven Transcription Leading to Insulin Secretion in Pancreatic Beta-Cells. *PLOS ONE* **2012**, *7* (8), e44007. https://doi.org/10.1371/journal.pone.0044007.

(13) Kazan, K. The Multitalented MEDIATOR25. *Front. Plant Sci.* **2017**, *8*.

(14) Sela, D.; Conkright, J. J.; Chen, L.; Gilmore, J.; Washburn, M. P.; Florens, L.; Conaway, R. C.; Conaway, J. W. Role for Human Mediator Subunit MED25 in Recruitment of Mediator to Promoters by Endoplasmic Reticulum Stress-Responsive Transcription Factor ATF6α. *J. Biol. Chem.* **2013**, *288* (36), 26179–26187. https://doi.org/10.1074/jbc.M113.496968.

(15) Xu, J.-Y.; Wu, L.; Shi, Z.; Zhang, X.-J.; Englert, N. A.; Zhang, S.-Y. Upregulation of Human *CYP2C9* Expression by Bisphenol A via Estrogen Receptor Alpha (ERα) and Med25: BPA Upregulates Human *CYP2C9* Expression Through ERα and Med25. *Environ. Toxicol.* **2017**, *32* (3), 970–978. https://doi.org/10.1002/tox.22297.

(16) Doak, B. C.; Norton, R. S.; Scanlon, M. J. The Ways and Means of Fragment-Based Drug Design. *Pharmacol. Ther.* **2016**, *167*, 28–37. https://doi.org/10.1016/j.pharmthera.2016.07.003.

(17) Mapp, A. K.; Pricer, R.; Sturlis, S. Targeting Transcription Is No Longer a Quixotic Quest. *Nat. Chem. Biol.* **2015**, *11* (12), 891–894. https://doi.org/10.1038/nchembio.1962.

(18) Henley, M. J.; Koehler, A. N. Advances in Targeting 'Undruggable' Transcription Factors with Small Molecules. *Nat. Rev. Drug Discov.* **2021**, *20* (9), 669–688. https://doi.org/10.1038/s41573-021-00199-0.

(19) Ikeda, K.; Maezawa, Y.; Yonezawa, T.; Shimizu, Y.; Tashiro, T.; Kanai, S.; Sugaya, N.; Masuda, Y.; Inoue, N.; Niimi, T.; Masuya, K.; Mizuguchi, K.; Furuya, T.; Osawa, M. DLiP-PPI Library: An Integrated Chemical Database of Small-to-Medium-Sized Molecules Targeting Protein–Protein Interactions. *Front. Chem.* **2023**, *10*, 1090643. https://doi.org/10.3389/fchem.2022.1090643.

(20) Gambini, L.; Baggio, C.; Udompholkul, P.; Jossart, J.; Salem, A. F.; Perry, J. J. P.; Pellecchia, M. Covalent Inhibitors of Protein–Protein Interactions Targeting Lysine, Tyrosine, or Histidine Residues. *J. Med. Chem.* **2019**, *62* (11), 5616–5627. https://doi.org/10.1021/acs.jmedchem.9b00561.

(21) Jin, L.; Wang, W.; Fang, G. Targeting Protein-Protein Interaction by Small Molecules. *Annu. Rev. Pharmacol. Toxicol.* **2014**, *54* (1), 435–456. https://doi.org/10.1146/annurev-pharmtox-011613-140028.

(22) Modell, A. E.; Blosser, S. L.; Arora, P. S. Systematic Targeting of Protein–Protein Interactions. *Trends Pharmacol. Sci.* **2016**, *37* (8), 702–713. https://doi.org/10.1016/j.tips.2016.05.008.

(23) Bates, C. A.; Pomerantz, W. C.; Mapp, A. K. Transcriptional Tools: Small Molecules for Modulating CBP KIX-Dependent Transcriptional Activators. *Biopolymers* **2011**, *95* (1), 17–23. https://doi.org/10.1002/bip.21548.

(24) Choi, S.; Choi, K.-Y. Screening-Based Approaches to Identify Small Molecules That Inhibit Protein–Protein Interactions. *Expert Opin. Drug Discov.* **2017**, *12* (3), 293–303. https://doi.org/10.1080/17460441.2017.1280456.

(25) Mapp, A. K.; Ansari, A. Z.; Ptashne, M.; Dervan, P. B. Activation of Gene Expression by Small Molecule Transcription Factors. *Proc. Natl. Acad. Sci.* **2000**, *97* (8), 3930–3935. https://doi.org/10.1073/pnas.97.8.3930.

(26) Thompson, A. D.; Dugan, A.; Gestwicki, J. E.; Mapp, A. K. Fine-Tuning Multiprotein Complexes Using Small Molecules. *ACS Chem. Biol.* **2012**, *7* (8), 1311–1320. https://doi.org/10.1021/cb300255p.

(27) Wang, N.; Majmudar, C. Y.; Pomerantz, W. C.; Gagnon, J. K.; Sadowsky, J. D.; Meagher, J. L.; Johnson, T. K.; Stuckey, J. A.; Brooks, C. L. I.; Wells, J. A.; Mapp, A. K. Ordering a Dynamic Protein Via a Small-Molecule Stabilizer. *J. Am. Chem. Soc.* **2013**, *135* (9), 3363–3366. https://doi.org/10.1021/ja3122334.

(28) Magee, T. V. Progress in Discovery of Small-Molecule Modulators of Protein–Protein Interactions via Fragment Screening. *Bioorg. Med. Chem. Lett.* **2015**, *25* (12), 2461–2468. https://doi.org/10.1016/j.bmcl.2015.04.089.

(29) Ueda, T.; Tamura, T.; Kawano, M.; Shiono, K.; Hobor, F.; Wilson, A. J.; Hamachi, I. Enhanced Suppression of a Protein–Protein Interaction in Cells Using Small-Molecule Covalent Inhibitors Based on an *N* -Acyl- *N* -Alkyl Sulfonamide Warhead. *J. Am. Chem. Soc.* **2021**, *143* (12), 4766–4774. https://doi.org/10.1021/jacs.1c00703.

(30) Henderson, A. R.; Henley, M. J.; Foster, N. J.; Peiffer, A. L.; Beyersdorf, M. S.; Stanford, K. D.; Sturlis, S. M.; Linhares, B. M.; Hill, Z. B.; Wells, J. A.; Cierpicki, T.; Brooks, C. L.; Fierke, C. A.; Mapp, A. K. Conservation of Coactivator Engagement Mechanism Enables Small-Molecule Allosteric Modulators. *Proc. Natl. Acad. Sci.* **2018**, *115* (36), 8960–8965. https://doi.org/10.1073/pnas.1806202115.

(31) Erlanson, D. A.; Braisted, A. C.; Raphael, D. R.; Randal, M.; Stroud, R. M.; Gordon, E. M.; Wells, J. A. Site-Directed Ligand Discovery. *Proc. Natl. Acad. Sci.* **2000**, *97* (17), 9367–9372. https://doi.org/10.1073/pnas.97.17.9367.

(32) Henderson, A. R. Dissecting Transcriptional Coactivator Binding Networks To Enable Small Molecule Modulation.

(33) Narayanan, A.; Jones, L. H. Sulfonyl Fluorides as Privileged Warheads in Chemical Biology. *Chem. Sci.* **2015**, *6* (5), 2650–2659. https://doi.org/10.1039/c5sc00408j.

(34) Orita, M.; Ohno, K.; Warizaya, M.; Amano, Y.; Niimi, T. Lead Generation and Examples Opinion Regarding How to Follow up Hits. *Methods Enzymol.* **2011**, *493*, 383–419. https://doi.org/10.1016/B978-0-12-381274-2.00015-7.

(35) Schulz, M. N.; Hubbard, R. E. Recent Progress in Fragment-Based Lead Discovery. *Curr. Opin. Pharmacol.* **2009**, *9* (5), 615–621. https://doi.org/10.1016/j.coph.2009.04.009.

(36) Tabuchi, Y.; Watanabe, T.; Katsuki, R.; Ito, Y.; Taki, M. Direct Screening of a Target-Specific Covalent Binder: Stringent Regulation of Warhead Reactivity at a Matchmaking Environment.

(37) Gentile, D. R.; Rathinaswamy, M. K.; Jenkins, M. L.; Moss, S. M.; Siempelkamp, B. D.; Renslo, A. R.; Burke, J. E.; Shokat, K. M. Ras Binder Induces a Modified Switch-II Pocket in GTP and GDP States. *Cell Chem. Biol.* **2017**, *24* (12), 1455-1466.e14. https://doi.org/10.1016/j.chembiol.2017.08.025.

(38) Nnadi, C. I.; Jenkins, M. L.; Gentile, D. R.; Bateman, L. A.; Zaidman, D.; Balius, T. E.; Nomura, D. K.; Burke, J. E.; Shokat, K. M.; London, N. Novel K-Ras G12C Switch-II Covalent Binders Destabilize Ras and Accelerate Nucleotide Exchange. *J. Chem. Inf. Model.* **2018**, *58* (2), 464–471. https://doi.org/10.1021/acs.jcim.7b00399.

(39) Abo, M.; Li, C.; Weerapana, E. Isotopically-Labeled Iodoacetamide-Alkyne Probes for Quantitative Cysteine-Reactivity Profiling. *Mol. Pharm.* **2018**, *15* (3), 743–749. https://doi.org/10.1021/acs.molpharmaceut.7b00832.

(40) Chen, F.-J.; Gao, J. Fast Cysteine Bioconjugation Chemistry. *Chem. – Eur. J.* **2022**, *28* (66), e202201843. https://doi.org/10.1002/chem.202201843.

(41) Isor, A.; Chartier, B. V.; Abo, M.; Currens, E. R.; Weerapana, E.; McCulla, R. D. Identifying Cysteine Residues Susceptible to Oxidation by Photoactivatable Atomic Oxygen Precursors Using a Proteome-Wide Analysis. *RSC Chem. Biol.* **2021**, *2* (2), 577–591. https://doi.org/10.1039/D0CB00200C.

(42) Fu, H. W.; Moomaw, J. F.; Moomaw, C. R.; Casey, P. J. Identification of a Cysteine Residue Essential for Activity of Protein Farnesyltransferase. Cys299 Is Exposed Only upon Removal of Zinc from the Enzyme. *J. Biol. Chem.* **1996**, *271* (45), 28541–28548. https://doi.org/10.1074/jbc.271.45.28541.

(43) Ebalunode, J. O.; Zheng, W. Molecular Shape Technologies in Drug Discovery: Methods and Applications. *Curr. Top. Med. Chem.* **2010**, *10* (6), 669–679. https://doi.org/10.2174/156802610791111489.

(44) Nicola, G.; Vakser, I. A. A Simple Shape Characteristic of Protein–Protein Recognition. *Bioinformatics* **2007**, *23* (7), 789–792. https://doi.org/10.1093/bioinformatics/btm018.

(45) Gainza, P.; Wehrle, S.; Van Hall-Beauvais, A.; Marchand, A.; Scheck, A.; Harteveld, Z.; Buckley, S.; Ni, D.; Tan, S.; Sverrisson, F.; Goverde, C.; Turelli, P.; Raclot, C.; Teslenko, A.; Pacesa, M.; Rosset, S.; Georgeon, S.; Marsden, J.; Petruzzella, A.; Liu, K.; Xu, Z.; Chai, Y.; Han, P.; Gao, G. F.; Oricchio, E.; Fierz, B.; Trono, D.; Stahlberg, H.; Bronstein, M.; Correia, B. E. De Novo Design of Protein Interactions with Learned Surface Fingerprints. *Nature* **2023**, *617* (7959), 176–184. https://doi.org/10.1038/s41586-023-05993-x.

(46) Kortagere, S.; Krasowski, M. D.; Ekins, S. The Importance of Discerning Shape in Molecular Pharmacology. *Trends Pharmacol. Sci.* **2009**, *30* (3), 138–147. https://doi.org/10.1016/j.tips.2008.12.001.

(47) Von Eichborn, J.; Günther, S.; Preissner, R. Structural Features and Evolution of Protein-Protein Interactions. *Genome Inform. Int. Conf. Genome Inform.* **2010**, *22*, 1–10.

(48) Gatiatulin, A. K.; Ziganshin, M. A.; Gorbatchuk, V. V. Smart Molecular Recognition: From Key-to-Lock Principle to Memory-Based Selectivity. *Front. Chem.* **2020**, *7*.

(49) Kumar, A.; Zhang, K. Y. J. Advances in the Development of Shape Similarity Methods and Their Application in Drug Discovery. *Front. Chem.* **2018**, *6*.

(50) Rudmann, D. G. On-Target and off-Target-Based Toxicologic Effects. *Toxicol. Pathol.* **2013**, *41* (2), 310–314. https://doi.org/10.1177/0192623312464311.

(51) Hao, Y.; Moore, J. H. TargetTox: A Feature Selection Pipeline for Identifying Predictive Targets Associated with Drug Toxicity. *J. Chem. Inf. Model.* **2021**, *61* (11), 5386–5394. https://doi.org/10.1021/acs.jcim.1c00733.

(52) Lin, A.; Giuliano, C. J.; Palladino, A.; John, K. M.; Abramowicz, C.; Yuan, M. L.; Sausville, E. L.; Lukow, D. A.; Liu, L.; Chait, A. R.; Galluzzo, Z. C.; Tucker, C.; Sheltzer, J. M. Off-Target Toxicity Is a Common Mechanism of Action of Cancer Drugs Undergoing Clinical Trials. *Sci. Transl. Med.* **2019**, *11* (509), eaaw8412. https://doi.org/10.1126/scitranslmed.aaw8412.

(53) Srivastava, R. Theoretical Studies on the Molecular Properties, Toxicity, and Biological Efficacy of 21 New Chemical Entities. *ACS Omega* **2021**, *6* (38), 24891–24901. https://doi.org/10.1021/acsomega.1c03736.

(54) Feldmann, C.; Miljković, F.; Yonchev, D.; Bajorath, J. Identifying Promiscuous Compounds with Activity against Different Target Classes. *Molecules* **2019**, *24* (22), 4185. https://doi.org/10.3390/molecules24224185.

(55) Ji, H.-F.; Kong, D.-X.; Shen, L.; Chen, L.-L.; Ma, B.-G.; Zhang, H.-Y. Distribution Patterns of Small-Molecule Ligands in the Protein Universe and Implications for Origin of Life and Drug Discovery. *Genome Biol.* **2007**, *8* (8), R176. https://doi.org/10.1186/gb-2007-8-8-r176.

(56) Schneider, P.; Röthlisberger, M.; Reker, D.; Schneider, G. Spotting and Designing Promiscuous Ligands for Drug Discovery. *Chem. Commun.* **2016**, *52* (6), 1135–1138. https://doi.org/10.1039/C5CC07506H.

(57) Feldmann, C.; Bajorath, J. Machine Learning Reveals That Structural Features Distinguishing Promiscuous and Non-Promiscuous Compounds Depend on Target Combinations. *Sci. Rep.* **2021**, *11* (1), 7863. https://doi.org/10.1038/s41598-021-87042-z.

(58) Gilberg, E.; Gütschow, M.; Bajorath, J. Promiscuous Ligands from Experimentally Determined Structures, Binding Conformations, and Protein Family-Dependent Interaction Hotspots. *ACS Omega* **2019**, *4* (1), 1729–1737. https://doi.org/10.1021/acsomega.8b03481.

(59) Vojnic, E.; Mourão, A.; Seizl, M.; Simon, B.; Wenzeck, L.; Larivière, L.; Baumli, S.; Baumgart, K.; Meisterernst, M.; Sattler, M.; Cramer, P. Structure and VP16 Binding of the Mediator Med25 Activator Interaction Domain. Nat. Struct. Mol. Biol. **2011**, 18 (4), 404–409. https://doi.org/10.1038/nsmb.1997.

CHAPTER IV Conclusions and Future Directions

Chapter 4.1 Conclusions

Since the coactivator Med25 plays significant regulation roles in healthy and in diseased tissues, there is a need to identify small molecule probes that would allow us to better control Med25 protein-protein interactions (PPIs). However, as outlined in **Chapter 1**, Med25 PPIs are of a class that are particularly challenging to target with small molecules.

In **Chapter 2**, I demonstrated how the site-directed ligand discovery method of disulfide Tethering can be utilized to first identify fragments with innate affinity for the dynamic coactivator Med25 AcID in a high throughput manner, and then adapted to quickly investigate how changes in structure affect the ability of a probe to covalently tether to Med25 AcID.

Med25 is perfectly suited for disulfide Tethering as it has two solvent-exposed cysteines that are reactive enough to participate in a reversible disulfide exchange. The two cysteines are also close enough to Med25's binding surfaces that the disulfide exchange results in the formation of a favorable complex detectable by mass spectrometry.

I dissected compound **5** (identified from the 2017 Tethering screen) into sub-fragments and demonstrated that each piece contributes to the overall binding affinity. More specifically, both the nipecotic acid moiety and the benzothiophene have some affinity for Med25 AcID; however, neither sub fragment is comparable to compounds **5**. Additionally, I demonstrated that the Tethering moiety (the 'tail' portion of a fragment) can be a thiol **PW4**, a homodisulfide **PW6**, or as is typical, a heterodisulfide **PW5** since the Boc isonipecotic HEAD fragment could bind to Med25 in all instances. The TAIL portion of the disulfide does however play roles in the solubility of the overall fragment and can alter the kinetics of the disulfide exchange and will

allow the attached HEAD fragment to reach the same equilibrium concentrations despite the attached TAIL.

It is also important to emphasize that the disulfide ligands all function as reversible covalent ligands for Med25, meaning these probes are sensitive to redox conditions. This limits the use of these probes to in vitro studies, as they would not survive within the reductive cellular environment. As the probes become reduced from their targets resulting in off target effects. Because of this I decided to convert the nipecotic acid-based and benzothiophene-based analogs of **Chapter 2** into irreversible probes by converting the disulfide tail into a more thiol-reactive electrophile. To create the irreversible probe the representative amine analog of each fragment was coupled to bromo acetyl bromide. The experiments of **Chapter 3** catalogue how stereochemical alterations of these sub fragments and other SAR considerations affect their ability to alkylate Med25.

Here I showed that the stereochemistry of the nipecotic acid- derivatives does not affect the fragments' abilities to effectively alkylate Med25. Considering how each of the sub-fragments were able to effectively Tether Med25 20-30%, and how at least the R-Nipecotic Acid fragment appeared frequently in the Med25 hits from the initial disulfide Tethering screen, we chose to test both (R)-nipecotic acetyl bromide and (S)-nipecotic acetyl bromide derivatives in conjunction with isonipecotic acetyl bromide analogs, testing the hypothesis that one isomer would be able to bind Med25 AcID better than the other. Surprisingly, each fragment alkylated Med25 similarly, suggesting that the changes in stereochemistry do not affect binding to at least this dynamic protein. This may relate to the protein altering its overall structure to accommodate

ligand binding. This result was corroborated when the Benzothiophene-Nipecotic Acid-based fragments all alkylated Med25 in similar ways. It can be noted that the Benzothiophene isoNipecotic Acid seems to be the worst performing out of the three.

Interestingly, both Benzothiophene (R)-Nipecotic Acetyl Bromide **PW19R** and Benzothiophene (S)-Nipecotic Acetyl Bromide **PW20S**, which were not fragments from the original tethering screen, were shown to stabilize Med25 AcID by lowering its Melting Temperature (T_m) by more than 3 standard deviations of the mean.

Chapter 4.2 Future Directions

To further investigate the role these benzothiophene-based ligands play regarding Med25 AcID PPIs, a few different directions can be explored. By using fluorescence polarization (FP) relying on fluorescently labeled peptide to compete off prelabeled small molecule, we can evaluate if these ligands can act as inhibitors of Med25 related PPIs by looking for changes in Kd between Med25 and a related activator versus Med25-Small Molecule complex and a related activator. Changes can be seen both allosterically and orthosterically as Med25 AcID is known to change structure upon ligand binding. However, simply binding to a protein of interest (poi) does not indicate that molecule's effectiveness at altering PPIs. While it was interesting to see that these molecules bound to Med25, the results presented in a follow-up experiment for the KIX protein suggested that the binding of a small molecule to a specific binding site does not correlate to the molecule's ability to alter related PPI activity.[1–3]

Additionally, it has been recently shown that modifying the thiol-reactive electrophile can tune the reactivity of the electrophile as well as have disparate orthosteric or allosteric effects depending on complexation changes Med25 AcID's structure.[1] Various different thiol reactive tails can be attached to the benzothiophene-based analogues to tune the fragments overall

reactivity.[4–12] It would be interesting to consider how an acrylamide tail and a vinyl sulfonamide tail compared to the bromo acetyl tail alter Med25 PPIs.

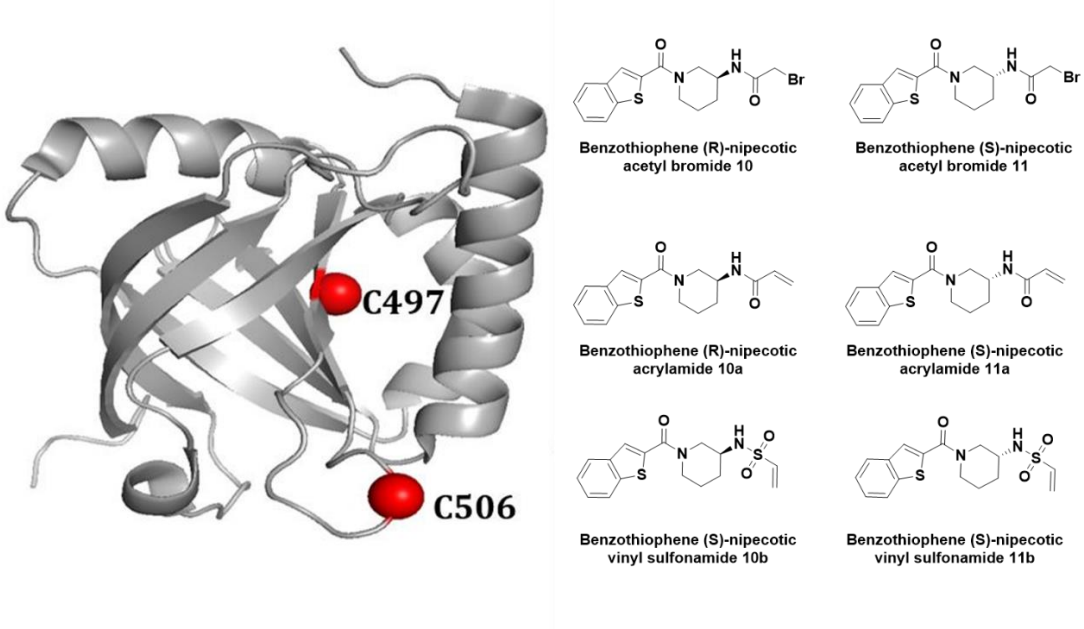

Figure 4.1 Modifications of PW19R and PW20S For Use in Biological Experiments. ***Figure 4.1 shows the next steps for PW19R and PW20S. By changing their electrophile TAIL to different thiol reactive moieties, we expect to see differences in Med25 PPI regulation.***

Since many of the initial Tethering fragments can be seen both singly and doubly labeling Med25, it could be useful to do additional experiments that help differentiate which Cysteine (C497 or C506) is being targeted by which fragments. To do this one could perform site directed mutational analysis on wtMed25 AcID to make Cysteine mutants Med25 C497A, Med25 C506A, Med25 C497S or Med25 C506S or even a double alanine mutant Med25 C497A C506A. By mutating out one of the Cysteines, double labeling should be significantly decreased if not completely abolished allowing for the rational design of cysteine-specific probes or the identification of patterns or sub features that help us identify significant scaffolds that add specificity to these binding interactions. Generally, alanine mutants are used, but it may be more

useful to create serine mutants which only differs from cysteine by replacement of Cysteine's S with Serine's O.[13,14]

Chapter 4.3 References

(1) Lodge, J. M.; Majmudar, C. Y.; Clayton, J.; Mapp, A. K. Covalent Chemical Cochaperones of the P300/CBP GACKIX Domain. *ChemBioChem* **2018**, *19* (18), 1907–1912. https://doi.org/10.1002/cbic.201800173.

(2) Henderson, A. R. Dissecting Transcriptional Coactivator Binding Networks To Enable Small Molecule Modulation.

(3) Lodge, J. M.; Justin Rettenmaier, T.; Wells, J. A.; Pomerantz, W. C.; Mapp, A. K. FP Tethering: A Screening Technique to Rapidly Identify Compounds That Disrupt Protein–Protein Interactions. *MedChemComm* **2014**, *5* (3), 370–375. https://doi.org/10.1039/C3MD00356F.

(4) Allen, C. E.; Curran, P. R.; Brearley, A. S.; Boissel, V.; Sviridenko, L.; Press, N. J.; Stonehouse, J. P.; Armstrong, A. Efficient and Facile Synthesis of Acrylamide Libraries for Protein-Guided Tethering. *Org. Lett.* **2015**, *17* (3), 458–460. https://doi.org/10.1021/ol503486t.

(5) Xu, H.; Qin, X.; Zhang, Y.; Wan, C.; Wang, R.; Hou, Z.; Ding, X.; Chen, H.; Zhou, Z.; Li, Y.; Lian, C.; Yin, F.; Li, Z. A Bifunctional Vinyl-Sulfonium Tethered Peptide Induced by Thio-Michael-Type Addition Reaction. *Chin. Chem. Lett.* **2022**, *33* (4), 2001–2004. https://doi.org/10.1016/j.cclet.2021.09.071.

(6) Berka, K.; Laskowski, R.; Riley, K. E.; Hobza, P.; Vondrášek, J. Representative Amino Acid Side Chain Interactions in Proteins. A Comparison of Highly Accurate Correlated Ab Initio Quantum Chemical and Empirical Potential Procedures. *J. Chem. Theory Comput.* **2009**, *5* (4), 982–992. https://doi.org/10.1021/ct800508v.

(7) Yang, J.; Tabuchi, Y.; Katsuki, R.; Taki, M. BioTCIs: Middle-to-Macro Biomolecular Targeted Covalent Inhibitors Possessing Both Semi-Permanent Drug Action and Stringent Target Specificity as Potential Antibody Replacements. *Int. J. Mol. Sci.* **2023**, *24* (4), 3525. https://doi.org/10.3390/ijms24043525.

(8) Prins, L. J.; Scrimin, P. Covalent Capture: Merging Covalent and Noncovalent Synthesis. *Angew. Chem. Int. Ed.* **2009**, *48* (13), 2288–2306. https://doi.org/10.1002/anie.200803583.

(9) Tabuchi, Y.; Watanabe, T.; Katsuki, R.; Ito, Y.; Taki, M. Direct Screening of a Target-Specific Covalent Binder: Stringent Regulation of Warhead Reactivity at a Matchmaking Environment.

(10) Orita, M.; Ohno, K.; Warizaya, M.; Amano, Y.; Niimi, T. Lead Generation and Examples Opinion Regarding How to Follow up Hits. *Methods Enzymol.* **2011**, *493*, 383–419. https://doi.org/10.1016/B978-0-12-381274-2.00015-7.

(11) Schulz, M. N.; Hubbard, R. E. Recent Progress in Fragment-Based Lead Discovery. *Curr. Opin. Pharmacol.* **2009**, *9* (5), 615–621. https://doi.org/10.1016/j.coph.2009.04.009.

(12) Narayanan, A.; Jones, L. H. Sulfonyl Fluorides as Privileged Warheads in Chemical Biology. *Chem. Sci.* **2015**, *6* (5), 2650–2659. https://doi.org/10.1039/c5sc00408j.

(13) Coombs, G. S.; Corey, D. R. Chapter 4 - Site-Directed Mutagenesis and Protein Engineering. In *Proteins*; Angeletti, R. H., Ed.; Academic Press: San Diego, 1998; pp 259–I. https://doi.org/10.1016/B978-012058785-8/50006-2.

(14) Barik, S. Site-Directed Mutagenesis In Vitro by Megaprimer PCR. In *In Vitro Mutagenesis Protocols*; Trower, M. K., Ed.; Methods In Molecular Medicine™; Humana Press: Totowa, NJ, 1996; pp 203–215. https://doi.org/10.1385/0-89603-332-5:203.

APPENDICIES

Appendix 1 Abbreviations

You can find a list of abbreviations here

Appendix 2 Small Molecule Characterization

You can see the NMR data analysis for new compound synthesized here.

You can see the MS data analysis for new compounds synthesized here.